



Università degli Studi di Udine

Corso di dottorato in
Scienze e Tecnologie Cliniche
Ciclo XXVIII

Tesi di dottorato

**Low-grade gliomas: from Glioma-Associated
Stem Cells (GASCs) to new prognostic and
predictive markers.**

Relatore:

Prof.ssa Carla Di Loreto

Dottorando:

Dott.ssa Marisa Sorrentino

Correlatore:

Dott.ssa Daniela Cesselli

TABLE OF CONTENTS

LIST OF ABBREVIATIONS.....	4
1. INTRODUCTION	8
1.1 GLIAL CELLS.....	8
1.1.1 MACROGLIA.....	9
1.1.2 EPENDYMAL CELLS	10
1.1.3 MICROGLIA.....	11
1.2 GLIOMA.....	11
1.2.1 EPIDEMIOLOGY.....	12
1.2.2 GLIOMA CLASSIFICATION	13
1.2.3 LOW-GRADE GLIOMA (LGG).....	15
1.2.4 MOLECULAR ABNORMALITIES IN LOW-GRADE GLIOMA (LGG)	16
1.2.5 HIGH-GRADE GLIOMA (HGG).....	21
1.3 GLIOMA STEM CELLS (GSC) IN HGG AND LGG	24
1.4 CANCER STEM CELL NICHE.....	26
1.5 TUMOR MICROENVIRONMENT (TME).....	28
1.6.1 TUMOR MICROENVIRONMENT CELLS	30
1.6.1 SOLUBLE FACTORS INVOLVED IN GLIOMA PROGRESSION.....	33
2. AIM OF THE STUDY.....	37
3. METHODS AND MATERIALS	39
3.1 SAMPLE STUDY.....	39
3.2 GLIOMA HISTOLOGICAL CHARACTERIZATION.....	39
3.3 GASC ISOLATION AND CULTURE	40
3.4 SURFACE IMMUNOPHENOTYPE CHARACTERIZATION	41
3.5 IMMUNOFLUORESCENCE ASSAY ON GASC.....	41
3.6 SOFT AGAR ASSAY	41
3.7 RNA EXTRACTION AND SEQUENCING FROM HUMAN GASC.....	42
3.8 IMMUNOHISTOCHEMICAL VALUATION OF <i>UPSTREAM REGULATORS</i>	43
3.9 TISSUE MICROARRAY (TMA) CONSTRUCTION.....	43
3.10 TMA PROCESSING.....	45
3.11 TMA ANALYSIS.....	45
3.12 STATISTICAL ANALYSIS.....	45
4. RESULTS.....	46

4.1	CHOICE AND CHARACTERIZATION OF GASC FROM LGG.....	46
4.1.1	LGG GASC WERE CHARACTERIZED BY AN UNDIFFERENTIATED PHENOTYPE...	47
4.1.2	LGG GASC RETAINED ABERRANT GROWTH PROPERTIES.....	50
4.2	TRANSCRIPTOMIC ANALYSIS OF GASC	51
4.3	IMMUNOHYSTOCHEMICAL EVALUATION OF THE EXPRESSION OF <i>UPSTREAM REGULATORS</i> AT TISSUE LEVEL.....	54
4.4	IL-1 β , IL-6 AND p65 EXPRESSION IN TMA: PATIENTS INCLUDED IN THE STUDY ..	57
4.5	EVALUATION OF THE PROGNOSTIC VALUE OF <i>GOLD STANDARD</i> BIOMARKERS.....	60
4.6	EVALUATION OF THE PROGNOSTIC VALUE OF IL-1 β , IL-6 AND p65.....	63
5.	DISCUSSION	64
6.	CONCLUSION AND FUTURE PERSPECTIVES	67
	References.....	69

LIST OF ABBREVIATIONS

ALT: Alternative Lengthening of Telomeres

APC: Adenomatous Polyposis Coli

ATRX: α Thalassemia/Mental retardation syndrome X-linked

BB: Basic Buffer

BBB: Blood-Brain Barrier

BCL-2: B Cell Lymphoma 2

BRAF: v-raf murine sarcoma viral oncogene homolog B1

BSA: Bovine Serum Albumin

CAF: Cancer Associated Fibroblast

CCL2: C-C Motif Ligand 2

CD: Cluster of Differentiation

CIC: Capicua Transcriptional Repressor

CNS: Central Nervous System

CO₂: Carbon Dioxide

COX-2: cyclooxygenase 2

CSC: Cancer Stem Cell

CSF1: Colony Stimulating Factor 1

CSF: Cerebrospinal Fluid

DAPI: 4',6-Diamidino-2-Phenylindole

DMEM: Dulbecco's Modified Eagle Medium

EC: Endothelial Cell

ECM: Extracellular Matrix

EGF: Epidermal Growth Factor

EGFR: Epidermal Growth Factor Receptor

EMR1: EGF-like module containing Mucin-like hormone Receptor-like 1

FGF: Fibroblast Growth Factor

FITC: Fluorescein Isothiocyanate

FUBP1: Far Upstream element-Binding Protein 1

G-CIMP: CpG Island Methylator Phenotype
GASC: Glioma-Associated Stem Cells
GAM: Glioma-Associated Microglia And Macrophages
GBM: Glioblastoma
GFAP: Glial Fibrillary Acid Protein
GFP: Green Fluorescent Protein
GIC: Glioma-Initiating Cells
GLUT1: Glucose Transporter Type 1
GSC: Glioma Stem Cells
HGF: Hepatocyte Growth Factor
HGG: High-Grade Glioma
HIF: Hypoxia-Inducible Factors
HLA-DR: Human Leukocyte Antigen - D Related
IAP2: Inhibitor of Apoptosis 2
IDH: Isocitrate Dehydrogenase
I κ B α : Inhibitor of κ B α
IL: Interleukin
JAK: Janus Kinase
JNK: c-Jun N-terminal Kinase
KPS: Karnofsky Performance Status
LGG: Low-Grade Glioma
LPS: Lipopolysaccharide
MAPK: Mitogen-Activated Protein Kinase
MDSC: Myeloid-Derived Suppressor Cell
MGMT: O⁶-Methylguanine-DNA Methyltransferase
MIF: Macrophage Migration Inhibitory Factor
MMPs: Matrix Metallo Proteinase
MPFS: Malignant Progression-Free-Survival
mRNA: Messenger RNA
miRNA: MicroRNA

NADH: Nicotinamide Adenine Dinucleotide Dehydrogenase

NF1: Neurofibromin 1

NF- κ B: Nuclear Factor- κ B

NFKBIA: NF- κ B inhibitor α

NPC: Neural Progenitor Cell

NPTX1: Neuronal Pentraxin 1

NSC: Neural Stem Cells

Oct-4: Octamer-binding Transcription factor 4

OS: Overall Survival

PBS: Phosphate Buffered Saline

PDGF: Platelet-Derived Growth Factor

PE: Phycoerythrin

PFS: Progression Free Survival

PGE-2: Prostaglandin E2

PI3K: Phosphoinositide 3-Kinase

PTEN: Phosphatase and Tensin Homolog

PVN: Perivascular Niche

RB: Retinoblastoma Protein

RIG-1: Retinoic Acid-Inducible Gene 1

ROS: Reactive Oxygen Species

RTK: Receptor Tyrosine Kinase

SDF1: Stromal cell Derived Factor 1

Sox-2: Sex Determining Region Y Box 2

TAF: Tumor Associated Fibroblast

TCGA: The Cancer Genome Atlas

TERT: Telomerase Reverse Transcriptase

TGF: Transforming Growth Factor

TMA: Tissue Microarrays

TME: Tumor Microenvironment

TP53: Tumor Protein p53

VEGF: Vascular Endotelial Growth Factor

VZ: Ventricular Zone

WHO: World Health Organization

1. INTRODUCTION

1.1 GLIAL CELLS

The nervous system is composed of two major cell types: neurons and glia. Glial cells constitute 90% of cells in the human brain and have been considered for a long time as passive supporting cells for neurons ⁽¹⁾. However, there has been a growing interest in glia, and recent studies have provided convincing evidence that glia plays dynamic structural and signaling roles, both during the development as well as in adult and aging brains. The impairment of these properties are often present in most of the neurological conditions ⁽²⁾.

Glial cells play critical roles in neuronal homeostasis through their physical properties, in particular they:

- Perform a housekeeping role to remove extra neurotransmitters released by neurons during synaptic transmission and balance the ionic strength of the local neuronal environment.
- Function as scavengers to remove debris after nerve injury or neuronal death.
- Cooperate to form the blood–brain barrier that prevents large molecules/particles in the blood from entering the brain.
- Produce myelin, which insulates nerve cell axons that conduct electrical signals.
- Integrate neuronal inputs as well as release growth factors and neuromodulators, in association with synapses.

There are three types of glial cells in the central nervous system (CNS): macroglia, which comprises astrocytes and oligodendrocytes, ependymal cells and microglia (Figure 1.1).

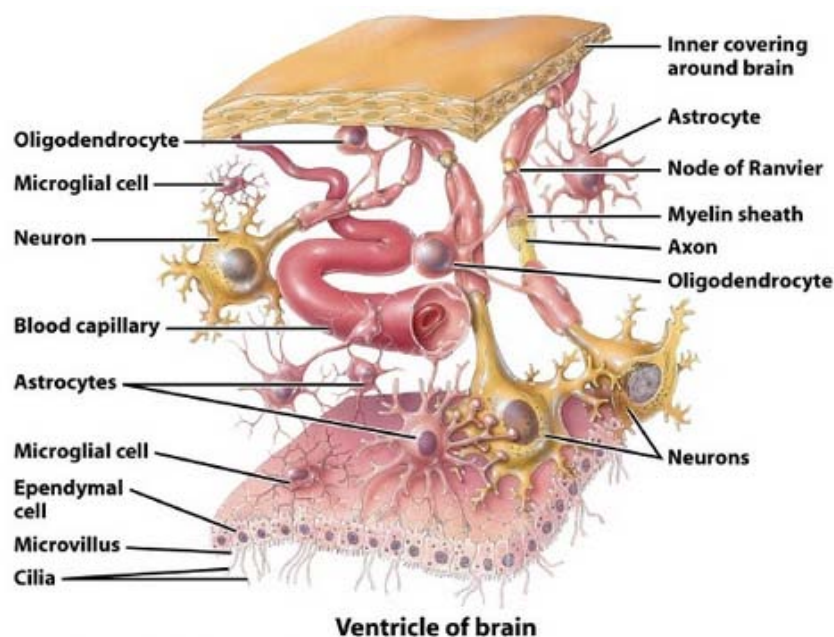


Figure 1.1. Schematic representation of the different types of glial cells in the central nervous system (CNS) and their interactions, among themselves and with neurons. (*Introduction to the Human Body, 7/e 2007 John Wiley & Sons*).

1.1.1 MACROGLIA

Macroglia originates from a single layer of proliferating neuroepithelial cells. These neural progenitor cells (NPC) line the ventricles, forming the ventricular zone (VZ). NPCs in the VZ proliferate and sequentially give rise to astrocytes and oligodendrocytes⁽³⁾.

ASTROCYTES

Astrocytes are the most abundant glial cells with irregular star-shaped cell bodies and broad end-feet on their processes⁽⁴⁾. They can be divided into two main subtypes, protoplasmic or fibrous, on the basis of differences in their cellular morphology and anatomical location. Protoplasmic astrocytes are found throughout all gray matter and, as first demonstrated using classical silver impregnation techniques, exhibit a morphology of several stem branches that give rise to many finely branching processes in a uniform globoid distribution. Fibrous astrocytes are found throughout all white matter and exhibit a morphology characterized by many long fiber-like processes. Classical and modern neuroanatomical studies also indicate that both astrocyte subtypes make extensive contacts with blood vessels. Electron microscopic analyses revealed that the processes of protoplasmic astrocytes envelop synapses and that the processes of fibrous astrocytes contact nodes of Ranvier, and that both types of astrocytes form gap junctions between distal processes of neighboring astrocytes.

Astrocytes express and secrete many signaling molecules that mediate synapse formation and synaptic transmission. They also express neurotransmitter receptors, through which they potently regulate neurotransmitter recycling at synaptic sites through the formation of “tripartite” synapses consisting of astroglial projections and neuronal pre- and postsynaptic terminals. Astrocytic end-feet are an essential constituent of the blood brain barrier (BBB). Through these widespread contact properties, astroglia have the ability to adjust blood flow for oxygen, ATP and glucose supplies, in addition to maintaining ionic concentrations in the extracellular matrix. Through the expression of aquaporin 4 water channels in the astrocytic vascular end-feet, astroglia play a vital role in the newly discovered glymphatic system, which is a brain drainage system implicated in the clearance of the amyloid β A β and tau proteins (Figure 1.2).

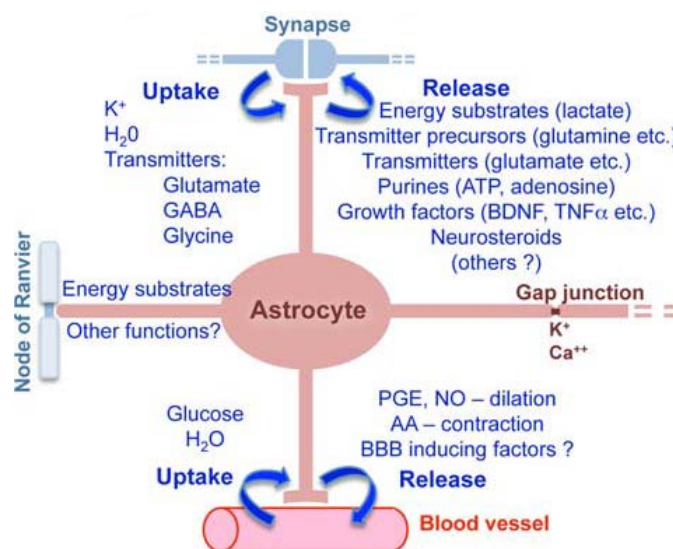


Figure 1.1.1. Schematic representations that summarize astrocyte functions in healthy CNS⁽⁴⁾.

Among the molecular marker that has been used for identification of astrocytes is the glial fibrillary acid protein (GFAP) that has become a prototypical marker for immunohistochemical identification of astrocytes. Other markers include glutamine synthetase and S100 β .

Astrocytes become reactive in response to various triggers, and this process is associated with morphological, molecular and functional changes. Reactive astrogliosis, marked by GFAP immunoreactivity, is a common feature associated with both acute brain injury and chronic neurological conditions.

OLIGODENDROCYTES

The term oligodendroglia was introduced by Rio Hortega to describe those neuroglial cells that show few processes in material stained by metallic impregnation techniques ⁽²⁾. The oligodendrocyte is mainly a myelin-forming cell, but there are also satellite oligodendrocytes that may not be directly connected to the myelin sheath. Satellite oligodendrocytes are perineuronal and may serve to regulate the microenvironment around neurons. A number of features consistently distinguish oligodendrocytes from astrocytes, in particular their smaller size, the greater density of both cytoplasm and nucleus (with dense chromatin), the absence of GFAP and of glycogen in the cytoplasm, and the presence of a large number of microtubules (25 nm in diameter) in their processes that may be involved in their stability. An oligodendrocyte extends many processes, each of which contacts and repeatedly envelopes a stretch of axon with subsequent condensation of this multispiral membrane-forming myelin. On the same axon, adjacent myelin segments belong to different oligodendrocytes. The number of processes that form myelin sheaths from a single oligodendrocyte varies according to the area of the CNS ⁽⁵⁾.

1.1.2 EPENDYMAL CELLS

Ependymal cells are ciliated cells that derives from the neuroectoderm ⁽³⁾. They constitute an epithelium, the ependyma, which lines the ventricles throughout the brain, including the dorsal part of the third ventricle next to the hypothalamus. There is a transitional zone at the middle of the third ventricle where another type of cells can be found, the tanycytes, specialized glial cells with long processes that directly access the circulation through fenestrations of the BBB.

The morphology of ependymocytes is very characteristic as they have numerous cilia, although ependymal cells with a long basal body and only two cilia have been described in the lateral ventricular zone. These cells secrete cerebrospinal fluid (CSF), with their numerous cilia participating in the transport of this fluid.

Ependymocytes play key roles in the central nervous system physiology. These roles depend on mechanisms related to cell polarity, sensory primary cilia, motile cilia, tight junctions, adherens junctions and gap junctions, machinery for endocytosis and molecule secretion, and water channels ⁽⁵⁾.

1.1.3 MICROGLIA

Microglia is constituted by specialized macrophages of the central nervous system (CNS) that are distinguished from other glial cells by their origin, morphology, gene expression pattern and functions⁽²⁾.

Microglia constitutes 5–20% of total glial cells, depending on the specific region of the CNS. It is found either in the brain parenchyma, often with a typical ramified appearance, or as perivascular microglia closely attached to the vasculature and within the perivascular ECM. In contrast to neurons and other glial cells, microglia is of haematopoietic origin and acts as primary responding cells for pathogen infection and injury.

These cells express many macrophage-associated markers, such as CD11b, CD14 and EGF-like module-containing mucin-like hormone receptor-like 1 (EMR1). Microglia exhibits several features that distinguishes it from other populations of macrophages, such as their ‘ramified’ branches that emerge from the cell body and communicate with surrounding neurons and other glial cells. Microglia rapidly responds to infectious and traumatic stimuli and adopts an ‘amoeboid’ activated phenotype⁽⁶⁾.

Activated microglia produces many pro-inflammatory mediators, including cytokines, chemokines, reactive oxygen species (ROS) and nitric oxide, which contribute to the clearance of pathogen infections. However, prolonged or excessive microglial cell activation may result in pathological forms of inflammation that contribute to the progression of neurodegenerative and neoplastic diseases⁽⁷⁾.

1.2 GLIOMA

Glioma is the most common primary malignant brain tumor and arises throughout the central nervous system (CNS) from glia⁽⁸⁾.

The incidence of primary brain tumors worldwide is approximately 7 per 100,000 individuals per year, accounting for about 2% of primary tumors and 7% of the years of life lost from cancer before the age of 70⁽⁹⁾.

Histopathologically, gliomas can grossly be divided into astrocytic, oligodendrocytic, and ependymal phenotypes. Classification by the World Health Organization (WHO) distinguishes malignancy by grade (I-IV). The most common and biologically aggressive of these tumors is glioblastoma (GBM), (WHO) grade IV, and is defined by the hallmark features of uncontrolled cellular proliferation, diffuse infiltration, propensity for necrosis, robust angiogenesis, intense resistance to apoptosis, and rampant genomic instability⁽¹⁰⁾. Despite implementation of multidisciplinary approaches which includes surgical resection, radiation and chemotherapy, survival rate is less than 5% at five years after treatment, and is worse in old patients⁽⁸⁾. Furthermore these cancers exhibit resistance to new targeted therapeutic approaches against angiogenesis mechanism. These poor results drive on new opportunities for understanding the fundamental basis for development of this devastating disease and also novel therapies that, for the first time, portend meaningful clinical responses⁽¹¹⁾.

While grade I glioma are characterized by an excellent prognosis, 70% of grade II low-grade gliomas, although slow-growing tumours, will almost invariably transform over time to a more

malignant phenotype; besides, early diffuse infiltration of the surrounding brain renders them incurable by surgery⁽¹²⁾. Recent advances highlight the cellular heterogeneity⁽¹³⁾, and their classification based on phenotypic resemblance to normal glial cells (astrocytomas, oligodendrogliomas, mixed oligoastrocytomas) and pathological grading cannot predict the clinical development of disease. Recently, genomewide analyses from multiple platforms delineated new molecular classes of lower-grade gliomas that were able to prognostically stratifying grade II and grade III LGG^(14; 15). However, the evidence that this classification is working on LGG only (being grade III glioma per se characterized by a worse prognosis, with respect to the grade II ones), is still missing.

1.2.1 EPIDEMIOLOGY

Central Nervous System (CNS) cancers comprise a group of different tumour entities anatomically close to each other but diverse in terms of morphology, site, molecular biology and clinical behavior and, presumably, etiology.

In Europe, the standardized (World) incidence of primary CNS cancers ranges from 4.5 to 11.2 cases per 100,000 men and from 1.6 to 8.5 per 100,000 women. The two most common CNS cancers, high-grade glioma and brain metastases occur more frequently during adulthood and especially among the elderly. In Europe, the peak of incidence is 18.5/100,000 in people aged \geq 65 years. The relative frequency of CNS tumors is however highest during childhood, when they account for 23% of all the cancers diagnosed. In adults the 5-year survival rate for the primary CNS cancers in Europe was 17% for males and 19% for females (1995–2002), with differences across European regions. Survivorship is higher for young European patients – 63% – than for the elderly ones⁽¹⁶⁾.

Gliomas represent 81% of malignant brain and CNS tumors. Their incidence rates vary significantly by histologic type, age at diagnosis, gender, race, ethnicity and geographic location. In general, gliomas are more common with increasing age, male gender, white race and non-Hispanic ethnicity. The most common type of glioma is glioblastoma, which ranges in age-adjusted incidence rate from 0.59 to 3.69 per 100,000 persons depending on reporting country/organization. Anaplastic astrocytoma (WHO grade III) and GBM are highest in incidence among those 75-84 years old, but oligodendroglioma and oligoastrocytomas are most common in those 35-44 years old.

Many potential risk factors for gliomas have been studied to date, but few provide explanation for the number of brain tumors identified. A meta-analysis conducted on a great number of patients population for use of mobile phones with a latency period of 10 years, give a consistent pattern of increased risk for acoustic neurinoma and glioma⁽¹⁷⁾.

For other potential risk factors, exposure to some substances, such pesticides, fertilizers, and therapeutic irradiation to the head are suggestive but not conclusive of a risk pattern for glioma⁽¹⁸⁾.

A very small proportion of glioma cases can be attributed to inherited genetic disorders. The genetic syndromes associated with the nervous system are: neurofibromatosis type 1, neurofibromatosis type 2 (associated to neurofibromin 1 and 2 genes mutations, respectively), Li-Fraumeni syndrome (associated to p53 gene mutations), Cowden disease (associated to Phosphatase and tensin homolog -PTEN- gene mutations) and Turcot syndrome (associated to

adenomatous polyposis coli -APC- gene mutations). They are characterized by the direct involvement of the underlying genetic abnormality in their pathogenesis and may have different clinical, histological and genetic features compared to their sporadic counterparts^{(19), (20)}.

1.2.2 GLIOMA CLASSIFICATION

Gliomas can be classified using different criteria.

The international classification of human tumors published by the World Health Organization (WHO) was initiated through a resolution of the WHO Executive Board in 1956 and the World Health Assembly in 1957. Its objectives have remained the same until today: to establish a classification and grading of human tumors that is accepted and used worldwide. Without clearly defined histopathological and clinical diagnostic criteria, epidemiological studies and clinical trials could not be conducted beyond institutional and national boundaries. The last edition on the histological typing of tumours of the nervous system was edited by a group of 25 pathologists and geneticists in November 2006 and the results of their deliberations and those of an additional 50 contributors are contained in the 2007 WHO classification of tumors of the central nervous system⁽⁹⁾ (Table 1.1).

Gliomas are:

- classified histologically, immunohistochemically, and/or ultrastructurally as astrocytomas, oligodendrogliomas, or tumors with morphological features of both astrocytes and oligodendrocytes, termed oligoastrocytomas.
- graded on a WHO consensus-derived scale of I to IV according to their degree of malignancy as judged by various histological features accompanied by genetic alterations.
 - grade I tumors are biologically benign and can be cured if they can be surgically resected;
 - grade II tumors are low-grade malignancies that may follow long clinical courses, but early diffuse infiltration of the surrounding brain renders them incurable by surgery;
 - grade III tumors exhibit increased anaplasia and proliferation over grade II tumors and are more rapidly fatal;
 - grade IV tumors exhibit more advanced features of malignancy, including vascular proliferation and necrosis, and as they are recalcitrant to radio/chemotherapy they are generally lethal within a year.

WHO grade is one component of a combination of criteria used to predict a response to therapy and outcome. Other criteria include clinical findings, such as age of the patient, neurologic performance status and tumors location; radiological features such as contrast enhancement; extent of surgical resection; proliferation indices; and genetic alterations. As regards molecular abnormalities, large-scale genetic sequencing efforts have identified key genomic alterations across glial subtypes, including mutations in CIC, FUBP1, 1p/19q co-deletion, IDH1/2, TERT promoter, ATRX, and the alternative lengthening of telomeres (ALT) phenotype⁽²¹⁾. For this reason, recent and ongoing translational studies in neuro-oncology have investigated the role of molecular markers as potential predictors of outcome in patients⁽¹³⁾. For each tumor entity, combinations of these parameters contribute to an overall estimate of prognosis.

Gliomas are further categorized from a clinical point of view in ⁽⁸⁾:

- Low-grade gliomas (LGG), which are categorized by the WHO as grade I and grade II; they tend to have a low proliferative potential and are well differentiated;
- High-grade gliomas (HGG), which are grade III or IV and have anaplastic features, high mitotic activity with or without vascular proliferation and necrosis.

These subgroups correlate to epidemiologic readouts and are functional to predict prognosis, therapy and follow-up. However, it's often difficult to distinguish between a LGG and a HGG. Moreover, as explained above, gliomas, in particular LGG, display a large degree of heterogeneity, both among tumors histopathologically similar and among tumor cells within the same tumor, making difficult to predict clinical outcome and hindering the decision-making process ⁽¹²⁾.

In order to explore glioma heterogeneity possible gaining insights into possible novel prognostic/predictive factors and therapies, three different approaches have been recently exploited, for both LGG and HGG: wide and integrated genome analyses, study of the glioma microenvironment and study of glioma stem cells (GSCs).

1.2.3 LOW-GRADE GLIOMA (LGG)

Low-grade gliomas represent up to 30% of gliomas and affect patients at a younger age than high-grade gliomas. LGG are commonly located in or close to eloquent areas, i.e. those areas of the brain involved in motor, language, visuospatial and memory function. The 5-year overall (OS) and progression-free survival (PFS) rates in randomized studies range from 58% to 72% and 37% to 55%, respectively ⁽²³⁾.

LGG categories include subependymal giant cell astrocytoma, pilocytic astrocytoma, pilomyxoid astrocytoma, diffuse astrocytoma, pleomorphic xanthoastrocytoma, oligodendroglioma, oligoastrocytoma and certain ependymomas. Among these subtypes, diffuse astrocytomas, mixed oligoastrocytomas and oligodendroglioma are the most common. These tumors are improperly defined as benign because they have a slow growth rate and a high degree of cellular differentiation, but unlike pilocytic astrocytomas, they grow diffusely into the normal brain parenchyma and are prone to malignant progression ⁽¹⁴⁾. Although LGG are clinically stable over a long period of time, some of them eventually transform into higher-grade tumours (WHO grade III–IV) at some point during the course of the disease. It is estimated that about 70 % of grade II gliomas progresses to an anaplastic form within 5-10 years with aggressive clinical manifestation and fatal outcome ^{(24), (25)}. Moreover, survival rate can range between 1 to 15 years and some LGG can be sensitive to standard therapies ^{(26), (27)}.

Therapeutic decisions in the management of patients with LGG (28) have traditionally been based on widely accepted clinical prognostic factors, which are:

- Age over 40 years
- Presence/absence of pre-operative neurological deficits
- Tumor size

Historically, standard care for LGG consists of surgical resection (if feasible) or biopsy and subsequent radiotherapy, yet alkylating chemotherapy and targeted drugs are increasingly

recognized as equivalent upfront treatment alternatives. However, complete neurosurgical resection is impossible, and the presence of residual tumor results in recurrence and malignant progression, albeit at highly variable intervals. Besides radiotherapy of the involved part of the brain, is not associated with an overall survival (OS) benefit but possibly with long-term *sequelae*, i. e. leucoencephalopathy and cognitive deficits, especially in patients with a favorable prognosis⁽²⁷⁾.

Although diagnosis has traditionally been made on the basis of histology, it suffers from high intraobserver and interobserver variability, does not adequately predict clinical outcomes and it is impossible to distinguish a secondary glioblastoma, defined as a tumor that was previously diagnosed as a lower-grade glioma, from a primary tumor (13).

Patient management is a challenge therefore clinicians increasingly rely on genetic classification to guide clinical decision-making.

1.2.4 MOLECULAR ABNORMALITIES IN LOW-GRADE GLIOMA (LGG)

Molecular abnormalities involve mutation of several genes, including isocitrate dehydrogenase 1 (IDH 1) and 2 (IDH 2), TP53 (tumor protein p53), ATRX (alpha-thalassemia/mental retardation syndrome X-linked), telomerase reverse transcriptase (TERT) promoter, deletion of chromosomes 1p and 19q, O⁶-methylguanine-DNA methyltransferase (MGMT) promoter methylation status and mutations in the v-raf murine sarcoma viral oncogene homolog B1 (BRAF) oncogene^{(14), (29), (30), (31) (15)}.

IDH1 AND IDH2 MUTATIONS

The molecular aberrations most intensely investigated in LGG during the past few years are point mutations in the IDH1 and IDH2 genes. IDH normally catalyzes the oxidative decarboxylation of isocitrate, producing alpha-ketoglutarate and CO₂. This enzyme has 3 isoforms: IDH1, IDH2 and IDH3. IDH3 catalyzes the third step of the citric acid cycle within the mitochondria. IDH1 and IDH2 catalyze this same reaction, but outside of the context of the citric acid cycle. Whereas IDH3 reduces NAD⁺ to NADH in this process, IDH1 and IDH2 use NADP⁺ instead. IDH1 is the only isoform localized to the cytoplasm⁽²⁸⁾. When mutations occur in IDH1 or IDH2, the mutant enzyme develops a preferential affinity for alpha-ketoglutarate instead of isocitrate, which leads to the production and accumulation of the oncometabolite 2-hydroxyglutarate.

Both IDH1 and IDH2 mutations occur in infiltrating gliomas, though IDH2 mutations are much less common than IDH1⁽³²⁾. IDH1 mutations are found in approximately 70–80% of histologic grades II and III infiltrating gliomas and secondary GBMs, yet are much less frequent in primary GBM (about 5%)^{(14), (26), (28), (33), (34), (35)}. These mutations aid diagnosis of diffuse brain lesions and differentiate diffuse LGG from pilocytic astrocytomas or ependymomas that lack IDH mutations. Moreover, IDH1/IDH2 mutations have been confirmed as early mutations in LGG and are associated with a younger age.

IDH mutant gliomas progress more slowly over time than those lacking IDH mutations, suggesting that these are biologically distinct forms of disease. Therefore, diffuse gliomas with IDH mutations are associated with a better prognosis, grade for grade, than those without⁽¹³⁾.

The importance of IDH mutations was recently corroborated by the identification of a CpG island methylator phenotype in a distinct subset of gliomas (G-CIMP), characterized by hypermethylation at a large number of CpG loci including the MGMT promoter-associated CpG island. Patients with G-CIMP are younger at the time of diagnosis and have a significantly longer survival. Moreover, the G-CIMP is more prevalent among LGG and tightly associated with IDH1 mutations. Most importantly, the IDH1 point mutation R132H was recently demonstrated to be causative to G-CIMP by remodelling the tumour methylome and transcriptome. It will be intriguing to see whether G-CIMP stands its ground as a prognostic or even a predictive biomarker in the framework of translational studies to be conducted in the near future^{(34), (35)}.

O⁶-METHYLGUANINE-DNA METHYLTRANSFERASE (MGMT) PROMOTER METHYLATION

Standard therapy for GBM includes radiation and chemotherapy with temozolomide, which acts by crosslinking DNA by alkylating multiple sites including the O position of guanine⁽³⁶⁾. DNA crosslinking is reversed by the DNA repair enzyme MGMT. Therefore, low levels of MGMT would be expected to enhance response to alkylating agents. The expression level of MGMT is determined in large part by the methylation status of the gene's promoter. In low grade diffuse astrocytomas and secondary GBM, MGMT promoter methylation is tightly correlated with TP53 mutation and overexpression of the p53 protein^{(33), (37)}. A recent study found that MGMT promoter hypermethylation is significantly associated with *IDH1/IDH2* mutations in grade II–III gliomas, whereas it had a borderline association with 1p deletion in oligodendrogliomas⁽³⁸⁾.

IDH MUTATIONS AND 1p/19q CO-DELETION

The loss of chromosomal material on 1p and/or 19q resulting from an unbalanced translocation, named loss of heterozygosity (LOH) 1p/19q, most strongly associated with oligodendroglial brain tumours, was first recognized as a predictor of chemosensitivity and later on of sensitivity to radiotherapy, and as a prognostic factor as well. More recent interpretations have emphasized that the combination of *IDH* mutation and 1p/19q co-deletion is the molecular signature of LGG rather than an association⁽²¹⁾.

Recently, the Cancer Genome Atlas project (TCGA) have characterized LGG^{(13), (39)}. TCGA is a global genomic profiling project that utilized high-throughput microarray technologies to identify molecular subtype classifications of cancers, multigene clinical predictors, new targets for drug therapy, and predictive markers for these therapies. The project delineated three molecular classes of 293 lower-grade gliomas from adults that were more concordant with IDH, 1p/19q codeletion, and TP53 status than with histologic class⁽¹⁴⁾.

The results are so described:

- **LLG with an IDH mutation and no 1p/19q codeletion** (94%) harbored TP53 mutations, which suggests that this tumor class is defined by a loss of p53 function.

Inactivating alterations of ATRX were frequent (86%) and included mutations (79%), deletions (3%), gene fusion (2%), or a combination of these events (2%).

- **LLG with an IDH mutation and 1p/19q codeletion** presented CIC (capicua transcriptional repressor) mutations in 62%, FUBP1 (far upstream element (FUSE) binding protein 1) mutations in 29%, NOTCH1 mutations (31%) and TERT (telomerase reverse transcriptase) promoter mutations in 96%; ATRX mutations were rare in these tumors, a finding consistent with the mutual exclusivity of ATRX and TERT mutations.
- **LLG with wild-type IDH** had more mutations than did samples with an IDH mutation and 1p/19q codeletion or those with an IDH mutation and no 1p/19q codeletion and showed remarkable genomic and clinical similarity to primary (wildtype IDH) glioblastoma (Figures 1.2.1 and 1.2.2).

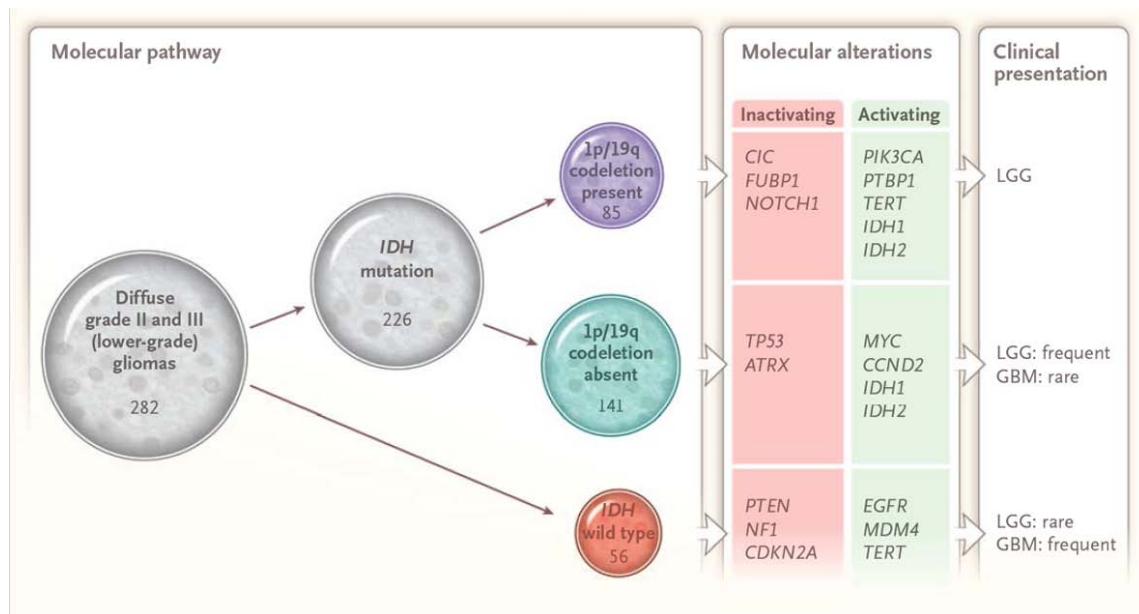


Figure 1.2.1. Summary of major findings. Schematic representation that summarizes the major molecular findings and distinct clinical presentations of grade II and grade III gliomas. GBM denotes glioblastoma, and LGG lower-grade glioma⁽¹⁴⁾.

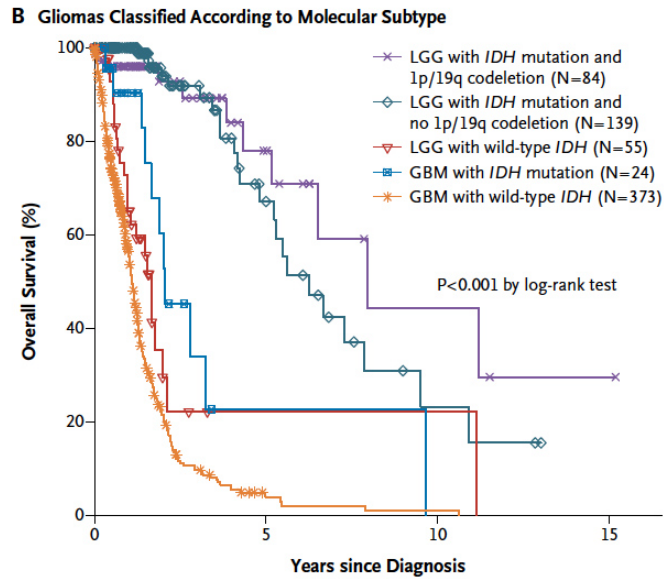


Figure 1.2.2. Clinical outcomes. Panel shows Kaplan–Meier estimates of overall survival among patients with LGGs that are classified according to *IDH* mutation and 1p/19q codeletion status. GBM samples classified according to *IDH* mutation status are also included⁽¹⁴⁾.

Similarly, another recent study defined five glioma molecular groups with the use of three alterations: mutations in the *TERT* promoter, mutations in *IDH*, and codeletion of chromosome arms 1p and 19q (1p/19q codeletion). The five groups are called: triple-positive, with *TERT* and *IDH1* mutations, with *TERT* mutations only, with *IDH* mutations only, triple-negative⁽¹⁵⁾.

The results are so described:

- **Triple-positive gliomas** are most strongly associated with the oligodendroglial histologic type and have better overall survival.
- **Gliomas with *TERT* and *IDH1* mutations** without an accompanying 1p/19q codeletion are relatively rare, accounting for 4% of all gliomas in the combined data set, and carried a lower risk for patient mortality.
- **Gliomas with only *TERT* mutations** are primarily grade IV gliomas; however, 9.6% in this study were grade II or III. Grade II or III gliomas in this group have an aggressive course and are associated with poor survival, which suggests the need for early adjuvant therapies and meticulous follow-up.
- **Gliomas with only *IDH* mutations** have the earliest mean age at onset (37 years) and an intermediate prognosis; they also account for half of all patients who have gliomas with an oligodendroglial component and two thirds of those who have grade II or III astrocytomas. These tumors almost always acquire mutations in *TP53* and *ATRX*. On the basis of their uniform mutational profile, gliomas with only *IDH* mutations become an important group for experimental modeling and novel therapeutic discovery.
- **Triple-negative gliomas** constitute 7% of grade II or III gliomas and 17% of grade IV gliomas. Although they typically develop in younger patients (approximately 10 years younger) than do gliomas with *TERT* mutations only, these two types of gliomas have a similar level of *MGMT* promoter methylation and similar associations with germline variants (Figure 1.2.3).

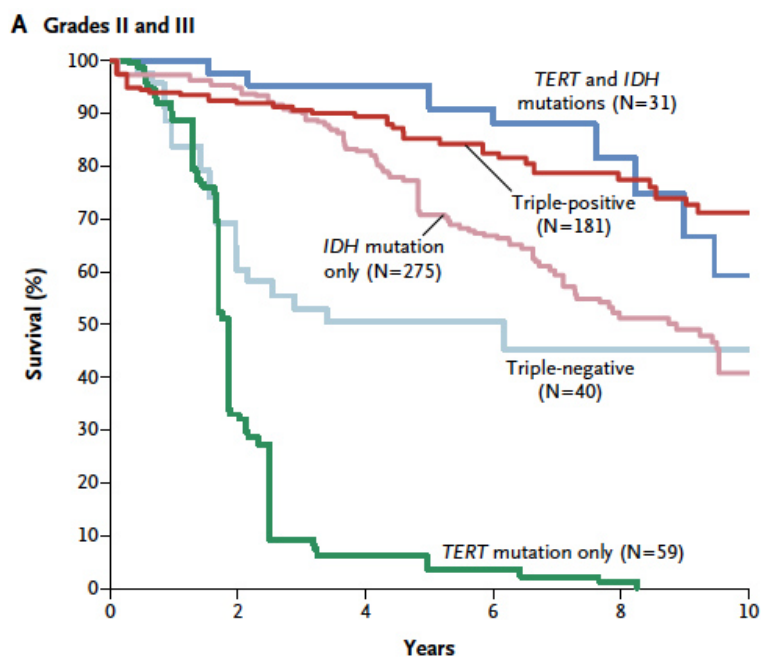


Figure 1.2.3. Overall survival of grade II and III gliomas. Adjusted Kaplan–Meier Estimates of Overall Survival in the five Glioma Molecular Groups⁽¹⁵⁾.

As seen above, beside association between IDH mutation and 1p/19q co-deletion, there is a molecular subset defined by IDH mutation, TP53 mutations and loss of ATRX, a gene that encodes a chromatin-remodeling regulator.

Studies based on morphologic class have consistently shown that the large majority of grade II and III diffuse astrocytomas and secondary glioblastomas have TP53 mutations^{(32), (33)}. When restricted to IDH-mutated infiltrating astrocytomas, an even higher percentage has TP53 mutations, since IDH wild-type diffuse gliomas have lower frequencies of TP53 mutation. In a study of 939 tumors of diverse histologies, 80% of IDH-mutated (IDH1 or IDH2) anaplastic astrocytomas and GBM also harbored TP53 mutations⁽³²⁾. Conversely, others have shown that 63% of grade II diffuse astrocytomas that contained a TP53 mutation also harbored an IDH1 mutation. More recently, The Cancer Genome Atlas project demonstrated that 94% of IDH mutant grade II and III diffuse gliomas that lacked 1p/19q co-deletion had TP53 mutations⁽³⁹⁾.

The combination of IDH and TP53 mutations is strongly coupled to inactivating alterations in ATRX. In one large analysis of 363 brain tumors, ATRX mutations were most frequent in grades II and III astrocytomas and oligoastrocytomas (67–73%) as well as secondary GBM (57%), but were uncommon in primary GBM, oligodendroglial tumors and pediatric GBM (4%, 14% and 20%, respectively)⁽³⁴⁾. Nearly all diffuse gliomas with an ATRX mutation had an IDH1 mutation as well. In tumors with IDH and ATRX mutations present, 94% had a TP53 mutation. ATRX mutations are associated with the Alternative Lengthening of Telomeres (ALT) phenotype⁽³⁴⁾, an alternative mechanism for maintaining telomere length in tumors that do not have constitutive telomerase activity. In establishing the diagnosis of an IDH mutant diffuse glioma, loss of immunohistochemical staining for ATRX in neoplastic cells is an excellent surrogate for ATRX gene inactivation and supports the diagnosis of an astrocytoma. The evidence to date indicates that the molecular signature of IDH mutant astrocytoma includes TP53 mutation and ATRX alteration and is associated with ALT^{(14), (35), (39)}.

With this emerging definition of disease, the optimal morphologic or molecular prognostic and predictive markers will need to be defined.

1.2.5 HIGH-GRADE GLIOMA (HGG)

High-grade gliomas are characterized by their invasiveness and lack of differentiation. This group of gliomas includes anaplastic astrocytoma, anaplastic oligodendroglioma, and anaplastic oligoastrocytoma, which are grade III, and glioblastoma (GBM), which is grade IV⁽³⁶⁾. GBM carries the worst prognosis, while pure oligodendroglioma has a protracted natural history and better outcome, and excellent response to therapy. Prognosis of mixed anaplastic oligoastrocytoma and anaplastic astrocytoma is intermediate between GBM and pure anaplastic oligodendroglioma⁽⁴⁰⁾.

The recent trend towards genomic profiling of gliomas has led to the exploration of classifying lesions into molecular groups based on multi-gene predictors. This classification may allow for the identification of new targets with the additional benefits of predictive markers for target therapies. The Cancer Genome Atlas (TCGA) database first sequenced GBM in 2008⁽³⁷⁾.

Genetic abnormalities involving gain and loss of heterozygosity (LOH) of chromosome 7 and 10 respectively with associated EGFR amplification and PTEN loss drive tumorigenesis in high-grade gliomas. Similarly, the presence of mutations involved in the receptor tyrosine kinase (RTK), p53, or RB pathways has similar associations with high-grade gliomas. Frequent mutations of cell cycle regulatory genes in glioma have underscored the importance of these genes in cellular proliferation and senescence. The RB and p53 pathways, which regulate the cell cycle primarily by governing the G1-to-S-phase transition, are major targets of inactivating mutations in GBM. The absence of these cell cycle guardians renders tumors particularly susceptible to inappropriate cell division driven by constitutively active mitogenic signaling effectors, such as phosphoinositide 3-kinase (PI3K) and mitogen-activated protein kinase (MAPK). Ultimately, patient specific data from high throughput screening will be utilized for diagnosis, prognostication, and patient-specific therapy based on the unique genetic signature of their neoplasm.

All GBM can be divided into two subtypes based on the presence or absence of a precursor lesion of a lower grade. Primary GBM is the most common type (>90%) and diagnosed as a de novo lesion without progression from a lower grade tumor in older patients (>60 years). Secondary GBMs result from progression of LGGs (WHO grade II/III) and are commonly found as a recurrence in younger patients ([Figure 1.2.4](#)). The time to GBM progression from a grade II in contrast to a grade III lesion is also longer (5 and 2 years respectively)^{(41), (42)}.

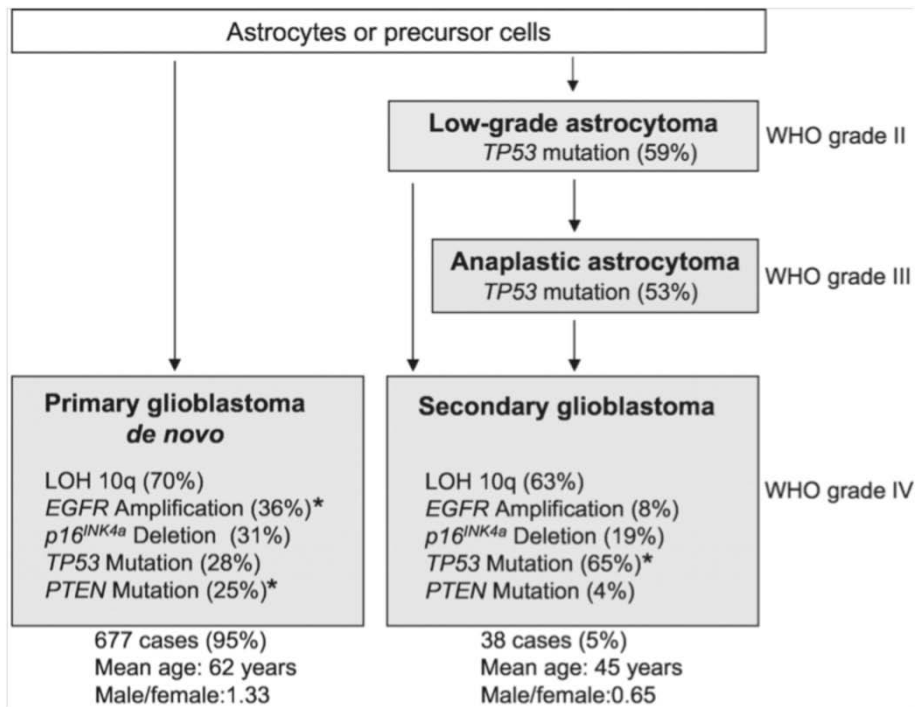


Figure 1.2.4. Molecular abnormalities in primary and secondary GBM⁽³²⁾.

Analysis of GBM genomics reveals multiple tumor suppressor and oncogenes that are inactive and active, respectively, during tumor progression and *de novo* formation⁽⁴³⁾. The three main pathways implicated in GBM formation are: RTK-RAS-MAPK PI3KA, the p53 pathway, and the RB pathway (Figure 1.2.5).

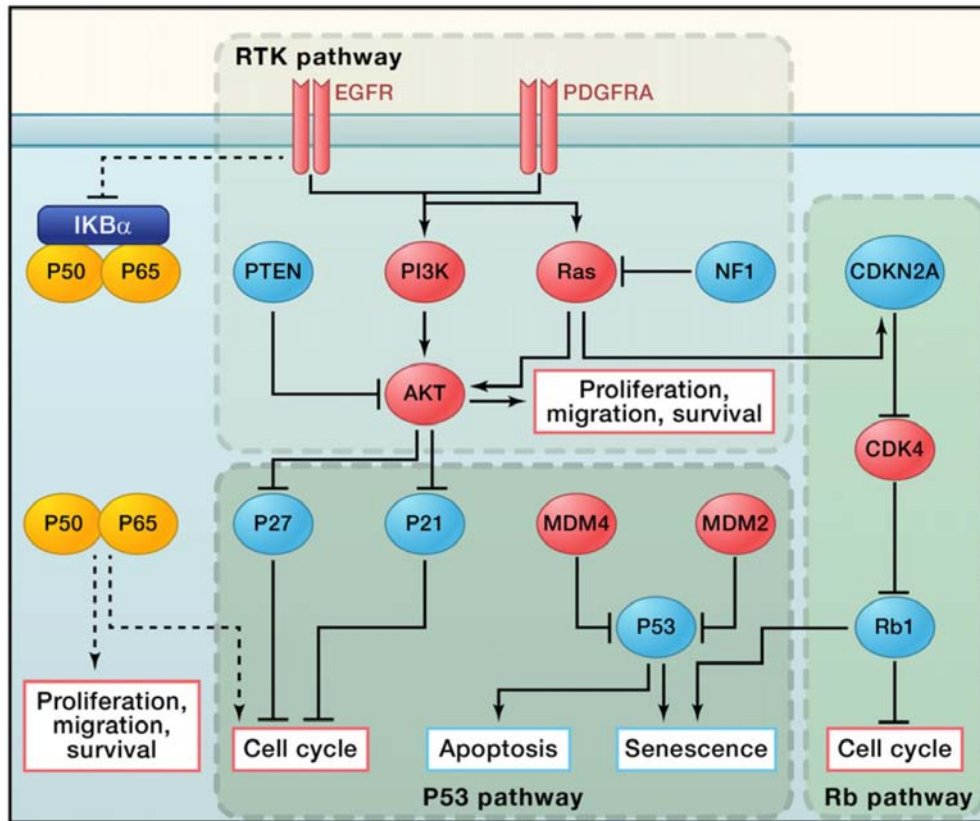


Figure 1.2.5. Core Signaling Pathways in Glioma Tumorigenesis. The receptor tyrosine kinase (RTK), p53, and Rb pathways are the core signaling pathways in glioma oncogenesis. Red indicates oncogenes that are either overexpressed or amplified in GBM samples, and blue indicates tumor suppressor genes that are somatically mutated or deleted (except for P27 and P21)⁽⁴³⁾.

The gain of copies of chromosome 7 along with losses of chromosome 10 contributes to the EGFR and PTEN mutations commonly identified in primary GBM. IDH mutations, TP53 mutations, and ATRX mutations are characteristic of secondary GBM. These mutations cluster specifically into gene expression profiles that are characteristic of recently described GBM subgroups.

In addition to the core signaling pathways identified through genome-wide screening studies, Harsh et al. recently reported that heterozygous deletion of the NF- κ B inhibitor α (NFKBIA) gene was present in GBM⁽⁴⁴⁾. The NFKBIA gene encodes the protein I κ B α , a crucial negative regulator in the canonical NF- κ B signaling pathway. Under basal conditions, I κ B α sequesters the NF- κ B transcription factor heterodimer (p50/p65) in the cytoplasm. Upon stimulation with ligand such as tumor necrosis factor α (TNF- α) or lipopolysaccharide (LPS), I κ B α is phosphorylated by the signalosome. This phosphorylation leads to rapid ubiquitination and degradation of I κ B α , which releases the inhibition of NF- κ B and allows translocation of p50/p65 into the nucleus to activate transcription of downstream target genes, including many cytokines that can promote tumor growth and infiltration⁽⁴⁵⁾.

In GBM, NFKBIA deletion and EGFR amplification are mutually exclusive, raising the possibility that the two genetic events converge on the same pathway. Indeed, overexpression of NFKBIA reduced the viability of primary glioma cells in which NFKBIA was downregulated or EGFR was upregulated⁽⁴⁴⁾. In addition, both genetic events were associated with similar

prognostic outcome, which is inferior to that of patients with normal expression levels of these two genes. However, the detailed molecular mechanism for the role of NF- κ B in glioma development and progression and its connection with EGFR signaling remain to be investigated. Researchers have examined DNA, mRNA, microRNA and epigenetic profiling to identify multiple glioma subtypes with different clinical outcomes⁽⁴⁶⁾. In the case of GBM, two major studies of the TCGA data identified three major subtypes. Two of the subgroups consistently replicate similar profiles in various studies and are in stark contrast to each other: proneural and mesenchymal. Proneural GBM is a secondary GBM that is present in young adults and has neuronal differentiation that is associated with better outcomes. Proneural GBM have IDH and TP53 mutations, a glioma-CpG island methylator phenotype, and a normal expression of EGFR/PTEN. This group represents close to 10% of all GBM, consistent with the known prevalence of secondary GBM. The mesenchymal GBM is common in older adults and is associated with a worse prognosis and characterized by neurofibromin 1 (NF1) loss or mutations (Neurofibromin acts as a tumor suppressor protein), abnormalities in Akt signaling, increased expression of angiogenic peptides, and overexpression of genes related to motility, the extracellular matrix, and cell adhesion. The final TCGA subtypes are the neural and the classical ones that are associated with PTEN loss and EGFR amplification and constitute the majority of GBM.

1.3 GLIOMA STEM CELLS (GSC) IN HGG AND LGG

The cancer stem cell theory postulates that tumors are sustained by a cell population with specific features, such as self-renewal ability and the capacity to give rise to a heterogeneous mass of tumor cells. Glioma stem cells (GSCs) were among the first cancer stem cell (CSC) that have been described in solid tumor^{(47), (48)}. It was reported that as few as 100 CD133+ GSCs, could give rise to tumors that recapitulated the parental tumors when implanted into immunodeficient mice, whereas as many as 1,000,000 CD133- GSC could not⁽⁴⁷⁾. This evidence indicated that only a selected cell population is responsible for sustaining and propagating tumors. Existence of GSC, then, could explain the gliomas resistance to existing therapies.

According to their name, GSC should be cells with stemcell-like properties present within all types of glioma. However, most studies describe GSC isolated from primary glioblastomas^{(47), (48), (49), (50), (51)}, and whereas a few describe stem-like cells obtained from low-grade gliomas (LGGs)⁽⁴⁷⁾, several others report that no stem-cell-like population could be established from LGGs or even secondary glioblastomas^{(52), (53)}. Several factors might underlie the difficulty in isolating LGG stem cells. One possible explanation is that the number of stem-like cells might be proportional to the degree of malignancy, with grade I gliomas having few stem cells and secondary glioblastomas in the incipient phase having fewer GSC than primary glioblastomas. Alternatively, the current isolation and culture techniques, namely neurosphere formation in growth-factor-supplemented medium, may enrich for glioblastoma stem cells but may not be permissive for LGG stem cells. LGG stem cells might thus require soluble factors other than basic fibroblast growth factor and epidermal growth factor for their maintenance, or their dependence on the *in vivo* niche might be greater than that of glioblastoma stem cells⁽⁵⁴⁾.

GSC are not necessarily the cells of origin for the initial tumor: GSC isolated from human specimens act as glioma-initiating cells (GIC) in experimental models, a fact that sometimes leads to reciprocal use of these terms. However, present knowledge suggests that whereas glioma cells of origin, GIC, and GSC might have overlapping characteristics, they are not identical entities. Despite continued efforts, there is yet no definite answer as to what type of cell constitutes the cell of origin for malignant gliomas. Theoretically, glioma cells of origin are cells that give rise to the initial tumor. They are the cells that undergo the initial transformation events and acquire just enough tumorigenic capacity to escape control mechanisms and proliferate. They might, but do not necessarily, include cells that will later sustain the tumor, the GSC⁽⁵⁴⁾. Given that GBM are already highly heterogeneous at the time of diagnosis, retrospective analysis of clinical specimens is poorly suited to the unequivocal identification of a cell of origin. Analysis of animal models is therefore useful to complement the available information regarding the initial phase of GBM. A recent study used a murine glioblastoma model based on genetically modified neural stem cells (NSCs). The tumor cells isolated from the allografts and sorted for GFP expression were propagated as tumorspheres. These cells were serially transplantable; they possessed self-renewal and differentiation potential and they truly represented the cell population that propagated the initial tumor. They could therefore be considered true GSC⁽⁵⁴⁾. Another characteristic of GSC, inferred from the properties of normal tissue stem cells and CSC of hematologic malignancies, is that they exist in and are protected by specific environments, the stem cell niches. Experimental data support this proposition and for GSC both perivascular and hypoxic niches have been described as such niches (see next paragraph). Whereas these observations require further validation, the niche represents an attractive target when considering future therapies.

According to cancer stem cell definition		
<i>Conceptual</i>		
Term	Glioma cell of origin	Glioma stem cell (GSC)
Definition	Cell that gives rise to the tumor = cell undergoing initial transformation event	Cell that sustains the tumor = cell with self-renewal ability and ability to give rise to heterogeneous offspring
Characteristics	Tumorigenic ability: ability to initiate primary tumor Preference for location in brain	Tumorigenic ability: ability to initiate recurrent tumor Preference for location in tumor: stem cell niche
<i>Experimental</i>		
Term	Glioma-initiating cell (GIC)	Glioma stem cell (GSC)
Requirement	(May be induced from normal cells in vitro)	Are or have been part of a tumor (in vivo or ex vivo)
Assessment	Capacity to form a tumor in a mouse model	Sphere formation ability Multilineage differentiation potential Capacity to recapitulate initial tumor pathology
<i>Clinical importance</i>		
Identification important in	Prevention Early diagnosis	Curative treatment Prevention of recurrence

Table 1.3 Similarities and differences between the terms GSCs, glioma cells of origin, and GICs⁽⁵⁴⁾.

Regarding LGG, evidences that murine oligodendroglioma arises from NG2-expressing cells in white matter regions, rather than NSC, has been recently given by Weiss's group, that linked the therapy-responsive nature of this tumor to a progenitor origin⁽⁵⁵⁾. Specifically, Authors demonstrated that NG2+ oligodendroglioma cells expressed genes and proteins associated with OPC rather than NSC, that NG2+ oligodendroglioma cells showed limited sphere-formation, consistent with a progenitor population, and that NG2+ oligodendroglioma cells were lineage

restricted, being able to differentiate only into oligodendroglial derivatives. Importantly, NG2-expressing cells, from both mouse and human oligodendroglioma, displayed high *in vivo* tumorigenicity and were sensitive to both alkylating and differentiating agents⁽⁵⁵⁾. Finally, they showed that these oligodendroglioma cells were neither chemoresistant nor quiescent and suggested that a progenitor origin for these cells could explain their chemosensitivity. Similarly, to analyze if OPC could serve as cell of origin for glioma, Lindberg et al. developed a new tv-a transgenic mouse line, Ctv-a, in which viral infection could be targeted to OPC expressing 2', 3'-cyclic nucleotide 3'-phosphodiesterase (CNP)⁽⁵⁶⁾. CNP is a highly specific marker that in the central nervous system is only expressed late in OPC development and in mature oligodendrocytes. With the Ctv-a mouse Authors could induce low-grade oligodendroglioma with RCAS-PDGF-B showing that the cell of origin for oligodendroglioma may be a committed glial progenitor cell⁽⁵⁶⁾.

In conclusion, several experimental evidences point to the fact that the cell of origin of low-grade gliomas has not been unequivocally identified. Nevertheless, establishing the cellular origin can be essential to give a more accurate representation of the biological properties of a particular glioma and thereby a better prediction of response to different therapeutic strategies⁽⁵⁷⁾.

1.4 CANCER STEM CELL NICHE

Niches are specialized microenvironments that regulate adult stem cell fate by providing cues in the form of both cell-cell contacts and secreted factors. Normal niches are comprised of fibroblastic cells, immune cells, endothelial and perivascular cells or their progenitors, extracellular matrix (ECM) components, and networks of cytokines and growth factors⁽⁵⁸⁾. The CSC niche itself is a part of the tumor microenvironment (TME), which is a collective term for the adjacent stroma along with the normal counterparts of the tumorigenic cells. Non-CSC tumor cells are also part the CSC niche. During the progression of tumors to a more malignant state, cells within the CSC niche produce factors that stimulate CSC self-renewal, induce angiogenesis, and recruit immune and other stromal cells that secrete additional factors to promote tumor cell invasion and metastasis.

In brain tumors the small population of tumor cells within the heterogeneous tumor mass with stem-like character is called brain tumor stem cell (BTSC). It is assumed that BTSC arise from stem/progenitor cells that have acquired various genetic and epigenetic alterations, enabling them to undergo neoplastic transformation and escape from vascular niche control. Alternatively, uncontrolled proliferation and transformation of BTSC may occur by deregulation of external signaling factors within the vascular niche^{(59), (60)}([figure 1.4](#)).

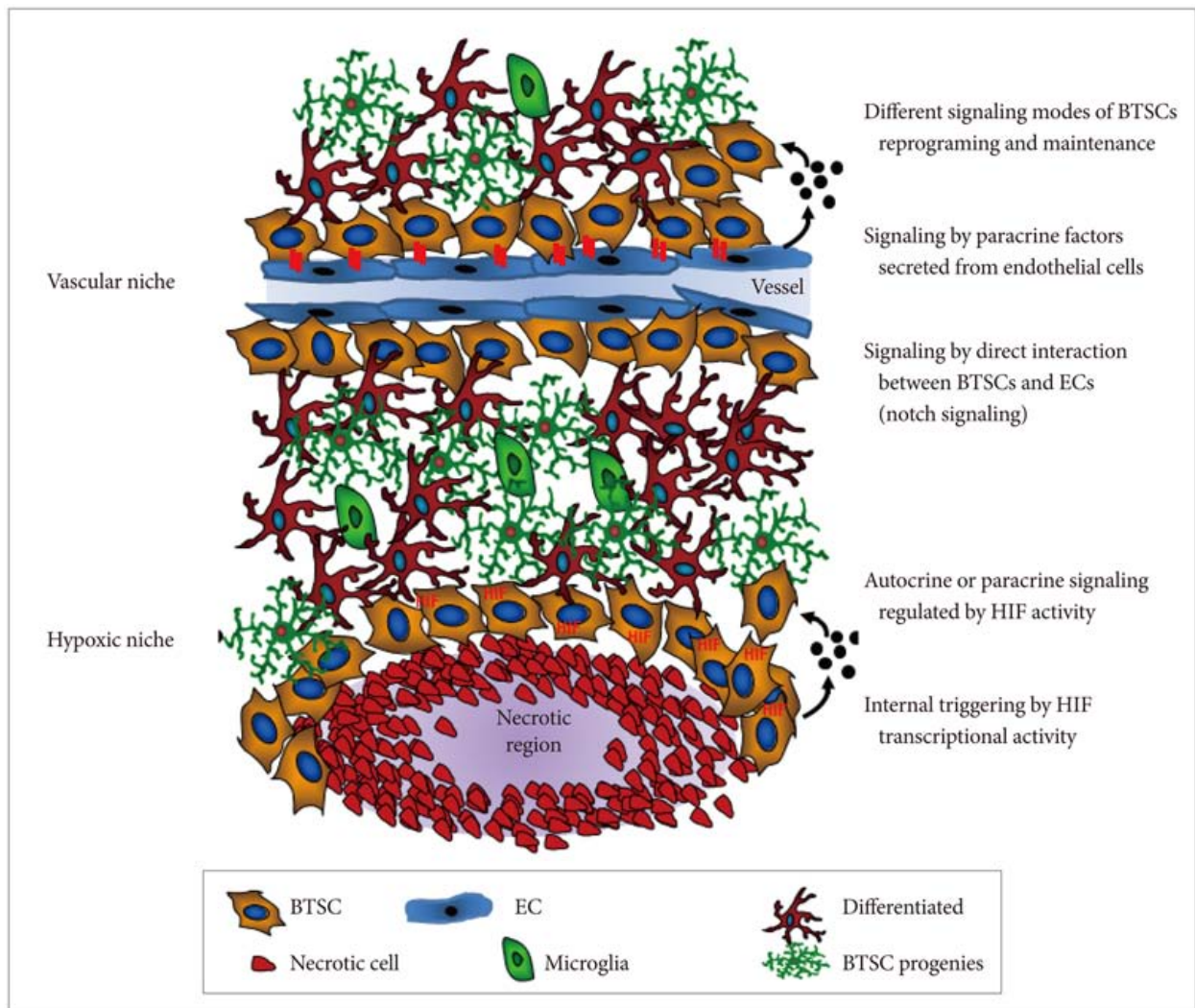


Figure 1.4. Two microenvironments of brain tumor stem cells: vascular and hypoxic niches regulated by various signaling modes. BTSC: brain tumor stem cell, HIF: hypoxia-inducible factor, EC: endothelial cell⁽⁶¹⁾.

In the primary tumor, hypoxia develops within the tumor mass due to impaired vascularization, and reactive oxygen species (ROS) are increased^{(62), (63)}. Both hypoxia and ROS up-regulate the CSC stress signaling pathways to enhance cancer cell survival and maintain cancer cell stemness⁽⁶⁴⁾. Hypoxia further promotes CSC survival and epithelial-to-mesenchymal transition (EMT) through ROS-activated stress response pathways and through ROS-induced TGF- β and TNF- α signaling pathways. Activation of TGF- β as well as WNT signaling pathways by hypoxia induces stemness by promoting an undifferentiated state in tumor cells. In various solid cancers, endothelial cells (EC) promote self-renewal of CSC by direct cell-cell contact or by nitric oxide (NO) production via the NOTCH signaling pathway. Hypoxia-inducible factor 1 alpha (HIF-1 α) also can directly increase NOTCH signaling. HIF-1 α antagonizes Myelocytomatosis viral oncogene homolog (c-Myc) activation, thus slowing down cell-cycle progression to protect CSCs from DNA damage and enhance stemness⁽⁶⁵⁾. Hypoxia induces CSC to express hypoxia-inducible factors (HIF), which are regulated and stabilized by TGF- β ⁽⁶⁶⁾. The HIF genes are the primary factors for driving angiogenesis via induction of Vascular Endothelial Growth Factor (VEGF). Under hypoxia, both ECs and CSCs produce VEGF to stimulate tumor angiogenesis. In the hypoxic regions of the tumor, VEGF-A can recruit monocytes and macrophages⁽⁶⁷⁾. Ultimately, blood vessels and their EC and hypoxia and its factors are the principal actors for the CSC survival in the niche and therefore for the tumor growth.

A characteristic feature of high-grade character in gliomas is the presence of microvascular proliferating structures. These angiogenic entities represent regions of hyper-proliferative tumor stromal and endothelial cells. The brain tumor perivascular niche (PVN)⁽⁶⁸⁾, defined as the area that borders angiogenic/tumor microvascular structures, is a prime location for GSC. Recent data suggest that establishment of the brain tumor PVN facilitates expansion and differentiation of GSC. Indeed, the density of these PVN regions appeared to correlate with the number of GSC across several brain tumor subtypes including oligodendrogliomas and glioblastomas.

A similar study identified PVN regions in medulloblastomas as prime locations for GSC that express both nestin and notch. These nestin-expressing GSC with respect to the tumor bulk, preferentially survived radiotherapy thus allowing repopulation and regeneration of the tumor after therapy. Several reports identify a variety of mechanisms that mediate these radioresistant effects. These studies highlight the growing recognition of the PVN as a critical participant in GSC regulation⁽⁶⁹⁾.

The major cell types known to reside in the brain tumor PVN⁽⁶⁹⁾, are pericytes, immune cells including lymphocytes, macrophages and microglia, astrocytes, fibroblasts and endothelial cells that line the vasculature. Each of these individual cell types makes distinct contributions to tumor progression by either contributing to the formation and stability of the microenvironment that supports the GSC population or by promoting conditions within the niche that facilitates tumor progression. In summary, the perivascular niche is a complex environment. It is composed of multiple cell types, some neoplastic cells derived from the tumor itself and other non-neoplastic cells derived from the stroma. The interplay between these cell types regulates differentiation and tumor progression.

1.5 TUMOR MICROENVIRONMENT (TME)

As explained above, the term tumor microenvironment (TME) is a collective term that includes the tumor's surrounding and supportive stroma, different cells of non-tumor origin (e.g. effectors of the immune system, fibroblast, EC) and soluble factors, including tumor- and stroma-derived extracellular vesicles⁽⁷⁰⁾. In normal epithelial tissues, homeostasis is maintained by a correct interpretation of the growth factor signaling present in the extracellular matrix (ECM) context. This control can be lost through impairment of the communication mechanisms between the epithelium and the surrounding stroma⁽⁷¹⁾([Figure 1.5](#)). For example, an epithelial cell might incorrectly initiate a signal into the stroma resulting in the stromal production of a growth factor that, in turn, can stimulate the incorrect proliferation of neighboring epithelial cells. Alternatively, an aberrant matrix component produced by stromal cells in response to a local stress might be perceived by neighboring cells as a signal to grow or to enter a new developmental pathway. Under normal homeostasis, these mistakes are corrected by cell cycle arrest or apoptotic cell death. Occasionally, if the abnormal signal persists, the behavior can become increasingly unbalanced, creating a growing, interdependent, heterogeneous tissue, defined as a tumor by its ability to grow and by its unresponsiveness to normal physiological controls.

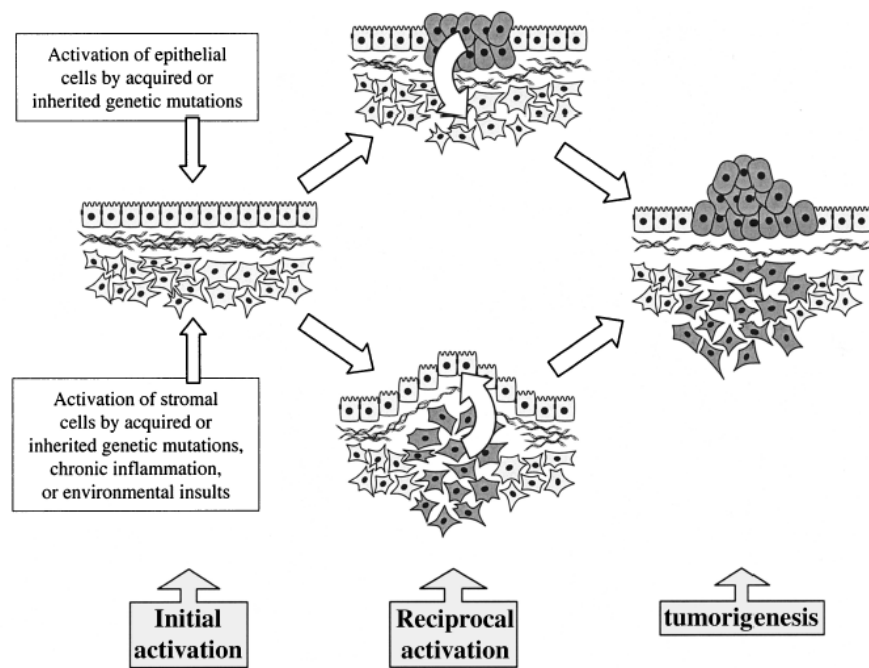


Figure 1.5. Tumorigenesis mechanisms. Tumor production can be the product of epithelial mutations that create an expanding, reactive tumor. However, it is also possible for mutations or environmental factors that create a reactive stroma in turn inducing an unstable epithelium thus favoring tumorigenesis through the establishment of epithelial mutations⁽⁷¹⁾.

As mentioned, TME is composed of both non-cellular (proteins, proteases, cytokines, etc.) and cellular components such fibroblasts, endothelial, immune cells and cancer associated fibroblasts (CAF)⁽⁷²⁾.

The role of CAF in tumour progression is multifaceted as they can either inhibit or promote malignant growth. CAF retain a major role in ECM remodelling since they are mainly responsible for the production of ECM proteins (i.e. collagens, fibronectin) as well as proteases and other enzymes involved in the posttranscriptional modification of ECM proteins themselves⁽⁷²⁾. In solid tumors, an increased matrix deposition and a concurrent, progressive stiffening of ECM are commonly observed. Two interactive pathways are established in the cross talk linking cancer and stromal cells (**Figure 1.5.1**):

- the **effluent pathway**, where cancer cells prompt a reactive response in the stroma;
- the **afferent pathway**, where the activated stromal cells influence cancer cell malignancy.

In the **effluent pathway**, tumour growth factor-1 (TGF- β 1) is one of the major pro-fibrotic tumour cell derived factors affecting CAF activation. Nevertheless, PDGF- α/β , basic fibroblast growth factor (bFGF) or interleukin (IL)-6 can also be secreted by cancer cells to activate CAF. The activation is a redox-regulated process. TGF- β 1 leads to the generation of ROS in CAF, which are responsible for messengers for their achievement of miofibroblasts phenotype and for the downregulation of gap junctions, promoting tumor activity⁽⁷³⁾. This transdifferentiation of CAF is commonly identified as mesenchymal–mesenchymal transition (MMT)⁽⁷⁴⁾.

In the **afferent pathway** CAF produce a series of growth factors and cytokines, such Hepatocyte Growth Factor (HGF), Epidermal Growth Factor (EGF), bFGF and IL-6, MMP and SDF-1 that

sustain tumor progression. In particular, HGF gives rise to an increased resistance of tumor cells to conventional tyrosine kinase inhibitors against EGF receptor⁽⁷⁵⁾.

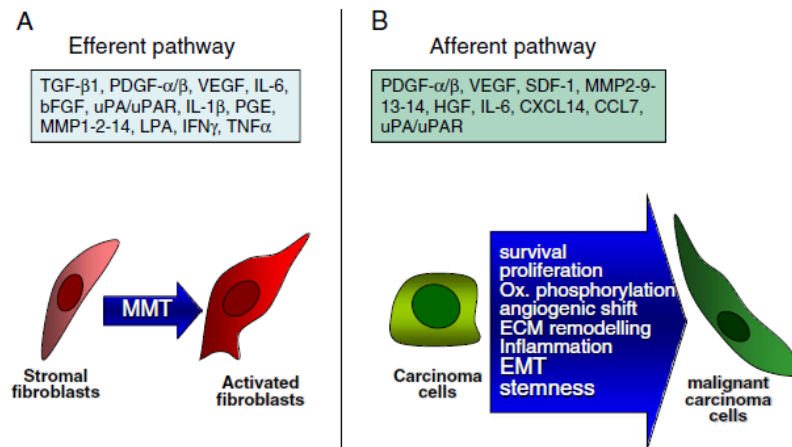


Figure 1.5.1. Interplay between CAFs and tumour cells: efferent and afferent pathways⁽⁷²⁾.

The continuously evolving and dynamic interplay between the tumor and its environment is finally responsible for the tumor progression since it progressively allow tumor cells to acquire new properties (evasion of natural anticancer mechanisms, infiltration, chemo-resistance)^{(70) (76)} that are hallmark of cancer.

1.6 GLIOMA MICROENVIRONMENT

1.6.1 TUMOR MICROENVIRONMENT CELLS

The microenvironment of glioma is composed of several stromal cell types, which are believed to make distinct contributions to tumor progression and invasion. These cells include but are not limited to astrocytes, macrophages, pericytes, fibroblasts and endothelial cells⁽⁶⁹⁾(**Figure 1.6.1**).

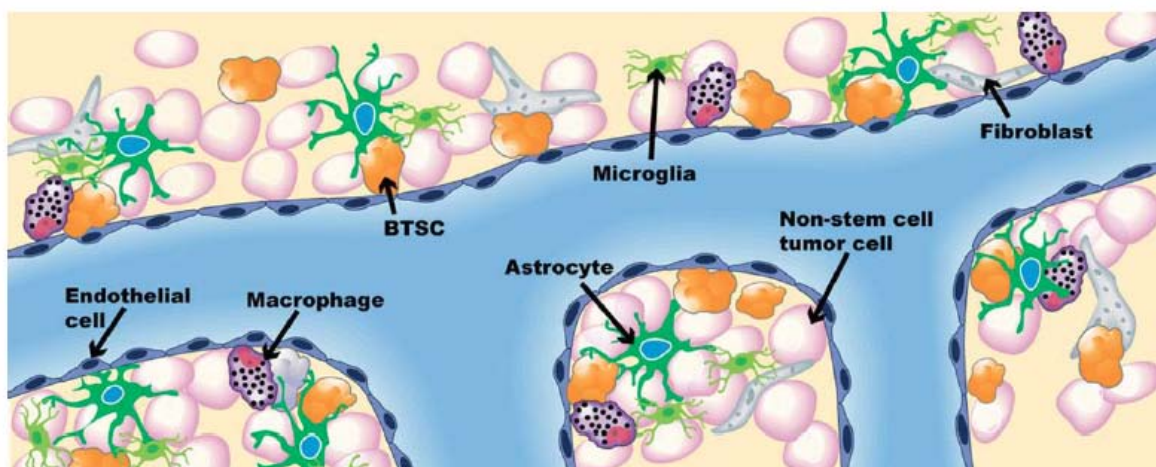


Figure 1.6.1. Microenvironment of gliomas⁽⁶⁹⁾(BTSC=brain tumor stem cells).

Pericytes are reportedly derived from mesenchymal stem cells or neural crest cells. They surround, stabilize and maintain the integrity of the walls of newly developed vasculature. In the

brain, pericytes have also been reported to be involved in immunological functions. They tend to be largely localized to microvessels where they are tightly associated with endothelial cells, separated only by a shared basement membrane. In addition, a codependent relationship appears to exist between pericytes and endothelial cells where they can each influence the mitotic activities of one another. Pericytes express various markers some of which include, nerve/glia antigen 2 proteoglycan (NG2), α -smooth muscle actin (α -SMA), desmin and platelet-derived growth factor receptor β (PDGFR β). However, none of these markers are absolutely specific for pericytes and their expression varies within specific tissues and developmental stages. Previous studies suggested a role for pericytes in microvascular proliferation in tumors. Pericyte recruitment has been identified to contribute to tumor vessel stabilization and survival of the vascular niche in pancreatic, melanoma and brain tumors. In addition, in gliomas and other malignant human brain tumors, perivascular localized pericytes are believed to play a critical role in shaping the angio-architecture of the tumor vascular niche⁽⁶⁹⁾.

Fibroblasts have been shown to play an important role in tumor progression in other cancers. Fibroblasts localized to the brain tumor microenvironment have been identified to promote the invasion of brain tumor cells. The expression of matrix metalloproteinases is critical for breakdown of the ECM for tumor invasion. Fibroblasts were shown to produce and mediate activation of proMMP-2, a metalloproteinase associated with increased invasiveness and malignant progression of gliomas⁽⁶⁹⁾.

Astrocytes, in the normal brain, function as support cells as well as *bonafide* stem cells that express GFAP. In the context of the brain tumor microenvironment, astrocytes have been implicated in the progression of brain tumors. Reactive astrocytes are frequently associated with glioma cells in the central nervous system. Tumor-associated astrocytes have been demonstrated to mediate glioblastoma cell invasion via activation of proMMP2, a metalloproteinase that plays a critical role in glioma invasion⁽⁶⁸⁾.

Perivascular astrocytes are closely associated with the endothelium. This close association is tied to its critical function in the induction and maintenance of the blood brain barrier (BBB). Crosstalk between perivascular astrocytes and endothelial cells can upregulate the expression of tight junction proteins, GLUT1 and Pgp transporters and BBB-associated enzyme activities of endothelial cells. These interactions ultimately enhance the stability of the vascular niche to support NSC. Some studies suggest that endothelial cells may mediate growth and differentiation of perivascular astrocytes⁽⁶⁹⁾.

Resident macrophages of the brain are termed microglia^{(77), (78)}. These cells invade the brain early in development and differentiate into the so-called resident, ramified microglia. Historically, the presence of these immune cells in gliomas was postulated as a host defense mechanism to suppress dividing neoplastic cells: however, recent studies have identified glioma cells to play a direct role in recruitment of immune cells into tumors to support tumor growth. Macrophage recruitment to brain tumors is suggested to be a primary source of cytokines and other mediators that promote glioma proliferation and migration.

A recent study, conducted by our research group, demonstrates that TME, both in LGG and in HGG, contains a population of nontumorigenic stem cells able to increase *in vitro* the GSC aggressiveness⁽⁷⁹⁾. These cells, named GASC (Glioma-Associated Stem Cells), present mesenchymal features and display aberrant growth properties *in vitro*. Nevertheless, they differ from GSC, since they are devoid of the genetic alterations characterizing the glioma of origin,

and are not able to originate a tumor when injected *in vivo*. Their aberrant growth reminds the distinguishing features of TAF which are characterized by the ability to modify the biological properties of tumor cell through the release of exosomes (Figure 1.6.2). These latter are membrane vesicles that originate in multivesicular bodies and are released in the extracellular space and in the body fluids from many cell types and, through their content in biologically active molecules (e.g., proteins, mRNAs, and miRNAs), they act as a potent intercellular communication system⁽⁷⁹⁾.

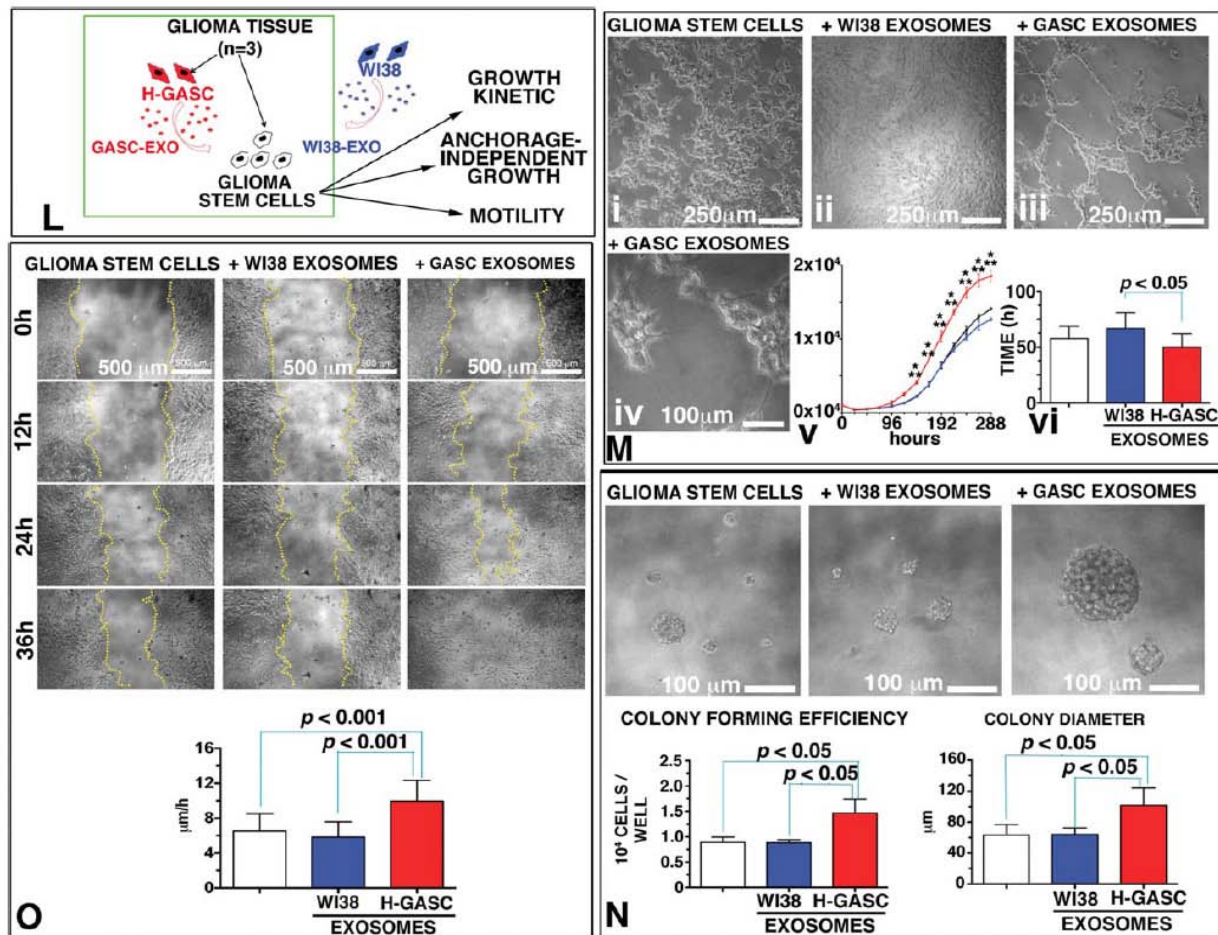


Figure 1.6.2. GSC, GASC and exosomes. GASC exert their tumor-supporting function through the release of exosomes.

Importantly, the *in vitro* features of GASC were the strongest predictor of LGG patients' overall survival and malignant progression free survival outperforming the state-of-the-art prognostic factors, including chromosome 1p-19q co-deletion, MGMT-promoter methylation and IDH1-IDH2 gene mutation⁸, thus supporting the notion that this patient-based approach could provide a groundbreaking method to exploit novel strategies aimed at targeting the tumor stroma⁽⁷⁹⁾.

1.6.1 SOLUBLE FACTORS INVOLVED IN GLIOMA PROGRESSION

As seen above, TME is composed of a variable combination of tumor cells, immune cells, inflammatory cells, endothelial cells and ECM. A variety of cytokines and other substances such as chemokines and growth factors are produced by different cells in the local tumor environment, resulting in complex cell-cell interaction and regulation of the differentiation, activation, functioning and survival of multiple cell types⁽⁸⁰⁾. The interaction between cytokines and their receptor results in the formation of a comprehensive network at the tumor site that is primarily responsible for the overall progression of tumors, the spread of antitumor immune responses and the induction of tumor rejection⁽⁸⁰⁾.

Cytokines are a heterogeneous group of soluble small polypeptide or glycoproteins that exert pleiotropic and redundant effects that promote the growth, differentiation and activation of normal cells. Immune cells are the major source of cytokines, but many human cells are also capable of producing them and their production acts as a means of communication between both cells and tissue⁽⁸¹⁾. Cytokines may be classified into the following categories: interleukin (IL) (1-15), growth factors, colony-stimulating factors, interferons (IFN) (α , β and γ), tumor necrosis factor (TNF) and chemokines. These cytokines can have either pro or anti-inflammatory activity and immunosuppressive activity, depending on the microenvironments⁽⁸¹⁾.

Glioma-associated microglia and macrophages (GAM) and myeloid-derived suppressor cells (MDSC) condition the glioma microenvironment to generate an immunosuppressed niche for tumour expansion⁽⁸²⁾. Glioma cells recruit GAM and MDSC to the tumour site and block their maturation. Glioma cell-derived factors subsequently skew these cells towards an immunosuppressive, tumour-promoting phenotype. Finally, GAM and MDSC enhance immune suppression in the glioma microenvironment and promote tumor growth, invasiveness, and neovascularization⁽⁸²⁾. The local and distant cross-talk between glioma cells and GAM and MDSC is regulated by a plethora of soluble proteins and cell surface-bound factors.

The population of GAM that is found in glioma is believed to predominantly contribute to the induction of an immunosuppressive glioma microenvironment⁽⁸²⁾([Figure 1.6.3](#)). They directly and indirectly interact with glioma cells in various ways:

1. GAM are recruited to the tumor via different glioma-derived factors that subsequently contribute to a switch from a tumor-suppressive M1 to a tumor-promoting M2 phenotype. This recruitment is mediated through various glioma-derived factors including chemokines, cytokines and matrix proteins. CSF-1 (M-CSF), TNF, VEGF, and GM-CSF have previously been reported to guide the recruitment and migration of GAMs into the glioma environment. Moreover, it has been suggested that such glioma stem-like cells recruit circulating monocytes via CSF-1 and the chemokine CCL2, and that this process is more effective than recruitment by regular glioma cells. Activated M1 GAM are stimulated by LPS and IFN γ and are able to effectively promote an anti-tumor immune response. M1 GAM produce pro-inflammatory mediators, phagocytose tumor cells, present tumor antigens to immune cells, and stimulate them to trigger an antigen-specific T cell response. Glioma cells actively secrete factors including IL-4, IL-6, IL-10, MIF,

TGF- β ¹, and PGE-2 that skew the phenotype of GAMs to a M2 phenotype. Acquisition of the M2 phenotype is accompanied by an incompetence to induce an anti-tumor T-cell response and by immunosuppressive features.

2. M2 GAM mediate immune suppression in the glioma microenvironment through secretion of immunosuppressive factors including IL-6, IL-10, and TGF- β 1 and interaction with other immune cells. IL-10 release has been found to be regulated by STAT3, and mediates a range of immunosuppressive mechanisms. These include amongst others the inhibition of an anti-tumor response by the down-regulation of HLA-DR expression on monocytes, and their decreased production of inflammatory cytokines. GAM in turn promote immune suppression via the induction of T-cell anergy and apoptosis, expansion of Treg cells, inhibition of T-cell activation and proliferation and decreasing the activity of Lymphokine Activated Killer (LAK) cells, Natural Killer (NK) cells and Cytotoxic T lymphocyte (CTL)⁽⁸³⁾.
3. M2 GAMs produce factors that stimulate glioma growth, neovascularization, and invasiveness. An important example is represented by the glioma-induced production of matrix metalloproteases (MMP), especially MMP-2 and MMP-9. MMP-2 is produced by both glioma cells and microglia, and is believed to promote matrix remodeling and to manipulate glioma cells in various other ways, by affecting glioma cell metabolism, receptor turnover and apoptosis resistance. MMP-9, the second key MMP in glioma progression, is also secreted by microglia and glioma cells. The expression of MMP-9 can be triggered by multiple factors derived from GAM.

Multiple lines of evidence suggest that immunosuppressive cytokines expressed by GAM might also play an important role in the promotion of glioma proliferation and motility. IL-6, IL-10, and TGF- β have all been reported as potent inducers of glioma invasiveness. Beside its effects on immune suppression, TGF- β 1 has been demonstrated to enhance MMP-9 expression in glioma stem-like cells and consequently promote their invasiveness. Moreover, TGF β 1 can induce up-regulation of VEGF in glioma cells and thus potentially contribute to glioma angiogenesis. In addition, GAM stimulate glioma proliferation and angiogenesis by various other mechanisms including the production of EGF and, again, VEGF.

¹ Transforming growth factor β (TGF- β) is a family of pleiotropic cytokines consisting of three members, TGF- β 1, TGF- β 2, and TGF- β 3. It activates a serine/threonine-kinase receptor. TGF- β proteins as well as their functional receptors are expressed in glioblastoma and anaplastic astrocytoma but are just detectable in low-grade gliomas and normal brain.

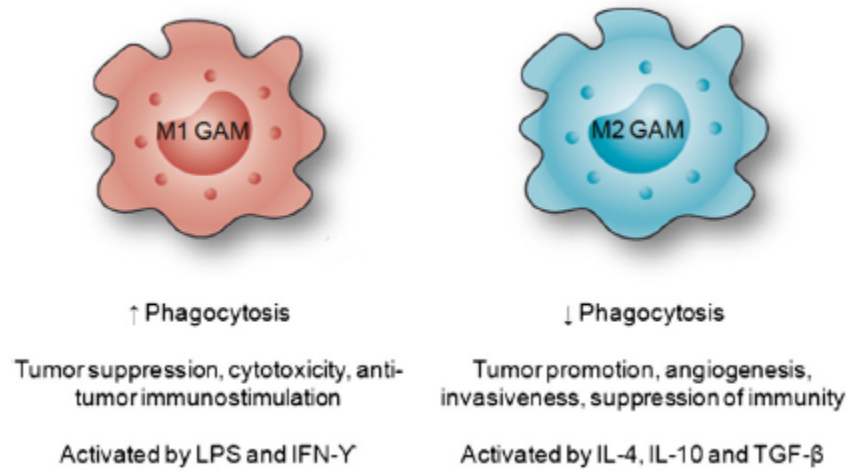


Figure 1.6.3. M1 and M2 GAMs. Schematic representation of the two different GAM subtypes with opposing immunological functions⁽⁸²⁾.

Myeloid Derived Suppressor Cells (MDSC) are known to exert remarkable immunosuppressive activities in cancer⁽⁸²⁾. MDSC mediate immune suppression by depleting essential nutrients for lymphocytes, hampering their trafficking and viability, producing reactive nitrogen species and ROS, as well as activating and inducing expansion of Treg cells. IL-6, M-CSF, COX-2/PGE-2 (Cyclooxygenase 2 / prostaglandin E2), IL-1 β , TNF- α , and VEGF were previously shown to stimulate the differentiation of normal human peripheral blood mononuclear cells into MDSCs *in vitro*. As gliomas are known to over-express these factors, it is likely that they also induce the generation of MDSC *in vivo*.

In the TME glioma cells have been found to express multiple factors such as IL-1 β , IL-6 and IL-8^{(83), (84)}. IL-1 β may directly stimulate glioma cell proliferation and induce the secretion of other cytokines like IL-6 and IL-8 by an autocrine loop⁽⁸⁵⁾. IL-1 β , IL-6 and IL-8 share the capacity to induce the expression and secretion of MMP-2, MMP-9 in normal and tumor cells. Thus, these factors may contribute to invasion of glioma cells through the induction of matrix degrading proteinases^{(86), (87), (88)}. Besides, IL-1 β can enhance gene expression of TGF- β 2. Increased transcription of TGF- β 2 can lead to suppression of anti-glioma responses by inhibiting the proliferation of lymphocytes, reducing immune cell activation, blocking antitumor activity, and inhibiting antigen presentation⁽⁷⁾.

The expression of these cytokines is up-regulated by Nuclear Factor- κ B (NF κ B), an inducible transcription factor that plays a key role in regulating the expression of numerous immune and inflammatory response genes. NF κ B family consists of five members and the predominant form of NF κ B is a dimer composed of p65 and p50 proteins. It is normally expressed in an inactive state in the cytoplasm where it is bound by its inhibitor protein family I κ B. NF κ B activation involves I κ B phosphorylation and proteasome-mediated degradation leading to NF κ B release. Once released, NF κ B translocates to the nucleus where it becomes phosphorylated, binds to DNA and induces the expression of genes involved in inflammation such as IL-8 and IL-6, as well as anti-apoptotic genes including cIAP2, Bcl-2 and Bcl-xL⁽⁸⁹⁾. Several studies have demonstrated that the activity of NF κ B is elevated in many cancers, including GBM^{(89), (90)}. A work conducted in 2004 evaluated immunohistochemical changes of this transcription factor in human brain glioma and human brain metastatic carcinoma (HBMC) and the role of NF κ B in the

biological behavior of the tumors⁽⁹⁰⁾. Normal brain tissues had only trace expression of NFκB, whereas all tumor tissues examined expressed it. The level of NFκB in HGG, HBMC and recurrent glioma tissues was considerably higher than that in LGG tissues. Briefly, NFκB expression is associated with the malignant progression, invasion and angiogenesis of HBG and HBMC, and it may play a crucial role in the recurrence of glioma.

2. AIM OF THE STUDY

Gliomas are primary central nervous system tumors that arise most frequently in the cerebral hemispheres of adults⁽⁸⁾.

These tumors are graded on a WHO consensus-derived scale of I to IV according to their degree of malignancy as judged by various histological features accompanied by genetic alterations⁽⁹¹⁾. WHO grade I and grade II gliomas are summarized as low grade glioma (LGG) and WHO grade III and grade IV are summarized as high grade glioma (HGG). While HGG are characterized by a poor prognosis (e.g. grade IV gliomas have a median survival of 12-15 months), LGG are usually well differentiated, slow growing and have a better prognosis⁽⁹⁾⁽¹¹⁾.

However, although grade I LGG are characterized by an excellent prognosis, grade II LGG grow slowly but ineluctably evolve to anaplasia in turn leading to neurological disability and ultimately to death, within 5-10 years⁽²⁷⁾. Additionally, in grade II LGG, the natural course of the disease varies considerably and histological analyses, even when combined with newly identified molecular markers, partially fail in predicting the clinical evolution of the lesions⁽²⁹⁾. Therefore, the management of patients with grade 2 LGG is a challenge, because: 1. There are not definitive criteria to classify a lesion as at high risk or low risk to relapse and/or progression and 2. Current possible adjuvant therapies can produce or contribute to chronic neuro-cognitive function impairment, particularly radiotherapy. Therefore, to profoundly impact the outcome of glioma patients, new drugs and better prognostic/predictive factors are strongly required⁽⁹²⁾. In this regard, great interest is now focused on the tumor microenvironment (TME) considered to be crucial for tumor progression and metastasis⁽⁹³⁾.

In collaboration with the Neurosurgery Department of the Azienda Ospedaliero-Universitaria of Udine, we have recently isolated from both HGG and LGG a population of stem cells devoid of tumorigenic features but characterized by tumor-supporting activities, being able, through the release of exosomes, to increase the biological aggressiveness of glioma-initiating cells. Importantly, the *in vitro* features of these cells, named GASC (Glioma-Associated Stem Cells), were the strongest predictor of LGG patients' overall survival and malignant progression free survival outperforming the state-of-the-art prognostic factors, including chromosome 1p-19q co-deletion, MGMT-promoter methylation *status* and IDH1-IDH2 gene mutation⁸. This supports the notion that GASC could represent a patient-based approach and could provide a groundbreaking method to identify novel prognostic/predictive markers and to exploit innovative therapeutic strategies aimed at targeting the tumor stroma.

However, cellular culture approaches are not frequently used in pathology department whereas ancillary studies such immunohistochemistry and molecular biology remain the gold standard for the diagnosis of glioma. Since immunohistochemistry is less expensive and widely available, it is often used in favor of other methods. For this reason this thesis aims at analyzing the gene expression profile of GASCs derived from LGG to identify putative novel prognostic factors that have been finally validated in a case study including 175 formalin-fixed paraffin-embedded LGG. Specifically:

1. GASC from LGG characterized by two different prognosis were cultured and analyzed: GASC from LGG without clinical evidence of anaplastic progression at 7 year from

diagnosis (LGG-good) and GASC from LGG characterized by anaplastic transformation within 4 years (LGG-bad)

2. Taking advantage of next generation sequencing and bioinformatics techniques, the gene expression profile of GASCs isolated from LGG-good and LGG-bad were compared and molecules (“upstream regulators”) considered to be responsible for the differences in the gene signatures of the two groups, the so called “upstream regulators”, were identified;
3. The expression of putative novel markers obtained by analyzing GASC, was assessed by immunohistochemistry, in LGG and HGG;
4. The prognostic value of the novel biomarkers was finally evaluated in a case study including 175 LGG well characterized from a clinical and pathological point of view and with an updated follow-up.

3. METHODS AND MATERIALS

3.1 SAMPLE STUDY

Human glioma samples were collected by the Department of Neurosurgery of the Azienda Ospedaliero-Universitaria of Udine directed by Dr. Miran Skrap. Informed consents were obtained from patients and all clinical investigations were conducted according to the principles expressed in the Declaration of Helsinki. The independent ethic committee of the Azienda Ospedaliero-Universitaria of Udine and the regional ethic committee approved the research (Consent 102 / 2011 / Sper and Consent 196 / 2014 / Em).

After glioma resection, tumor fragments (with a weight ranging from 20mg and 2g) were sent to the Department of Pathology of Udine.

Samples were divided in three parts: part of the samples were immediately snap frozen and stored at -80°C, part formalin-fixed paraffin-embedded (FFPE), and part freshly used for GASC isolation⁽⁷⁹⁾.

Eligibility criteria included written informed consent and availability of follow-up data. Extensive surgical resection was done at diagnosis and radio- and/or chemotherapy was administered in case of tumor progression or malignant transformation. Regarding the selection of patients for the study of the expression profile of GASC, we considered LGG with a good prognosis, patients without malignant transformation after at least 7 years from the first surgery and, LGG with a poor prognosis, those patients who died of neoplasm or of malignant transformation within 48 months from the first surgical treatment. Patients' characteristics are shown in **tables 4.1** and **4.2**. As regards cases included in the comparison between HGG and LGG, patients' characteristics are shown in **tables 4.5** and **4.6**.

3.2 GLIOMA HISTOLOGICAL CHARACTERIZATION

The histological characterization of gliomas was conducted in collaboration with the Department of Pathology of Udine within a transboundary programme between Italy and Slovenia named: "Identificazione di nuovi marcatori di cellule staminali tumorali a scopo diagnostico e terapeutico".

Tumors were histologically reviewed by two expert neuropathologist according to the WHO classification of tumors of the central nervous system⁽⁹⁾. Mitotic index was evaluated on Hematoxylin/Eosin stained sections by the number of mitosis in 10 high-power fields. Immunohistochemistry was performed on 4 µm-thick formalin-fixed paraffin-embedded slides. Sections were deparaffinized and pretreated for heat induced epitope retrieval using EnVision™ FLEX citrate buffer, pH 6.1, in PT Link (Dako) then placed in an automated immunostainer, Autostainer Link 48, (Dako) and incubated for 30 minutes at room temperature with the following mouse anti-human monoclonal antibodies: Ki-67 (1:200, clone Mib-1, Dako), GFAP (1:400, clone 6F2, (Dako), EGFR (1:50, clone 31G7, Zymed Laboratories Inc.), p53 (1:200, clone D07 Dako) and IDH1^{R132H} (1:150, clone H09, Dianova), ATRX (1:200, rabbit polyclonal, Sigma). Primary antibodies were detected using EnVision™ FLEX system (Dako). Ki-67 was

scored as percentage of positive nuclei. All other markers were qualitatively evaluated as negative or positive. All negative IDH1R132H cases were then amplified for IDH1 and IDH2 gene status assessment.

FISH analysis for 1p36 and 19q13 deletions was performed on 4 µm-thick formalin-fixed paraffin-embedded sections using dual-color 1p36/1q25 and 19q13/19p13 probes (Vysis 1p36/1q25 and 19q13/19p13 FISH Probe Kit, Abbott Molecular). Briefly, sections were deparaffinized and pretreated with 1M sodium thiocyanate solution at 80°C for 30 minutes. After washing in 2x SSC buffer, slides were immersed in a protease solution at 37°C for 15-30 minutes, then washed twice in 0.4X SSC/0.3% NP-40 buffer and then air-dried. Probes and target were simultaneously denatured at 73°C for 5 minutes and hybridized at 37°C for 18-20 hours. Slides were then immersed in 2xSSC-0.3% NP-40 for 5 minutes at 73°C and, finally, counterstained with DAPI. For each case 50-100 non-overlapping nuclei were analyzed and 1p or 19q deletion status was defined if the 1p36/1q25 or 19q13/19p13 signal ratio was lower than 0.80, respectively. Co-deletion status was defined if both 1p and 19q ratio were lower than 0.80. IDH gene status and MGMT promoter methylation were assessed on DNA extracted from formalin-fixed paraffin-embedded tissue with QIAmp DNA mini kit (Qiagen). DNA concentration was estimated with NanoDrop2000c spectrophotometer (Thermoscientific). IDH1 and IDH2 genes regions spanning codon 132 (IDH1) and codon 172 (IDH2) were amplified on Rotor-Gene 6000 (Corbett) and pyrosequencing of PCR products were performed on Pyromark Q96 ID (Qiagen) as previously reported⁽⁹⁴⁾ and analyzed with Pyromark ID 1.0 (Biotage AB) software. After DNA bisulfite conversion with EpiTect Bisulfite Kit (Qiagen), methylation levels of the MGMT promoter in position 17-39 of exon 1 were investigated, by PyroMark Q96 CpG MGMT (Qiagen) according to manufacturers' instructions.

3.3 GASC ISOLATION AND CULTURE

Cells from glioma were isolated and cultured applying, with minor modifications, a protocol optimized for culturing multipotent adult stem cells from normal⁽⁹⁵⁾,⁽⁹⁶⁾ and neoplastic human tissues⁽⁹⁷⁾. Briefly, glioma fragments were first disaggregated mechanically with scalpels and then enzymatically dissociated, in a 0.0125% Collagenase type II solution (Worthington) in Joklik modified Eagle's Medium (Sigma-Aldrich), for 5 minutes at 37°C. Collagenase activity was stopped by the addition of 0.1% bovine serum albumin (Sigma-Aldrich) solution in Joklik modified Eagle's Medium (Sigma-Aldrich). Cell suspension was centrifuged at 500g for 10 minutes and filtered through a sieve (BD Falcon) in order to select a population less than 40 µm in diameter. 2.0×10^6 freshly isolated human cells were plated onto 100 mm in diameter, human fibronectin (Sigma-Aldrich)-coated dishes (BD Falcon), in an expansion medium composed as follows: 60% low glucose DMEM (Invitrogen), 40% MCDB-201, 1mg/mL linoleic acid-BSA, 10^{-9} M dexamethasone, 10^{-4} M ascorbic acid-2 phosphate, 1X insulin-transferrin-sodium selenite (all from Sigma-Aldrich), 2% fetal bovine serum (Stemcell Technologies Inc.), 10 ng/ml human PDGF-BB, 10 ng/ml human EGF (both from Peprotech). Cells were cultured in an incubator at 37°C, 5% O₂/5% CO₂. Medium was replaced with fresh one every 4 days. Once cells reached 70-

80% of confluence, they were detached with TrypLE Express (Invitrogen) and re-plated at a density of $1-2 \times 10^3/\text{cm}^2$.

3.4 SURFACE IMMUNOPHENOTYPE CHARACTERIZATION

Cells populations were detached with 0.25% trypsin-EDTA (Sigma-Aldrich) and then incubated with either properly conjugated primary antibodies: CD11b, CD13, CD29, CD45, CD49a, CD49b, CD49d, CD90, CD73, CD44, CD59, CD45, HLA-DR, CD117, CD271, CD34, CD325 (Becton Dickinson) CD105, CD66e (Serotec), CD133 (Miltenyi Biotec), E-Cadherin (Santa Cruz Biotechnology), ABCG-2 (Chemicon International), or with an unconjugated primary antibody: N-cadherin (Sigma-Aldrich). Unconjugated antibody was revealed using PE or FITC conjugated secondary antibodies (Dako). Properly conjugated isotype matched antibodies were used as a negative control. The analysis was performed either by FACS-Calibur (Becton Dickinson) or by CyAn (Dako).

3.5 IMMUNOFLUORESCENCE ASSAY ON GASC

Cells cultured either in expansion or in differentiation medium were fixed in 4% buffered paraformaldehyde for 20 minutes at room temperature (RT). For intracellular stainings, fixed cells were permeabilized for 10 minutes at RT with 0.1% Triton X-100 (Sigma-Aldrich) before exposing them to primary antibodies. In order to block unspecific binding of the primary antibodies, cells were incubated with 10% donkey serum in PBS for 30 min. Primary antibody incubation was performed over-night at 4°C to detect: Oct-4 (Abcam, 1:150); Sox-2 (Chemicon International, 1:150); Nanog (Abcam, 1:150); Nestin (Millipore, 1:100); GFAP (Dako, 1:50); Vimentin (Dako, 1:500). To detect primary antibodies, A488- and A555- labeled secondary antibodies, diluted 1:800, were employed (Molecular Probe, Invitrogen). Finally, Vectashield (Vector Laboratories Inc.) added with 0.1 µg/ml DAPI (Sigma-Aldrich) was used as mounting medium. Epifluorescence and phase contrast images were obtained utilizing a live cell imaging dedicated system consisting of a Leica DMI 6000B microscope connected to a Leica DFC350FX camera (Leica Microsystems) and equipped with a 63X oil immersion objective (numerical aperture: 1.40) or a 40X oil immersion objective (numerical aperture: 1.25). Adobe Photoshop software was utilized to compose, overlay the images and to adjust contrast (Adobe). There were analyzed almost 300 cells for quantification of the protein expression.

3.6 SOFT AGAR ASSAY

To evaluate the ability of GASC to grow in an anchorage-independent way, 3×10^5 cells at the third passage in culture, were plated in a 0.25% soft agar solution in 35-mm plates containing a basal layer of 1% agarose. After 4 weeks, the total number of formed colonies were counted

under a phase contrast microscope (Leica DM IL, Leica Microsystems) equipped with a 10X objective (numerical aperture: 0.25). Assays were performed in triplicate.

3.7 RNA EXTRACTION AND SEQUENCING FROM HUMAN GASC

Total RNA was extracted from GASC using the TRIzol Reagent (Invitrogen) following the company's instructions and then it was suspended in nuclease-free water.

For each sample it was extracted at least 4 µg (Nanodrop) of RNA according to criteria established from the Institute of Applied Genomics (IGA, Udine, Italy) for the sequencing; the criteria were: ratio 260/280 > 1.8; RNA Integrity Number (RIN) > 8 (Agilent Bioanalyzer 2100); minimum RNA concentration of 40ng/µL.

Transcriptome GASC sequencing was performed by IGA using the Illumina mRNASeq Sample Prep kit v2.0. The poly-A mRNA was fragmented 3 minutes at 94°C and every purification step was performed by using 1X Agencourt AMPure XP beads.

Single read sequencing was performed on the HiSeq2000 (Illumina) generating 50-base reads. The platform permitted an analysis of 30 million sequence/sample.

3 GASC lines from glioma with a good prognosis and 3 GASC lines from glioma with a bad prognosis were sequenced.

Bioinformatic analysis was performed by Laboratorio Nazionale del Consorzio Interuniversitario per le Biotecnologie (LNCIB) which verified data availability removing linker sequence, marking sequence errors and mapping on the genome reference sequence (hg19) (preprocessing and mapping phases)⁽⁹⁸⁾. These preliminary phases showed that obtained data were of good quality and that over 90% of reads were available for the following analysis phases. It was provided a list of genes that were differently expressed between the two GASC groups. The results supplied the differential expression levels and the statistical power of the difference (p and q value).

The miRNA list was analyzed by using *Upstream regulators prediction* instrument included in *Ingenuity Pathway Analysis* software. This analysis identifies regulators, relationships, mechanisms, functions, and pathways relevant to changes observed in cells studied. The analyses provided tables, which show molecules able to modify the transcriptional program observed. The prediction score (z score), the overlay p-value and the genes regulated list included in the analyzed dataset were defined for each molecule.

3.8 IMMUNOHISTOCHEMICAL VALUATION OF *UPSTREAM REGULATORS*

To evaluate a possible difference in the expression of three upstream regulators (IL-1 β , IL-6 and p65/NF κ B) between LGG (n=5) and HGG (n=5), an immunohistochemical assay on sections, obtained from formalin-fixed paraffin-embedded, glioma tissues has been optimized.

4 μ m-thick sections were deparaffinized and pretreated for heat induced epitope retrieval using EnVision™ FLEX Target Retrieval Solution, High pH (IL-1 β) or EnVision™ FLEX Target Retrieval Solution, Low pH (IL6, p65/NF κ B).

Endogenous peroxidase was blocked with a solution of hydrogen peroxide (3,5% H₂O₂ in distilled H₂O), for 10 minutes at room temperature. Slides were then incubated with the following primary antibodies: IL-1 β (Abcam, clone 3E1, 1:50, overnight); IL6 (Abcam, rabbit polyclonal, 1:250, overnight); P65/NF κ B (Abcam, rabbit polyclonal, 1:500, 60 minutes at room temperature). Primary antibodies were detected using Dako EnVision + Dual Link System-HRP (DAB+) system, according to company's instructions. Slides were counterstained with Gill's Hematoxylin, dehydrated and mounted with Eukitt.

Positive controls were breast cancer- (IL-6 and p65/NF κ B) and endometrial cancer- (IL-1 β) tissues, while negative controls were obtained by omitting the primary antibody.

Slides were scanned at 40x magnification by using Aperio CS2 digital scanner (Leica Biosystems).

Images were then analyzed by Image J program quantifying optic mean density of each sample for area's unit.

3.9 TISSUE MICROARRAY (TMA) CONSTRUCTION

14 tissue microarrays (TMA) including 163 glioma samples (161 LGG and 2 HGG) were built. Glioma samples are well characterized both histopathologically and clinically and up-to-date clinical follow-up of the patients is available.

From formalin-fixed paraffin-embedded glioma's blocks, 4 μ m-thick sections were obtained and stained by Hematoxylin/Eosin (H&E). An expert neuropathologist on the basis of specific criteria (i.e. atypia, differentiation grade, cellular and nuclear polymorphism, microvascular proliferation, necrosis, heterogeneity, as well as hypercellularity) located and labeled in the H&E sections of each glioma sample, three areas representative of the glioma.

The TMA construction was then performed by using the GALILEO CK4500 instrument (Integrated System Engineering).

The areas of interest, previously marked, were matched to its approximate position in the donor block. A core of wax (1 mm diameter) was removed from the recipient block using a stylet before the donor core was taken and placed in this hole using a second stylet (Figure 3.1). Three cores were taken for each sample and the TMA was created with multiple different cases.

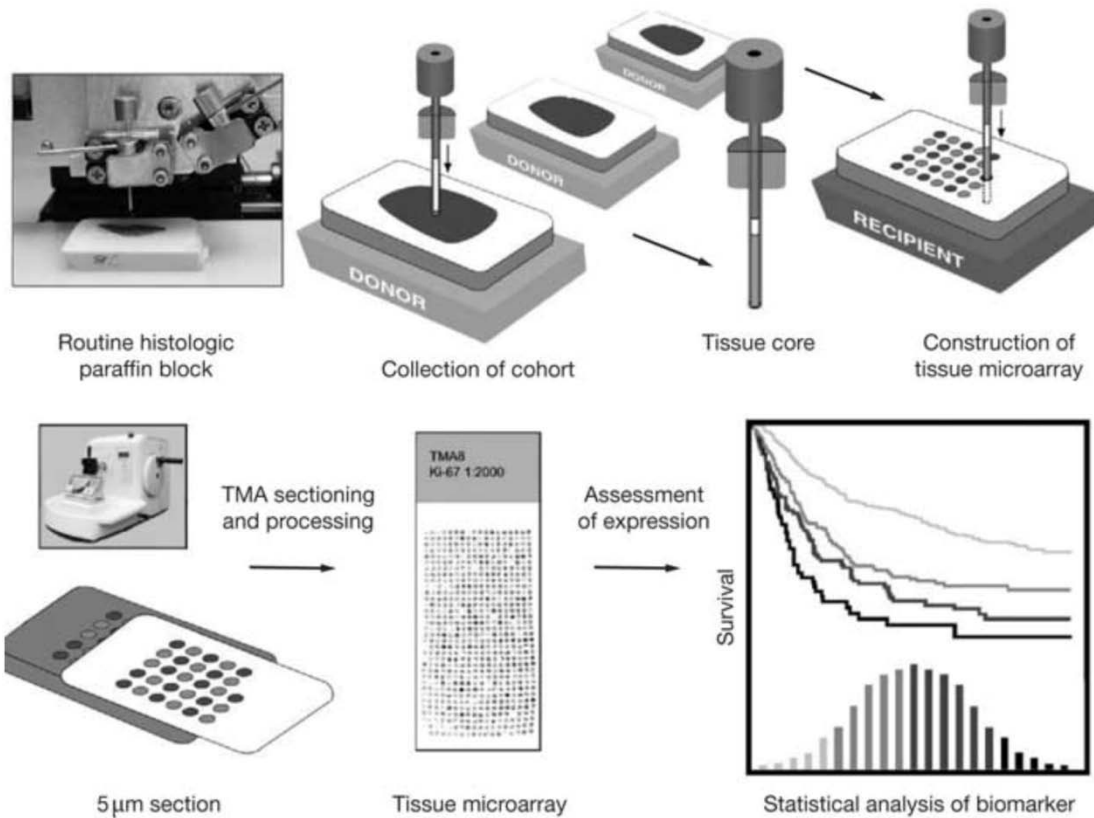


Figure 3.1. Steps of TMA construction using a manual tissue microarrayer. For details see paragraph 2.9⁽⁹⁹⁾.

Orientation of the cores was guaranteed by using two non-glioma tissues (i.e. murine tissue and human placenta) as point of reference (**Figure 3.2**).

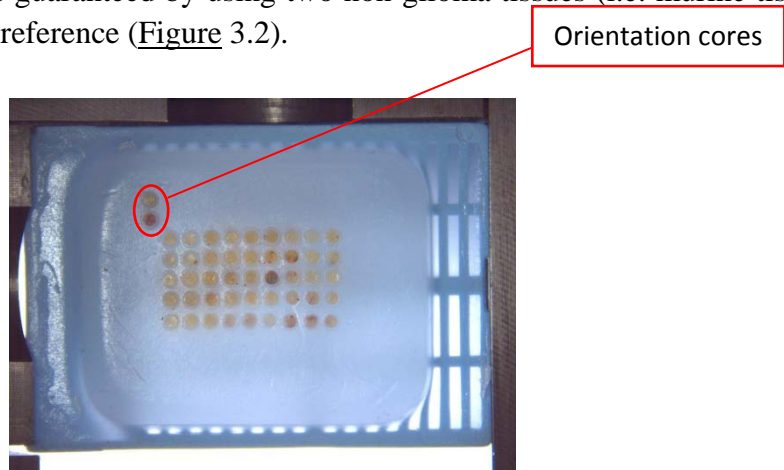


Figure 3.2. TMA block obtained after construction.

In TMA, samples were grouped on the basis of histopathology.

3.10 TMA PROCESSING

4 μ m-thick sections were obtained from TMA blocks and treated for immunohistochemical assays as previously described in paragraph 3.8.

3.11 TMA ANALYSIS

TMA slides were scanned at 40x magnification by using Aperio CS2 digital scanner (Leica Biosystems). IL-6 images were then analyzed by Image J program quantifying optic mean density of each sample for area's unit. For IL-1 β and p65, characterized by nuclear and cytoplasmic localization, images were evaluated by three independent observers that semiquantitatively scored nuclear and cytoplasm positivity. In the first case, the following parameters were quantified: fraction of positive nuclei; nuclear staining intensity (from 1 to 4); nuclear score (product of the fraction of positive nuclei and nuclear intensity). The cytoplasm score (an arbitrary number between zero and three) has been assigned on the basis of the staining intensity.

3.12 STATISTICAL ANALYSIS

As regards GASC analysis (surface immunophenotype, immunofluorescence and soft agar growth), characteristics of patients and valuation of IL-1 β , IL-6 and p65/NF κ B at tissue level, data are expressed as mean \pm standard deviation or as median and interquartile range, based on Gaussian distribution.

The comparison between two groups was performed by using *t* Student test or Mann Whitney test, as appropriate. A *p* value < 0.05 was considered significant.

As regards clinical and histological parameters and TMA analysis of IL-1 β , IL-6 and p65/NF κ B expression, in order to define a prognostic value, Overall Survival (OS), Progression-free Survival (PFS) and Malignant Progression-free Survival (MPFS) were described using the Kaplan-Meier method. In particular, OS was defined as time between initial surgery and death; PFS was defined as time between initial surgery and demonstration of unequivocal increase in tumor size on follow-up imaging, malignant progression, and/or death; MPFS was defined as time between initial surgery and demonstration of gadolinium enhancement on follow-up imaging and/or higher-grade tumor on subsequent biopsy or death. Analysis of survival was done using Cox proportional hazard model.

At the univariate analysis, age, sex, extent of tumor resection, histotype, p53 expression, IDH1/2 mutation presence, 1p/19q co-deletion, MGMT promoter methylation status and IL-1 β , IL-6 and p65/NF κ B expression were variables considered as possible prognostic factors.

At the multivariate analysis, covariates which presented a *p* < 0.010 at the univariate analysis were selected. Variables had to present a *p* < 0.05 to be considered in the stepwise model. Results are presented as hazard ratio (HR) and confidence interval at 95% (CI 95%).

4. RESULTS

4.1 CHOICE AND CHARACTERIZATION OF GASC FROM LGG

In this study we used 3 GASC lines obtained from 3 patients without malignant transformation after more than 7 years from the first surgery (LGG-good) and 3 GASC lines obtained from 3 patients who died of neoplasm or underwent malignant transformation within 48 months from the first surgery (LGG-bad). Table 4.1 and 4.2 illustrate clinical-pathological features of patients included in the study.

ID	Sex	Age at diagnosis	Histotype	Ki67 (%)	p53	1p deletion	19q deletion	1p/19q codel	IDH1	IDH2	IDH1/IDH2	MGMT	Alive/Dead	OS (months)	PFS (months)	MPFS (months)	
1	M	29	Diffuse astrocytoma	7	1	0	1	0	1	0	1	1	A	111	111	111	
13	F	39	Oligoastrocytoma	3	1	1	1	1	1	0	1	1	A	103	60	103	
27	F	41	Diffuse astrocytoma	4	1	0	0	0	1	0	1	1	A	98	70	95	
		36±6		5±2											104±7	80±27	103±8

Table 4.1. Clinical-pathological features of LGG-good patients included in the study.

Table reports data about histological analysis, common molecular features and patient prognosis, referred to 3 LGG with a good prognosis. F = female; M= male; p53 = p53 mutation; IDH1 = mutation of IDH1 gene; IDH2 = mutation of IDH2 gene; IDH1/IDH2: mutation of either IDH1 or IDH2 gene; MGMT = methylation of MGMT promoter; 0 = absent; 1 = present; D = dead; A = alive; n.d. = not determined. OS = overall survival; PFS = progression free survival; MPFS = malignant progression free survival.

ID	Sex	Age at diagnosis	Histotype	Ki67 (%)	p53	1p deletion	19q deletion	1p/19q codel	IDH1	IDH2	IDH1/IDH2	MGMT	Alive/Dead	OS (months)	PFS (months)	MPFS (months)	
2	M	63	Oligoastrocytoma	8	0	1	1	1	1	0	1	1	D	59	48	48	
25	M	54	Diffuse astrocytoma	20	0	0	0	0	0	0	0	0	D	26	12	12	
32	F	47	Oligoastrocytoma	4	1	0	0	0	1	0	1	1	D	25	18	18	
		55±8		11±8											37±19	16±19	26±19

Table 4.2. Clinical-pathological features of LGG-bad patients included in the study.

Table reports data about histological analysis, common molecular features and patient prognosis, referred to 3 LGG with a good prognosis. F = female; M= male; p53 = p53 mutation; IDH1 = mutation of IDH1 gene; IDH2 = mutation of IDH2 gene; IDH1/IDH2: mutation of either IDH1 or IDH2 gene; MGMT = methylation of MGMT promoter; 0 = absent; 1 = present; D = dead; A = alive; n.d. = not determined. OS = overall survival; PFS = progression free survival; MPFS = malignant progression free survival.

GASC lines were obtained according to the protocol optimized in our laboratory⁸ and cryopreserved in liquid nitrogen. These lines were thawed and expanded *in vitro* according to our protocol.

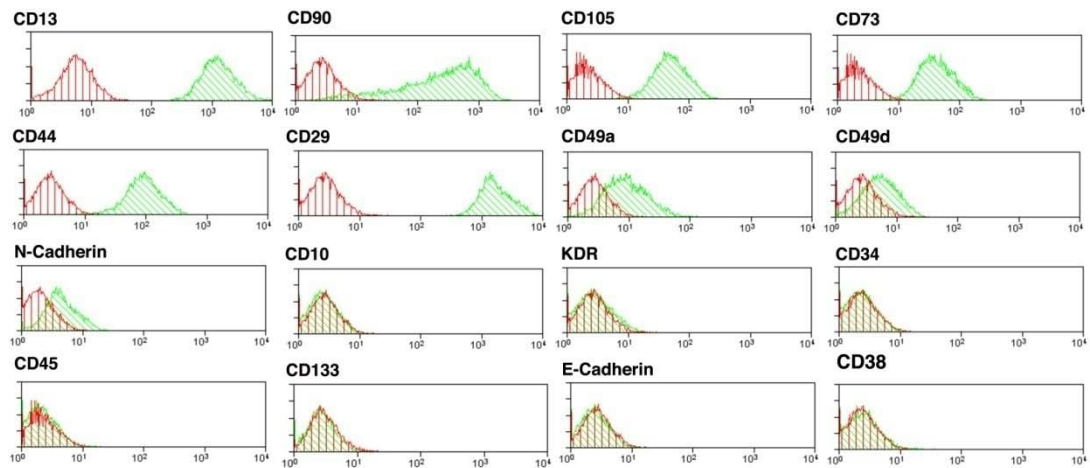
To establish whether GASC, even after seven years from collection, still possessed features of stem cells with tumor-supporting ability, we verified in thawed and expanded *in vitro* GASC:

1. The expression of an undifferentiated phenotype;
2. The ability to grow in anchorage-independent conditions (soft agar assay).

4.1.1 LGG GASC WERE CHARACTERIZED BY AN UNDIFFERENTIATED PHENOTYPE

Flow-cytometry analysis of the surface immunophenotype confirmed that GASC shared a mesenchymal phenotype (Figure 4.1), as they were markedly positive for antigens like CD90, CD105 and CD73 and they were negative for hematopoietic markers like CD45 and CD38.

A



B

Marker	GASC-LG-GOOD % positive cells			GASC-LG-BAD % positive cells		
	Media	±	DS	Media	±	DS
CD59	99,6	±	0,1	98,5	±	2,5
CD73	99,8	±	0,1	99,6	±	0,4
CD13	99,3	±	0,4	70,7	±	50,5
CD44	91,3	±	13,8	96,3	±	4,5
CD105	75,8	±	34,1	66,1	±	56,9
CD49A	97,9	±	2,3	52,1	±	43,1
CD49D	98	±	0,5	54,4	±	31,2
CD29	93,9	±	6,9	58,6	±	37,4
CD90	62,5	±	31,4	85,9	±	14,2
CD10	33,8	±	47,6	3	±	2,3
DR	0	±	0	0	±	0
CD117	27,5	±	44,5	0,5	±	0,4
N-CAD	28,8	±	39,9	22,5	±	36,5
E-CAD	0,8	±	0,7	24,9	±	36,9
CD271	0,2	±	0,2	1,3	±	1,6
ABCG2	0,8	±	0,5	2	±	1,9
CD34	0,3	±	0,4	0,7	±	0,8
CD66E	0,3	±	0,2	1,3	±	2,1
CD45	0,1	±	0,2	0,3	±	0,2
CD133	0,3	±	0,1	0,4	±	0,3

Figure 4.1. Surface immunophenotype of GASC included in the study.

A: Representative surface immunophenotype of LGG-GASC line.

Histograms overlays show isotype control IgG staining profile (red histograms) versus specific antibody staining profile (green histograms).

B: Table comparing GASC-LGG-GOOD versus GASC-LGG-BAD expression of the assayed surface markers (mean ± SD)

In order to test whether GASC were characterized by an undifferentiated state, we tested by immunofluorescence the expression of the pluripotent state-specific transcription factors Oct-4, NANOG and Sox-2. The [Figure 4.2](#) shows that most of the cultured cells expressed Oct-4, NANOG and Sox-2, confirming that cultured GASC maintained an undifferentiated transcriptional phenotype.

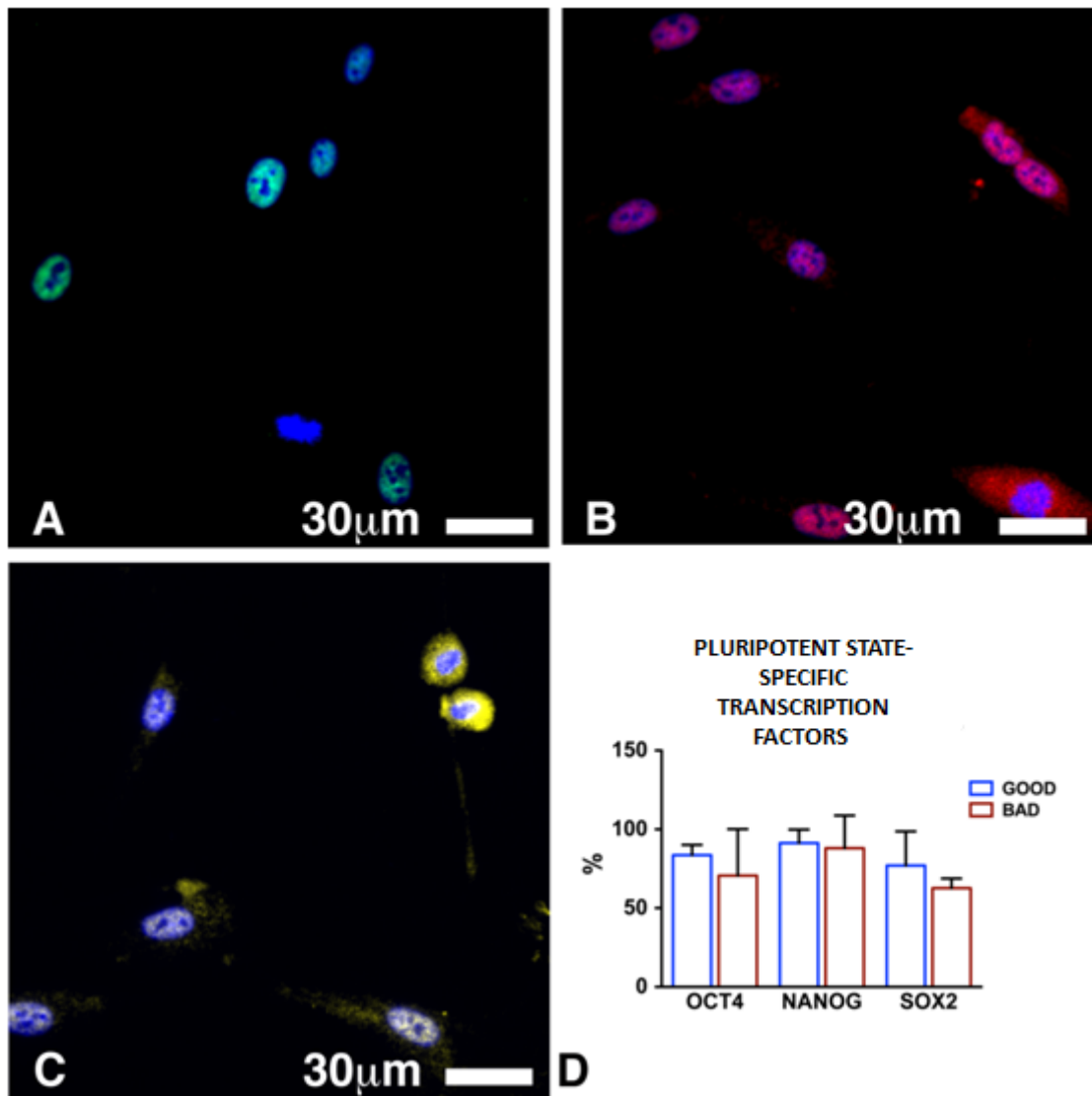


Figure 4.2. Pluripotent state-specific transcription factors expression.

A-C: representative images of Oct-4 expression (green fluorescence, **A**), NANOG expression (red fluorescence, **B**), and Sox-2 expression (yellow fluorescence, **C**) in LGG-GASC. Nuclei are depicted by the blue fluorescence of DAPI staining. **D:** Histograms comparing the expression of Oct4, NANOG and Sox-2 in GASC obtained, respectively, in LGG-GOOD and LGG-BAD. Data are expressed as mean \pm SD.

GASC lines were subsequently tested for the cytoplasmic expression of proteins characterizing undifferentiated neural cells, i.e. vimentin and nestin. Since tumors examined are of glial origin, it was also tested the expression of GFAP, an intermediate filament expressed in several glial cells. As shown in [Figure 4.3](#), a large number of GASC expressed both nestin, an intermediate filament characterizing primitive cells, and vimentin, an intermediate filament characterizing not only mesenchymal cells but also several cell types in the early phases of differentiation; conversely, GFAP was present and organized in filaments only in a minority of GASC ([Figure 4.3](#)).

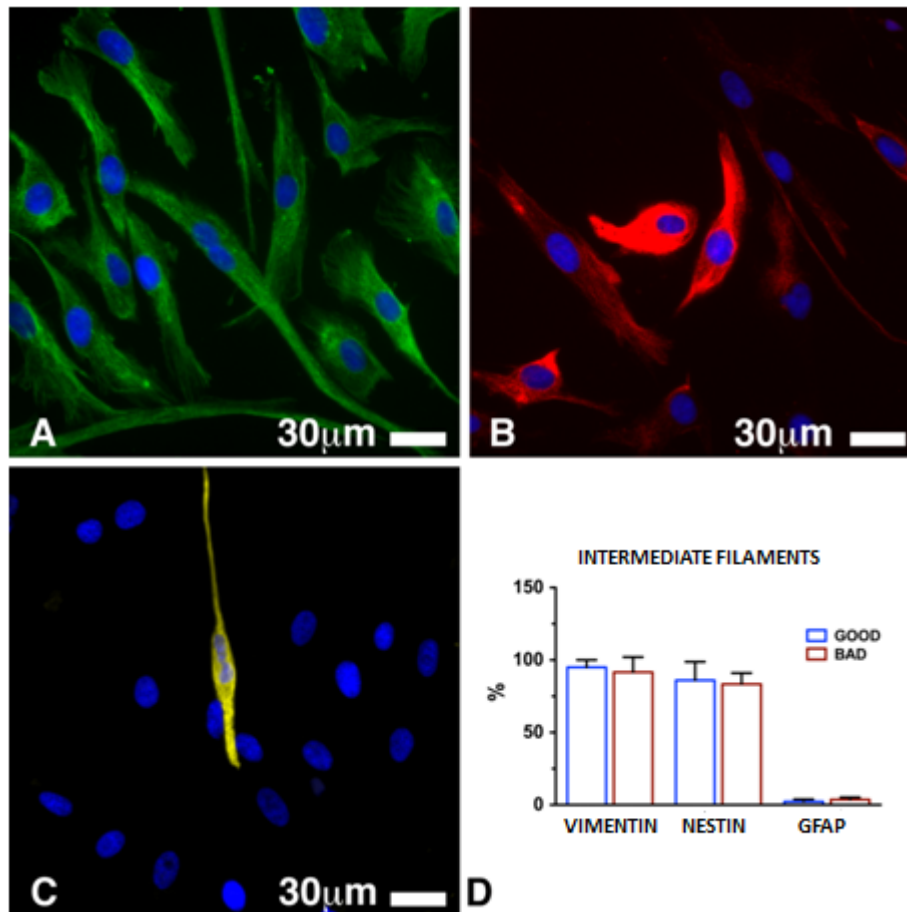


Figure 4.3. Expression of cytoplasmic filaments characterizing an undifferentiated state.

A, B: representative images of the expression in GASC of vimentin (green fluorescence, **A**), nestin (red fluorescence, **B**) and GFAP (yellow fluorescence, **C**). Nuclei are depicted by the blue fluorescence of DAPI staining. **D:** histograms depict as mean \pm SD the fraction of cells expressing the tested intermediate filaments in both GASC-LGG-BAD and GASC-LGG-GOOD.

In conclusion, GASC lines presented a surface immunophenotype, a transcriptional asset and an intermediate filament expression profile consistent with an undifferentiated phenotype.

4.1.2 LGG GASC RETAINED ABERRANT GROWTH PROPERTIES

Once it was proven that thawed GASC lines continue to present phenotypic stem cell features, we tested whether they retained also the typical property of tumor supporting cells, i.e. an anchorage-independent growth in a semisolid medium. With this purpose, GASC were cultured in soft agar (0,25% agar concentration). All GASC lines examined displayed the ability to grow in an anchorage-independent way, without significant statistical differences ([Figure 4.4](#)).

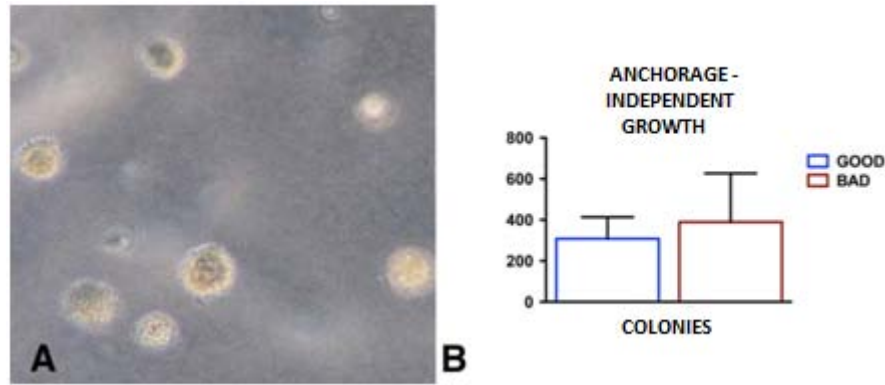


Figure 4.4. GASC anchorage-independent growth.

A: phase-contrast image (10x) of colonies grown for 4 weeks in a semisolid medium.

B: quantification of the absolute number of colonies $>100\mu\text{m}$ in diameter formed after 4 weeks (data are presented as mean \pm SD).

4.2 TRANSCRIPTOMIC ANALYSIS OF GASC

After checking that thawed GASC retained phenotypic features of stem cells with tumor-supporting ability, cells were expanded and RNA was extracted and analyzed by using deep-sequencing in collaboration with the Applied Genomic Institute (IGA).

82 genes (Table 4.3) resulted to be differentially expressed between GASC obtained from LGG characterized by a good prognosis (**q1**) and those obtained from LGG characterized by a poor prognosis (**q2**), respectively.

Only one of the 82 genes, NPTX1, resulted to be over expressed in GASC from LGG with a good prognosis, meanwhile all the other genes resulted to be up regulated in GASC from LGG with a bad prognosis.

As a whole, the gene expression profile of GASC from LGG with a bad prognosis was characterized by elements typical of an inflammatory response and, in part, of the so-called senescence-associated secretory phenotype (SASP).

GENE	LOCUS	value_1 (good)	value_2 (bad)	log2 (fold_change)	test_stat	p_value	q_value
CPXM2	chr10:125505151-125651500	0,0357066	10,6086	8,21483	-7,24916	4,19E-13	3,16E-09
RARRES2	chr7:150035406-150038763	0,266673	80,5709	8,23905	-7,32592	2,37E-13	3,16E-09
LRRC55	chr11:56949220-56959188	0,0348059	7,4269	7,73729	-7,09093	1,33E-12	6,69E-09
UNC5D	chr8:35092974-35652181	0,00918622	2,94237	8,32329	-6,79163	1,11E-11	4,18E-08
IL36RN	chr2:113816214-113822320	0,08191	21,8728	8,06088	-6,50506	7,77E-11	2,34E-07
COL4A4	chr2:227867426-228029275	0,131274	4,00436	4,93092	-6,11669	9,55E-10	2,40E-06
C15orf48	chr15:45722726-45725647	0,330422	67,9885	7,68484	-5,95667	2,57E-09	5,39E-06
CSF2	chr5:131409484-131411863	0,0618759	22,3282	8,49527	-5,93943	2,86E-09	5,39E-06
DHRS3	chr1:12627938-12677820	0,33111	11,8432	5,1606	-5,82189	5,82E-09	9,74E-06
COL4A3	chr2:228029280-228179508	0,0133608	1,08025	6,33722	-5,79029	7,03E-09	1,06E-05
IL1RN	chr2:113875469-113891593	0,0953215	29,5104	8,27421	-5,77141	7,86E-09	1,08E-05
GUCY1A2	chr11:106544737-106889171	0,0307103	2,30684	6,23105	-5,708	1,14E-08	1,44E-05
IL33	chr9:6215785-6257983	0,171093	23,4467	7,09846	-5,65319	1,57E-08	1,83E-05
SLAMF7	chr1:160709076-160724601	0,711663	14,6415	4,36273	-5,57554	2,24E-08	2,66E-05
CXCL2	chr4:74962753-74964997	1,47218	53,8745	5,19358	-5,23639	1,64E-07	1,21E-04
CXCL3	chr4:74902311-74904490	2,51675	123,713	5,61929	-5,23109	1,69E-07	1,21E-04
DAZL	chr3:16628300-16647006	0,0213078	5,27941	7,95285	-5,23528	1,65E-07	1,21E-04
IL1A	chr2:113531491-113542971	0,197288	8,69926	5,46251	-5,25011	1,52E-07	1,21E-04
IL36B	chr2:113779667-113810440	0,701937	202,715	8,1739	-5,27828	1,30E-07	1,21E-04
MEIS1	chr2:66662531-66799891	0,0149617	2,39824	7,32456	-5,25486	1,48E-07	1,21E-04
TNFRSF11B	chr8:119935795-119964383	0,520243	12,1145	4,54141	-5,27983	1,29E-07	1,21E-04
UPK1B	chr3:118892424-118924000	0,28799	10,4815	5,18568	-5,22276	1,76E-07	1,21E-04
CCL20	chr2:228678557-228682280	0,879665	120,2	7,09426	-5,17781	2,25E-07	1,47E-04
SULT1B1	chr4:70592685-70626430	0,0453819	5,99948	7,04658	-5,08732	3,63E-07	2,28E-04
ADAMTSL3	chr15:84322837-84708593	0,00634936	0,879891	7,11457	-5,05519	4,30E-07	2,58E-04
SULF1	chr8:70378858-70573147	0,0782839	5,34728	6,09395	-5,04862	4,45E-07	2,58E-04
FMOD	chr1:203309751-203320289	0,3278	8,51221	4,69865	-4,91676	8,80E-07	4,57E-04
PARM1	chr4:75858284-75975325	0,236247	4,95605	4,39083	-4,92966	8,24E-07	4,57E-04
RSPO3	chr6:127440047-127518184	0,0938318	4,70062	5,64663	-4,91957	8,67E-07	4,57E-04
HSD11B1	chr1:209859524-209908295	0,448669	77,3312	7,42926	-4,87367	1,10E-06	5,50E-04
EHF	chr11:34642587-34684834	0,0292247	2,97217	6,66819	-4,8196	1,44E-06	6,99E-04
CHI3L1	chr1:203148058-203155922	0,179121	10,0719	5,81326	-4,73075	2,24E-06	1,05E-03
PI3	chr20:43803539-43805185	0,0432537	26,0058	9,23179	-4,71996	2,36E-06	1,08E-03
KRT14	chr17:39738530-39743147	0,0204912	3,50101	7,41662	-4,64697	3,37E-06	1,49E-03
GJB2	chr13:20761603-20767114	0,305327	8,99268	4,88032	-4,55996	5,12E-06	2,20E-03
CACNG7	chr19:54415990-54446969	0,0172899	2,01059	6,86155	-4,5412	5,59E-06	2,34E-03
TMEM233	chr12:120031263-120079363	0,0507936	3,63338	6,16052	-4,52497	6,04E-06	2,46E-03
VNN1	chr6:133001996-133035194	0,0529256	1,85872	5,1342	-4,46713	7,93E-06	3,14E-03
DIRAS2	chr9:93372113-93405108	0,0270535	1,07918	5,31797	-4,44647	8,73E-06	3,37E-03
PI16	chr6:36916038-36932613	0,568253	41,7082	6,19765	-4,36826	1,25E-05	4,72E-03
NCAM1	chr11:112831968-113149158	0,0220552	1,58133	6,16388	-4,33047	1,49E-05	5,47E-03
PNLDC1	chr6:160221300-160241735	0,0169345	2,15276	6,99008	-4,27807	1,89E-05	6,61E-03
PTGDS	chr9:139871955-139876194	8,78118	307,535	5,13019	-4,28138	1,86E-05	6,61E-03
SFRP4	chr7:37945784-37956525	0,334111	5,40094	4,01481	-4,25695	2,07E-05	7,10E-03
CH25H	chr10:90965693-90967071	0,250897	5,94098	4,56553	-4,21419	2,51E-05	8,39E-03
NFB	chr6_ssto_hap7:3246430-3252571	1,56523	19,7885	3,66022	-4,20205	2,65E-05	8,59E-03
NPTX1	chr17:78440632-78450404	12,1585	0,378341	-5,00613	4,1992	2,68E-05	8,99E-03
ADAP1	chr7:937536-994289	0,1781	4,29845	4,59306	-4,13982	3,48E-05	1,09E-02
PTGES	chr9:132500614-132515344	6,09915	96,7688	3,98786	-4,11999	3,79E-05	1,17E-02
IL6	chr7:22766765-22771621	6,45137	274,677	5,41199	-4,10214	4,09E-05	1,23E-02
DKK2	chr4:107842958-107957453	0,468367	7,23007	3,9483	-4,02485	5,70E-05	1,68E-02
MFAP5	chr12:8798539-8815433	0,116746	2,05346	4,13661	-4,01584	5,92E-05	1,72E-02
C3	chr19:6677845-6720662	0,604522	175,949	8,18515	-4,008	6,12E-05	1,74E-02
SOX17	chr8:55370494-55373456	0,0200116	1,44468	6,17377	-3,99368	6,51E-05	1,82E-02
TMEM119	chr12:108983621-108991894	10,8899	0,891386	-3,61079	3,98682	6,70E-05	1,83E-02
IL24	chr1:207070787-207095378	0,216701	34,8981	7,3313	-3,97656	6,99E-05	1,88E-02
GPR37L1	chr1:202092028-202098634	0,442385	6,34548	3,84235	-3,97232	7,12E-05	1,88E-02
PID1	chr2:229888688-230136057	1,99642	30,9126	3,95271	-3,96688	7,28E-05	1,89E-02
GPRCSB	chr16:19870292-19896151	0,190175	2,73179	3,84444	-3,96058	7,48E-05	1,91E-02
DPP4	chr2:162848754-162931052	2,19102	98,5683	5,49145	-3,93026	8,49E-05	2,10E-02
LIPG	chr18:47088426-47119278	0,297673	4,98478	4,06573	-3,92349	8,41E-05	2,10E-02
GIMAP8	chr7:150147961-150176483	0,00572422	0,808907	7,14275	-3,90784	9,31E-05	2,23E-02
TMTC1	chr12:29653745-29937692	1,66804	14,1722	3,08684	-3,90915	9,26E-05	2,23E-02
NUPR1	chr16:28548661-28550495	6,19287	71,2316	3,52384	-3,873	0,0001075	2,53E-02
CCL7	chr17:32597234-32599261	0,330177	9,54153	4,85291	-3,86328	0,0001119	2,59E-02
MUM1L1	chrX:105412297-105452949	0,295297	5,33825	4,17613	-3,8229	0,0001319	3,01E-02
CD200	chr3:112051915-112081658	0,0945608	3,82179	5,33686	-3,81167	0,000138	3,03E-02
DCLK3	chr3:36753912-36781352	0,00430551	0,526902	6,9352	-3,81011	0,0001389	3,03E-02
LRRC15	chr3:194075975-194090472	0,192567	6,0953	4,98426	-3,81079	0,0001385	3,03E-02
ALDH1A3	chr15:101420008-101456830	2,62781	17,6117	2,7446	-3,80239	0,0001433	3,04E-02
ITGA8	chr10:15559087-15761770	31,0095	5,5426	-2,48407	3,80223	0,0001434	3,04E-02
HAND2	chr4:174447651-174451378	0,00668077	1,54279	7,85131	-3,77249	0,0001616	3,38E-02
PTGS2	chr1:186640943-186649559	1,99228	22,6921	3,50969	-3,75961	0,0001702	3,47E-02
SYT7	chr11:61281187-61348344	0,204321	4,28085	4,38898	-3,76213	0,0001685	3,47E-02
ICAM1	chr19:10381516-10397291	6,06048	42,8501	2,82179	-3,74497	0,0001804	3,62E-02
LCP1	chr13:46700057-46756459	2,33908	20,0884	3,10235	-3,73948	0,0001844	3,66E-02
CELF2	chr10:11047258-11378672	0,343772	3,43122	3,3192	-3,72091	0,0001985	3,88E-02
CLGN	chr4:141309606-141348815	0,701474	10,8642	3,95305	-3,70041	0,0002153	4,16E-02
EBI3	chr19:4229539-4237524	0,368407	5,29957	3,8465	-3,66939	0,0002431	4,64E-02
PAPPA2	chr1:176432306-176811970	0,107768	0,10106	4,22132	-3,65727	0,0002549	4,80E-02
CXCR7	chr2:237478379-237490994	1,02128	8,96387	3,13375	-3,65003	0,0002622	4,88E-02

Table 4.3. Genes differentially expressed between GASC isolated from LGG characterized by a good prognosis and those isolated by LGG with a poor prognosis (bad), respectively.

- Gene involved in inflammatory response
- Gene involved in SAP

Afterwards, the transcriptional program of GASC was verified at LNCIB (in collaboration with Doctor. S. Piazza and Doctor. Y. Ciani) by using *Upstream regulators* analysis (included in Ingenuity Pathway Analysis) and upstream regulators potentially responsible of the differences in the transcriptional profile between GASC isolated from LGG with different prognosis were identified (Table 4.3).

Upstream Regulator	Molecule Type	Activation z-score	p-value of overlap	Target molecules in dataset
IL1A	cytokine	3,902	1,44E-17	ALDH1A3,CCL20,CSF2,CXCL2,CXCL3,DPP4,HSD11B1,ICAM1,IL1A,IL1RN,IL36B,IL6,PI3,PTGES,PTGS2,TNFRSF11B
IL1B	cytokine	4,863	1,48E-17	CCL20,CCL7,CFB,CHI3L1,CSF2,CXCL2,CXCL3,DPP4,EBI3,EHF,HSD11B1,ICAM1,IL1A,IL1RN,IL24,IL33,IL36B,IL36RN,IL6,LC1,PI3,PTGDS,PTGES,PTGS2,TNFRSF11B
TNF	cytokine	4,845	6,42E-16	ACKR3,ALDH1A3,CCL20,CCL7,CFB,CH25H,CHI3L1,COL4A3,CSF2,CXCL2,CXCL3,DHRS3,DPP4,EBI3,EHF,HSD11B1,ICAM1,IL1A,IL1RN,IL24,IL33,IL36B,IL36RN,IL6,NCAM1,PI3,PTGES,PTGS2,RARRES2,TNFRSF11B
RELA	transcription regulator	2,922	4,82E-14	CCL20,CFB,CHI3L1,CSF2,CXCL2,CXCL3,EHF,ICAM1,IL1A,IL1RN,IL6,PI3,PTGDS,PTGES,PTGS2,TNFRSF11B
IFNG	cytokine	3,713	1,54E-13	ALDH1A3,CCL20,CCL7,CD200,CFB,CH25H,CSF2,CXCL2,CXCL3,DPP4,EBI3,EHF,GJB2,GPRC5B,ICAM1,IL1A,IL1RN,IL6,KRT14,NCAM1,NUPR1,PTGES,PTGS2,SYT7,TNFRSF11B
TLR5	transmembrane receptor	2,767	4,02E-13	CCL20,CSF2,CXCL2,CXCL3,ICAM1,IL1A,IL33,IL6
NFkB (complex)	complex	3,509	5,47E-13	ALDH1A3,CCL20,CCL7,CFB,CSF2,CXCL2,CXCL3,EHF,ICAM1,IL1A,IL1RN,IL24,IL6,NCAM1,PID1,PTGES,PTGS2,TNFRSF11B
TLR3	transmembrane receptor	3,141	1,46E-12	CCL20,CFB,CSF2,CXCL2,CXCL3,ICAM1,IL1A,IL1RN,IL33,IL6,LIPG,PTGES,PTGS2,CCL20,CCL7,CD200,CELF2,CSF2,CXCL2,CXCL3,DPP4,HSD11B1,ICAM1,IL1A,IL1RN,IL24,IL33,IL6,LIPG,PTGS2,SLAMF7,TNFRSF11B
IL4	cytokine	2,346	2,94E-12	IL24,IL33,IL6,LIPG,PTGS2,SLAMF7,TNFRSF11B
IL17F	cytokine	2,395	4,11E-12	CCL20,CSF2,CXCL2,CXCL3,ICAM1,IL6,PTGS2
NFKB1	transcription regulator	1,847	1,04E-11	CCL20,CFB,CSF2,CXCL2,CXCL3,EBI3,EHF,ICAM1,IL1RN,IL6,PI3,PTGS2
IL13	cytokine	1,316	2,48E-11	ACKR3,CCL20,CHI3L1,CXCL2,CXCL3,HSD11B1,ICAM1,IL1RN,IL6,PID1,PTGES,PTGS2,TNFRSF11B,VNN1
FOXL2	transcription regulator	2,804	2,50E-11	CCL20,CH25H,CXCL2,CXCL3,GPRC5B,ICAM1,PTGS2,RSPO3
IL17A	cytokine	3,023	3,20E-11	CCL20,CSF2,CXCL2,CXCL3,ICAM1,IL1A,IL1RN,IL33,IL6,PTGS2,TNFRSF11B
IKBKB	kinase	3,197	7,23E-10	CCL20,CH25H,CSF2,CXCL2,CXCL3,ICAM1,IL1A,IL1RN,IL6,PTGS2,TNFRSF11B
IL6R	transmembrane receptor	2,179	3,02E-09	CCL7,CXCL2,CXCL3,ICAM1,IL6,PTGS2,TNFRSF11B
IL6	cytokine	2,338	2,79E-06	CCL20,CCL7,CSF2,CXCL2,CXCL3,ICAM1,IL1RN,IL6,KRT14,PTGES,PTGS2,TNFRSF11B

Table 4.4. Upstream regulators analysis (included in Ingenuity Pathway Analysis).

Table reports a selection of molecules involved in the differences in the transcriptional program observed. z-score of prediction, p-value of overlap and the list of genes regulated in the analyzed dataset are shown.

The upstream regulators, which have the higher probability (z-score) to activate a molecular signature characterizing GASC of gliomas with a bad prognosis, were cytokine and transcriptional regulator of the inflammatory response. In particular, we decided to focus our attention on IL-1 β , IL-6 and p65/NF κ B (RELA) because they represent three different inflammatory pathways involved in the progression of glioblastoma⁽¹⁰⁰⁾.

4.3 IMMUNOHISTOCHEMICAL EVALUATION OF THE EXPRESSION OF *UPSTREAM REGULATORS* AT TISSUE LEVEL

In order to establish whether selected upstream regulators were expressed at tissue level, 5 LGG tissues were selected. Since we hypothesized that the “upstream regulators” could be related to an increased aggressiveness, 5 HGG were included as well. Tables 4.5 and 4.6 report features of glioma samples selected for the assessment of IL-1 β , IL-6 and p65/NF κ B expression.

ID	Sex	Age at diagnosis	Histotype	Ki67 (%)	p53	1p deletion	19q deletion	1p/19q code1	IDH1	IDH2	IDH1/IDH2	MGMT	Dead/Alive	OS (months)
13	F	40	Oligoastrocytoma	4	1	1	1	1	1	0	1	1	A	103
25	M	54	Diffuse astrocytoma	20	0	0	0	0	0	0	0	0	D	26
44	M	36	Oligoastrocytoma	5	1	1	1	1	1	0	1	1	A	80
72	M	45	Astrocytoma	5	1	0	0	0	0	0	0	n.d.	D	40
84	F	28	Diffuse astrocytoma	3	1	0	0	0	1	0	1	n.d.	D	51

Table 4.5. Clinical-pathological features of the 5 LGG included in the study. F = female; M= male; p53 = p53 mutation; IDH1 = mutation of IDH1 gene; IDH2 = mutation of IDH2 gene; IDH1/IDH2: mutation of either IDH1 or IDH2 gene; MGMT = methylation of MGMT promoter; 0 = absent; 1 = present; D = dead; A = alive; OS = overall survival; n.d. = not determined.

ID	Sex	Age at diagnosis	Histotype	Ki67 (%)	p53	IDH1	IDH2	IDH1/IDH2	MGMT	Dead/Alive	OS (months)
85	M	49	Glioblastoma multiforme	35	0	n.d.	n.d.	n.d.	n.d.	D	22
160	F	72	Glioblastoma	50	0	n.d.	n.d.	n.d.	n.d.	D	7
169	F	66	Glioblastoma	60	1	n.d.	n.d.	n.d.	n.d.	D	18
170	F	70	Diffuse astrocytoma	15	1	0	0	0	0	D	22
172	F	76	Glioblastoma	20	1	0	0	0	1	D	16

Table 4.6. Clinical-pathological features of the 5 HGG included in the study. F = female; M= male; p53 = p53 mutation; IDH1 = mutation of IDH1 gene; IDH2 = mutation of IDH2 gene; IDH1/IDH2: mutation of either IDH1 or IDH2 gene; MGMT = methylation of MGMT promoter; 0 = absent; 1 = present; D = dead; A = alive; OS = overall survival; n.d. = not determined.

Immunohistochemical analyses demonstrated that all markers were expressed either in LGG, (Figure 4.5) or in HGG tissues (Figure 4.6).

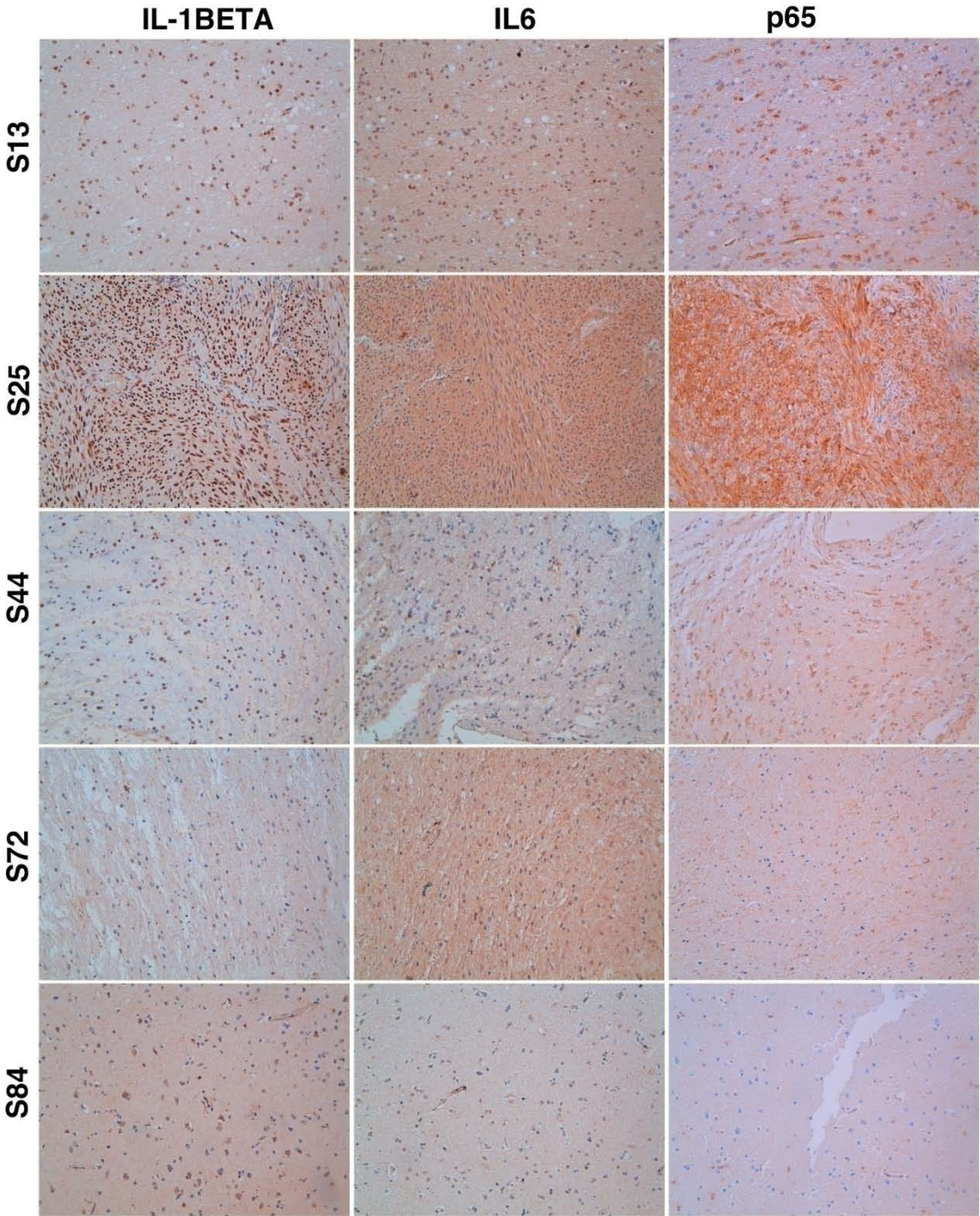


Figure 4.5. IL-1 β , IL-6 and p65/NF κ B expression in 5 LGG samples (20x).

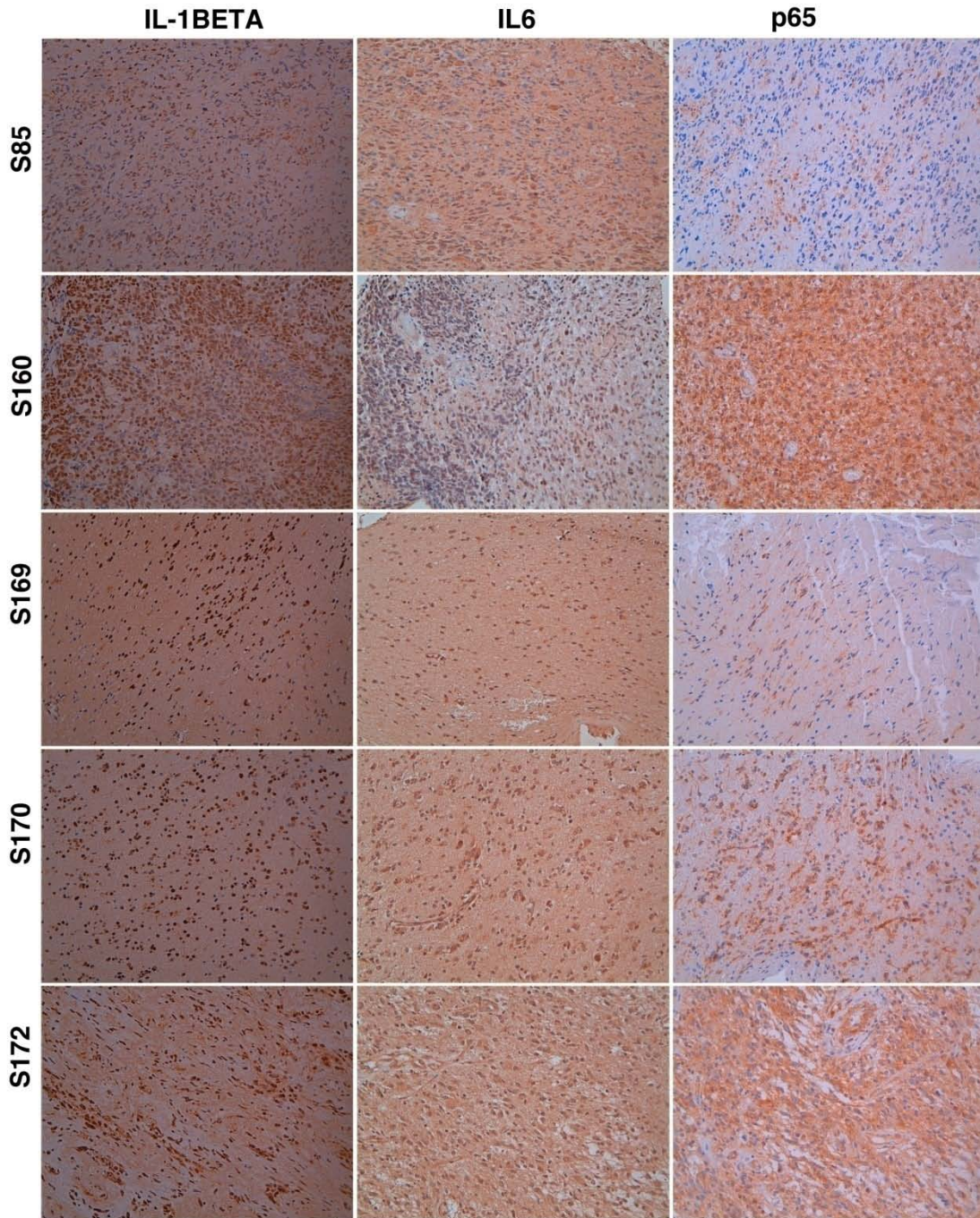


Figure 4.6. IL-1 β , IL-6 and p65/NF κ B expression in HGG samples (20x).

However, at a whole, it was apparent that IL-1 β , IL-6 and p65/NF κ B were expressed at higher level in HGG than in LGG.

Quantitative analysis of the marker expression, performed using Image J program, confirmed statistically significant differences in both IL-1 β and IL-6 expression between HGG and LGG (Figure 4.7).

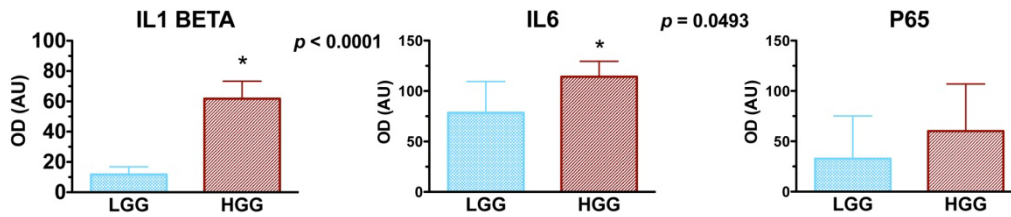


Figure 4.7. Differences in IL-1 β , IL-6 and p65/NF κ B expression between high-grade glioma (HGG) and low-grade glioma (LGG).

Results are expressed as mean \pm SD, * $p < 0.05$ vs. LGG.

p65 expression was not significantly different between HGG and LGG. In fact, its expression was extremely variable in HGG. In contrast, LGG, with the exception of S25, were mostly negative for p65 expression.

It was interesting to note that S25, a LGG characterized by an extremely poor prognosis, was characterized, with respect to the other LGG inserted in the dataset and characterized by a better prognosis, by an enhanced expression of all the three markers.

For this reason, we decided to include all the three markers in the subsequent analyses on a large LGG dataset.

4.4 IL-1 β , IL-6 AND p65 EXPRESSION IN TMA: PATIENTS INCLUDED IN THE STUDY

175 low grade glioma samples, included in the TMA, were obtained from the archive available at the Pathology Department of the Azienda Ospedaliero-Universitaria of Udine directed by doctor Skrap. However, material for immunohistochemical analyses was available for only 161 patients. Therefore, our immunohistochemical analyses was restricted to 161 patients. Table 4.7 summarizes the demographic, clinical and, histological data of the glioma samples analyzed. Patients were surgically treated at the Neurosurgery of Udine for a WHO grade II supratentorial astrocytoma *de novo* developed in a period between 1993 and 2013. Tumors were not chemo- or radio-treated before surgery. Grade I gliomas were excluded from the analysis because they are clinically and genetically different from WHO grade II gliomas.

CLINICOPATHOLOGIC FEATURES	PATIENTS, NO.	%	MEDIAN (RANGE)
SEX			
<i>MALE</i>	97	60	-
<i>FEMALE</i>	64	39	-
AGE AT SURGERY (YEARS)	-	-	39 (18-70)
EXTENT OF RESECTION (%)	-	-	86 (49-100)
TUMOR SUBTYPE			
<i>ASTROCYTOMA</i>	85	52	-
<i>OLIGOASTROCYTOMA</i>	53	30	-
<i>OLIGODENDROGLIOMA</i>	23	14	-
KI67 EXPRESSION (%)			5 (1 – 70)
≤ 4	77	47	-
>4	83	50	-
P53 EXPRESSION (N=158)	105	66	-
IDH1 MUTATION (N=158)	143	96.8	-
IDH2 MUTATION (N=158)	4	2.5	-
IDH1 OR IDH2 MUTATION (N=158)	147	93	-
CHROMOSOME 1P DELETION (N=155)	56	36	-
CHROMOSOME 19Q DELETION (N=155)	63	40	-
CHROMOSOME 1P AND 19Q CO-DELETION (N=155)	51	32	-
MGMT PROMOTER METHYLATION (N=158)	145	91.7	-
ATRX EXPRESSION (N=158)	78	49	
P65/NFKB (N=159)	-	-	107 (35.3-156.3)
NUCLEAR	-	-	7 (0-240)

CYTOPLASM	-	-	1 (0-3)
IL-1B (N=159)	-	-	250 (0-592)
NUCLEAR	-	-	160 (0-392)
CYTOPLASM	-	-	1 (0-3)
IL-6 (N=161)	-	-	75 (27-157.3)
NUMBER OF MITOSIS/10 HIGH POWER FIELDS	-	-	1 (0 - 10)
POST-OPERATIVE CHEMOTHERAPY	68	41	-
POST-OPERATIVE RADIOTHERAPY	94	57	-

Table 4.7. Clinicopathologic features of the n=161 low-grade glioma patients.

60% of patients was male and the median age was 39 years (range 18-70). The most common histotype was the astrocytoma (52%) and Ki67 was expressed in more than 4% of cells in 50% of patients.

As regards mutations, more than 90% of grade II gliomas presented IDH1 or IDH2 mutations, 32% presented 1p/19q co-deletion, 66% presented p53 expression, and 49% presented expression of ATRX. MGMT promoter resulted methylated in more than 90% of patients. After the surgery intervention, half of the patients were chemo- and/or radio-treated.

TMA construction allowed evaluating 159 samples of LGG for p65/NFκB and IL-1β and 161 sample for IL-6, out of 161 samples (Number of total TMA: 14).

IL-6 expression was analyzed by Image J program quantifying optic mean density of each sample for area's unit. The quantification values ranged from 27-157.3. Figure 4.8 shows IL-6 expression of a TMA core.

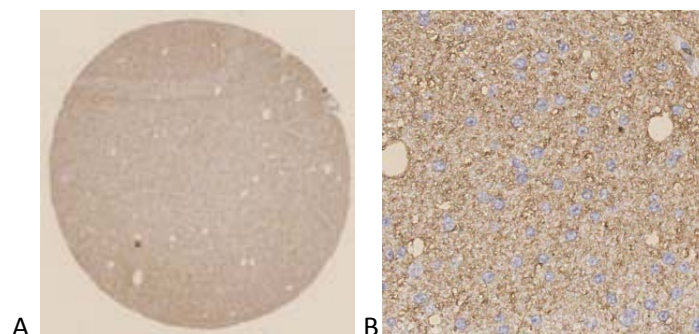


Figure 4.8. IL-6 expression. Representative image of IL-6 expression in TMA. Nuclei are counterstained with Hematoxylin of Gill (A: 20x; B: 40x).

As regards p65/NFκB and IL-1β expression, it was evaluated semiquantitatively nuclear and cytoplasm positivity. The score of p65/NFκB and IL-1β nuclear positivity ranged from 0 and 240 and from 0 and 392, respectively. 44.6% of LGG did not express p65 at nuclear level. 6.9% of LGG did not express IL-1β at nuclear level. The p65/NFκB and IL-1β cytoplasm score ranged

from 0 and 3. 20.7% of LGG did not express IL-1 β at cytoplasm level. Figure 4.9 and figure 4.10 show p65/NF κ B and IL-1 β TMA expression, respectively.

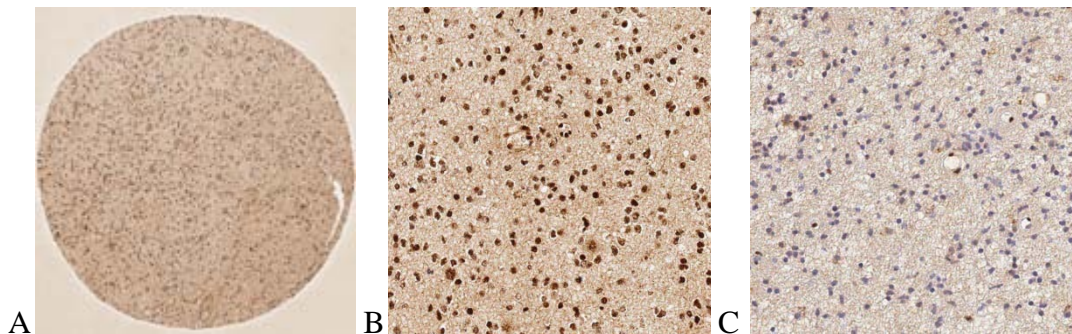


Figure 4.9. IL-1 β expression. Representative image of a core stained for IL1 β (A: 20x). Examples, at higher magnification, of LGG with a nuclear(B, 40x) and a cytoplasm (C, 40x) expression of IL1 β , respectively. Nuclei are counterstained with Hematoxylin of Gill (A: 20x).

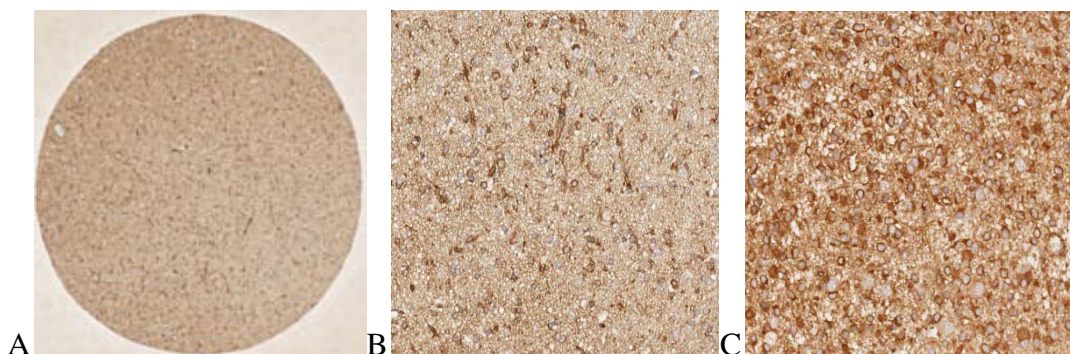


Figure 4.10. p65/NF κ B expression. Representative image of a core stained for p65/NF κ B (A: 20x). Examples, at higher magnification, of LGG with a nuclear (B, 40x) and a cytoplasm (C, 40x) expression of p65/NF κ B, respectively. Nuclei are counterstained with Hematoxylin of Gill.

4.5 EVALUATION OF THE PROGNOSTIC VALUE OF *GOLD STANDARD* BIOMARKERS

When the database was closed, disease progression was observed in 123 patients (76%), anaplastic transformation was observed in 102 cases (63%) and 77 patients died (48%). Median follow-up in patients still alive was 76 months (range 25-189), median overall survival (OS) was 65 months, median malignant progression-free-survival (MPFS) was 46 months, and median progression free survival (PFS) was 54 months. Estimated rate of OS, MPFS and PFS at 5 and

10 years was, respectively, 66% and 33% for OS, 46% and 17% for MPFS and 37% and 7% for PFS.

OVERALL SURVIVAL

As illustrated in table 4.8, prognostic factors which at the univariate analysis ($p < 0,005$) were positively associated with overall survival (OS) were the extent of tumor resection (EOR), the patient's clinical *status* evaluated as Karnosky Performance Status (KPS) and the presence of mutated IDH1 gene. Conversely, the age and the Ki67 expression ≥ 4 were associated with a poor prognosis.

At the multivariate Cox analysis, independent predictors of OS were Ki67 (hazard ratio –HR– 2.34, confidence interval at 95% –CI95%– 1.45-3.76, $p=0.000$), the extent of tumor resection (HR 0.93, CI95% 0.92-0.95, $p=0.000$), the KPS (HR 0.94, CI95% 0.91-0.97, $p=0.000$) and mutated IDH1 gene (HR 0.40, CI95% 0.19-0.84, $p=0.000$).

TUMOR PROGRESSION

As illustrated in table 4.8, prognostic factors which at the univariate analysis ($p < 0,005$) were positively associated with progression free survival (PFS) were the extent of tumor resection (EOR) and the patient's clinical *status* (KPS). Conversely, the Ki67 expression ≥ 4 and the presence of p53 mutation were associated with an high risk of progression.

At the multivariate Cox analysis, independent predictors of PFS were Ki67 (HR 1.55, CI95% 1.06-2.25, $p=0.022$), the extent of tumor resection (HR 0.96, CI95% 0.94-0.97, $p=0.000$), and p53 expression (HR 1.82, CI95% 1.19-2.80, $p=0.006$).

MALIGNANT TRANSFORMATION

As illustrated in table 4.8, prognostic factors which at the univariate analysis ($p < 0,005$) were positively associated with malignant progression-free-survival (MPFS) were the extent of tumor resection (EOR) and the patient's clinical *status* (KPS). Conversely, the Ki67 expression ≥ 4 was associated with an high risk of progression.

At the multivariate Cox analysis, independent predictors of MPFS were Ki67 (HR 1.69, CI95% 1.13-2.53, $p=0.010$), the extent of tumor resection (HR 0.95, CI95% 0.94-0.97, $p=0.000$), and the KPS (HR 0.95, CI95% 0.94-0.97, $p=0.000$).

	OS			PFS			MPFS		
	HR	95% CI	<i>p</i>	HR	95% CI	<i>p</i>	HR	95% CI	<i>p</i>
AGE (MODELED AS CONTINUOUS VARIABLE)	1.02	1.00-1.04	0.019	1.00	0.99-1.02	0.763	1.01	1.00-1.03	0.194
SEX (F VS M)	0.66	0.41-1.07	0.087	0.95	0.66-1.38	0.797	0.70	0.46-1.05	0.081
KPS (MODELED AS CONTINUOUS VARIABLE)	0.94	0.91-0.97	<0.0001	0.97	0.94-0.99	0.043	0.95	0.92-0.98	<0.0001
% EOR (MODELED AS CONTINUOUS VARIABLE)	0.93	0.91-0.95	<0.0001	0.96	0.94-0.97	<0.0001	0.95	0.94-0.97	<0.0001
HYSTOTYPE (OLIGOASTROCYTOMA VS OTHERS)	0.95	0.58-1.54	0.840	1.06	0.72-1.55	0.787	1.07	0.73-1.59	0.726
% Ki67 > 4 VS ≤ 4	2.10	2.32-3.35	0.002	1.44	1.01-2.06	0.046	1.64	1.01-2.43	0.015
NUMBER OF MITOSIS (MODELED AS CONTINUOUS VARIABLE)	1.02	0.88-1.19	0.782	1.02	0.90-1.16	0.727	1.04	0.92-1.17	0.558
IDH1 MUTATION (YES VS NO)	0.48	0.24-0.97	0.041	1.10	0.57-2.15	0.771	0.66	0.34-1.28	0.213
IDH2 MUTATION (YES VS NO)	1.35	0.33-5.51	0.678	1.88	0.69-5.13	0.218	1.75	0.55-5.55	0.340
IDH1 or IDH2 MUTATION (YES VS NO)	0.42	0.19-0.93	0.009	1.54	0.66-3.57	0.324	0.71	0.32-1.56	0.390
P53 MUTATION (YES VS NO)	0.90	0.55-1.47	0.670	1.65	1.09-2.48	0.017	1.30	0.84-2.02	0.237
ATRX EXPRESSION (YES VS NO)	1.44	0.91-2.28	0.119	0.84	0.58-1.22	0.356	1.08	0.72-1.60	0.714
MGMT PROMOTER METHYLATION (YES VS NO)	0.65	0.26-1.61	0.347	1.28	0.58-2.80	0.534	0.70	0.30-1.56	0.391
CHROMOSOME 1P DELETION (YES VS NO)	0.86	0.52-1.40	0.537	0.71	0.48-1.06	0.094	0.74	0.48-1.14	0.170
CHROMOSOME 19Q DELETION (YES VS NO)	1.09	0.68-1.75	0.724	0.87	0.59-1.27	0.457	0.91	0.60-1.37	0.640
CHROMOSOME 1p/19q CO-DELETION (YES VS NO)	0.91	0.55-1.51	0.706	0.75	0.50-1.13	0.170	0.82	0.53-1.27	0.370

Table 4.8. Univariate analysis of prognostic value of clinical and histological parameters with overall survival (OS), progression-free survival (PFS) and malignant progression-free survival (MPFS) in 161 patients with low-grade glioma. Abbreviations: HR = hazard ratio; CI = confidence interval; EOR = extent of surgical resection; KPS = Karnosky Performance Status. *p*<0.05 statistically significant.

4.6 EVALUATION OF THE PROGNOSTIC VALUE OF IL-1 β , IL-6 AND p65

TMA analysis of IL-1 β , IL-6 and p65/NF κ B expression was assessed by using the Cox regression. Table 4.9 illustrates Cox univariate analysis of IL-1 β , IL-6 and p65/NF κ B. At the univariate analysis, nuclear and cytoplasm IL-1 β expressions did not statistically correlate with OS, PFS and MPFS, while IL-6 expression had a protective effect with OS and MPFS. The prognostic factor associated with a poor OS was the nuclear p65 expression (Table 4.9). This result confirmed the previous evaluation of p65 expression in a LGG characterized by a poor prognosis; it is interesting to note that only the nuclear expression of P65/NF κ B was endowed with a prognostic significance, indicating that the protein localization is fundamental for the prognostic value.

	OS			PFS			MPFS		
	HR	95% CI	<i>p</i>	HR	95% CI	<i>p</i>	HR	95% CI	<i>p</i>
GLOBAL P65	1.003	0.994-1.012	0.499	0.999	0.992-1.006	0.772	1.002	0.994-1.010	0.612
NUCLEAR P65	1.004	1.000-1.008	0.044	1.002	0.999-1.006	0.230	1.003	1.000-1.007	0.087
GLOBAL IL6	0.983	0.972-0.995	0.005	0.992	0.983-1.000	0.061	0.984	0.979-0.999	0.032
GLOBAL IL1 β	1.000	0.999-1.002	0.684	1.000	0.995-1.001	0.942	1.001	1.000-1.002	0.184
NUCLEAR IL1 β	1.001	0.999-1.002	0.440	1.000	0.995-1.002	0.728	1.001	1.000-1.003	0.120

Table 4.9. Analysis of p65/NF κ B, IL-1 β and IL-6 expression with OS, PFS and MPFS in 161 patients with low-grade gliomas. Abbreviations: HR: hazard ratio, CI: confidence interval, OS: overall survival, PFS: progression free survival, MPFS: malignant progression free survival. *p*<0.05 statistically significant.

At the multivariate Cox analysis, including all factors resulted to be significantly associated with prognosis at the univariate analysis, nuclear p65 resulted to be an independent predictive factor of OS (HR 1.006, CI 95% 1.002-1.011, *p*=0.002), together with Ki67 (HR 2.324, CI95% 1.391-3.881, *p*=0.001), the extent of tumor resection (HR 0.924, IC95% 0.906-0.943, *p*=0.000), the KPS (HR 0.940, IC95% 0.906-0.974, *p*=0.001), and mutated IDH1 gene (HR 0.335, IC95% 0.149-0.751, *p*=0.008).

Moreover, nuclear p65 resulted to be an independent predictive factor of MPFS (HR 1.004, IC95% 1.000-1.008, *p*=0.028), together with Ki67 (HR 1.574, IC95% 1.044-2.374, *p*=0.003), the extent of tumor resection (HR 0.951, IC95% 0.936-0.967, *p*=0.000) and KPS (HR 0.949, IC95% 0.921-0.979, *p*=0.001).

The multivariate Cox analysis demonstrated that IL6 do not represent an independent predictive factor of OS and of MPFS.

5. DISCUSSION

Translational medicine aims at transferring advances in basic science research into new approaches for diagnosis and treatment of diseases. With this goal, our research group used a population of stem cell, isolated from human glioma, named Glioma-Associated Stem Cells (GASC), such an approach of personalized medicine to identify new prognostic and predictive factors that lead to personalized therapies⁽⁷⁹⁾.

GASC represent an *in vitro* model of the glioma microenvironment and they have a strong prognostic value in low grade glioma since their surface immunophenotype can predict patients' overall survival (OS) and malignant transformation risk⁽⁷⁹⁾.

Emerging studies highlight the importance of the tumor microenvironment in tumor progression⁽⁷⁰⁾ which can be considered a potential target for the development of new therapeutic strategies⁽¹⁰¹⁾.

For this reason, low grade glioma (WHO grade II), characterized by a better prognosis with respect to the high-grade ones, represent an important challenge for clinicians because: 1) complete surgical resection is quite impossible and about 70% of tumors transforms into anaplastic forms within 5-10 years with aggressive clinical manifestation and fatal outcome⁽²⁷⁾; 2) some of LGG progress to high-grade glioma and criteria for a correct patients' prognostic stratification don't exist⁽²⁹⁾; 3) current adjuvant therapies (radio- and chemo-therapies) cause neurocognitive deficits which affect negatively the patient's quality of life and well-being.

Recently, two independent studies of genome-wide molecular analysis have reported the clinical value of 1p/19q co-deletions, IDH1/2, TERT, TP53, and ATRX mutations in grade II and grade III gliomas. Both groups proposed a classification based on a combination of these molecular markers: the first study⁽¹⁴⁾ identified a combination of presence/absence of IDH mutations, 1p/19q co-deletions and TP53 status meanwhile the second study⁽¹⁵⁾ identified a combination of presence/absence of 1p/19q co-deletions, IDH1/2 mutations and TERT mutations. Both papers have demonstrated that the presence of IDH1/2 mutations is a factor of good prognosis.

As described in the previous paragraphs, our group isolated GASC from 40 cases of grade II glioma. We demonstrated that a score based on GASC characterization was the only independent predictor of both OS and MPFS, outperforming all the available criteria in stratifying LGG patients, such IDH1/2 mutations, 1p/19q co-deletions and TP53 status⁽⁷⁹⁾.

The use of GASC as predictor factor in LGG requires the presence of cellular culture laboratories and few pathology departments are provided with this type of laboratory. To introduce new markers related to the tumor microenvironment in the clinical practice, we have decided to analyze the gene expression profile of GASC to search for new key molecules and detect them at tissue level by immunohistochemical assays. In collaboration with the Institute of Applied Genomics, we decided, therefore, to sequence the exome of two groups of GASC lines obtained from glioma with different prognosis: glioma without malignant transformation after 7 years from treatment and glioma transformed in high grade forms within 48 months from treatment.

This was possible because we have built, in collaboration with the neurosurgery department of doctor Skrap, a bio-repository that includes cryopreserved lines of GSC (n=40), and GASC from both LGG (n=80) and HGG (n=100).

Thawed GASC lines continued to possess features of stemness (mesenchymal surface phenotype, expression of pluripotent state-specific transcription factors expression and intermediate filaments related to an undifferentiated phenotype and aberrant anchorage-independent growth. These evidences confirmed the value of our protocols optimized not only for the isolation but also for the cryopreservation of glioma cell lines.

The analysis of genes differentially expressed pointed out that the transcriptome of GASC obtained from glioma with a poor prognosis contains elements typical of the inflammatory response and of the so-called senescence-associated secretory phenotype (SASP) ⁽¹⁰²⁾. Senescence is now increasingly considered to be an integrated and widespread component that is potentially important for tumour development, tumour suppression and the response to therapy ⁽¹⁰³⁾. The core aspect of the senescent phenotype is a stable state of cell cycle arrest. However, this feature conceals a highly active metabolic cell state with diverse functionality. Both the cell-autonomous and the non-cell-autonomous activities of senescent cells create spatiotemporally dynamic and context-dependent tissue reactions ⁽¹⁰³⁾. For example, the senescence-associated secretory phenotype (SASP) provokes not only tumour-suppressive but also tumour-promoting responses ⁽¹⁰³⁾.

It has long been considered an important element the development of an inflammatory microenvironment for the tumor progression, particularly in the initiation and progression of glioblastoma. This tumor is surrounded by a pool of pro-inflammatory cytokines, such IL-1 β , IL-6 and IL-8, which activate the inflammatory pathways of JAK, p38 MAPK and JNK ⁽¹⁰⁰⁾.

Concordantly, *upstream regulators* analysis of genes differentially expressed between GASC from LGG with a good prognosis and LGG with a bad prognosis, by using Ingenuity Pathway Analysis (in collaboration with LNCIB), pointed out the presence of some cytokines and transcriptional regulators.

We selected three factors representatives of different inflammatory pathway, IL-1 β , IL-6 and p65, a component of the heterodimer NF κ B, from the *upstream regulators* list, on the base of their probability to activate a molecular signature characterizing GASC from LGG with a bad prognosis.

IL-1 may directly stimulate glioma cell proliferation and induce the secretion of other cytokines like IL-6 and IL-8 by an autocrine loop ⁽⁸⁵⁾. IL-1, IL-6 and IL-8 share the capacity to induce the expression and secretion of MMP-2, MMP-9 in normal and tumor cells ^{(86), (87), (88)}. Thus, these factors may contribute to invasion of glioma cells through the induction of matrix degrading proteinases.

Recent studies demonstrate that IL-1 is an inducer of pro-angiogenesis and pro-invasion factors such as VEGF and MMPs in glioblastoma cells ^{(104), (105)}.

Similarly, IL-6 act in a pracrine loop in the tumour microenvironment stimulating angiogenesis by inducing endothelial cell and pericyte proliferation and migration, generating an invasion permissive environment ⁽⁸⁰⁾.

The transcriptional factor NF κ B performs an important role for the production of a secretome enriched in inflammatory cytokines in senescent cells. NF κ B activation in senescent cells can be induced by different mechanisms: response to a DNA damage, Retinoic Acid-Inducible Gene 1(RIG-1) inflammasome, p38 MAPK pathway induced by stress, TGF β and inflammatory cytokines (such IL-1 β) ⁽¹⁰⁶⁾.

IL-1 β , IL-6 and p65 have been studied in high-grade glioma^{(107) (108) (109)} but not in low-grade glioma, therefore we have evaluated their expression at tissue level.

Firstly, we optimized the immunohistochemical assay on glioma sections belonging to a group of LGG (n=5) and to a group of HGG (n=5), to check a possible difference in the expression of the selected factors.

Expression quantification confirmed a high production of IL-1 β and IL-6 in high-grade glioma. These cytokines were expressed in significantly a lower quantity in low-grade glioma; however, it was interesting to note that the low-grade glioma sample characterized by with a poor prognosis was characterized by a high expression of IL-1 β and IL-6.

Differently, p65 expression was extremely variable among high-grade glioma and was particularly high in the LGG with a bad prognosis. Recently, it has been found that NF κ B expression in HGG can be associated with chemoresistance, thus identifying a group of HGG characterized by a poor prognosis⁽¹⁰⁷⁾.

Besides, it was demonstrated that neurosphere, isolated from proneural glioblastoma, can be induced to a mesenchymal phenotype in an NF κ B-dependent fashion, suggesting that NF κ B expression can be associated with an aggressive phenotype⁽¹⁰⁸⁾.

Since in our data IL-1 β , IL-6 and p65 expression was particularly high in the LGG with a poor prognosis, we considered including these markers in the evaluation of the case study available at the Neurosurgery Department of Azienda Ospedaliero-Universitaria of Udine and to test their possible prognostic value.

We constructed 14 TMA containing 161 samples of LGG and we evaluated with immunohistochemical assays the expression of IL-1 β , IL-6 and p65. The statistical analysis confirmed that nuclear p65 expression is an independent predictor factor of OS and MPFS in LGG and this evidence supports the use of GASC as a model to search new prognostic factors.

The nuclear localization of p65 indicates that the nuclear translocation of this transcription factor is fundamental for the activation of pathways that increase, in glioma, invasiveness as well resistance to therapies. In fact when p65 binds to DNA activates factors implicated in the inflammatory response (IL-6 and IL-8) and anti-apoptotic genes (cIAP2, Bcl-2)⁽⁸⁹⁾. Moreover, p65 is implicated in the transcriptional activation of the matrix metalloproteinase-9 (MMP-9) promoter in human glioma cells⁽¹⁰⁹⁾, demonstrating a role in the tumor invasiveness.

However, our study demonstrates that IL-6 expression has a protective effect with OS and MPFS and this result is in contrast with the nuclear expression of p65, because it induces the expression of IL-6⁽¹¹⁰⁾; then the multivariate analysis of our study demonstrated that IL6 do not represent an independent predictive factor of OS and of MPFS. This evidence suggests that the modulation of inflammatory cytokines is extremely complex: IL-6 expression is regulated by NF κ B and also by Notch, S1PR1 and STAT3 phosphorylation⁽¹¹¹⁾. Moreover, recent studies affirm that single nucleotide polymorphisms (SNP) in the promoter region of IL-6 are associated with the production of this cytokine and with cancer risk⁽¹¹²⁾.

6. CONCLUSION AND FUTURE PERSPECTIVES

We have studied gene expression profile of GASC obtained from gliomas with different prognosis and we have found that GASC from gliomas with a malignant progression are characterized by an inflammatory transcriptome which includes cytokines such IL-1 β and IL-6 and transcriptional regulator like NF κ B/p65.

We have evaluated the expression of IL-1 β , IL-6 and NF κ B/p65 at tissue level optimizing an immunohistochemical assay on high-grade and low-grade gliomas. The three markers were expressed at high levels in high-grade gliomas and in a low-grade glioma with a bad prognosis. Since low-grade gliomas expressed IL-1 β and IL-6 at quantifiable levels, we decided to validate the obtained results on the case study of LGG available in our department.

The analyses of our immunohistochemical assays suggest nuclear p65 as an independent predictor of OS and MPFS.

These promising data will enable us to extend our analyses to the case study of LGG available at the Neurosurgery Department of Azienda Ospedaliero-Universitaria of Udine. We have one of the most comprehensive case study of tissues obtained from patients with LGG in Europe and the corresponding clinical database is updated continuously. In particular, we have DNA, RNA and TMA of about 250 consecutive samples of supratentorial LGG characterized from a clinical point of view (age, sex, therapy, surgery, overall survival, progression free survival, malignant progression free survival), from a neuroradiologic point of view (extent of tumor resection, tumor bulk before the surgery and tumor bulk at the follow-up) and from a histological-molecular point of view (histotype, Ki67 and p53 expression, 1p-19q co-deletion, IDH1/2 mutation, MGMT promoter methylation).

Definition of new prognostic/predictive factors in LGG can provide:

- To clinician new instruments for the clinical management of the patients
- A new antibody panel useful for the immunohistochemical analyses for pathology departments with a low cost and a high benefit for patients and hospitals.

References

1. **D., Purves.** *Neuroscience*. s.l. : Sinauer Associates., 2004.
2. **Fei He, Yi E. Sun.** Glial cells more than support cells? *The International Journal of Biochemistry & Cell Biology* . 2007, Vol. 39: 661–665, p. 39: 661–665.
3. **Nikki A. Charles, Eric C. Holland,1 Richard Gilbertson, Rainer Glass, And Helmut Kettenmann.** The Brain Tumor Microenvironment. *GLIA* . 2011, Vol. 59:1169–1180 , p. 59:1169–1180. .
4. **Michael V. Sofroniew, Harry V.** Astrocytes: biology and pathology. *Acta Neuropathol* . 2010, Vol. 119:7–35, p. 119:7–35.
5. **Joachim Morrens, Wim Van Den Broeck, And Gerd Kempermann.** Glial Cells in Adult Neurogenesis. *GLIA* . 2012, Vol. 60:159–174, p. 60:159–174.
6. **Kettenmann, H., Hanisch, U. K., Noda, M. & Verkhratsky, A.** Physiology of microglia. *Physiol. Rev.* 2011, Vol. 91, 461–553 .
7. **K.Glass., Kaoru Saijo and Christopher.** Microglial Cell Origin And Phenotypes In Health And Disease. *Nature Reviews*. 2011, Vol. Vol 11, p. Volume 11.
8. **Furnari FB, Fenton T, Bachoo RM, Mukasa A, Stommel JM, Stegh A, Hahn WC, Ligon KL, DN, Brenn Louis an C, et al.** Malignant astrocytic glioma: genetics, biology, and paths to treatment. *Genes Dev.* 2007, Vol. 21: 2683–2710, p. 21: 2683–2710.
9. **Louis DN, Ohgaki H, Wiestler OD, Cavenee WK, Burger PC, Jouvet A, Scheithauer BW, Kleihues P.,** The 2007 WHO classification of tumours of the central nervous system. *Acta Neuropathologica*. 2007, Vol. 114(2): 97-109, p. 114(2): 97-109.
10. **Jovčevska I., Kočevar N., Komel R.** Glioma and Glioblastoma - how much do we (not) know? *Molecular and Clinical Oncology*. 2013, Vol. 1(6): 935-941, p. 1(6): 935-941.
11. **ML, Suvà.** Genetics and epigenetics of gliomas. *Swiss Med Wkly*. 2014, Vol. 144: w14018, p. 144: w14018.
12. **Wick., Markus Weiler and Wolfgang.** Molecular predictors of outcome in low-grade glioma. *Current opinion*. 2012, Vol. 25, 6.
13. **Christina L. Appin, Daniel J. Brat .** Biomarker-driven diagnosis of diffuse gliomas. *Molecular Aspects of Medicine* . 2015, Vol. 45: 87–96, p. 45: 87–96.
14. **Brat DJ, Verhaak RG, Aldape KD, Yung WK, Salama SR, Cooper LA, Rheinbay E, Miller CR, Vitucci M, Morozova O et al.** Comprehensive, Integrative Genomic Analysis of Diffuse Lower-Grade Gliomas. *N Engl J Med*. 2015, Vol. 372(26): 2481-2498.
15. **Eckel-Passow JE, Lachance DH, Molinaro AM, Walsh KM, Decker PA, Sicotte H, Pekmezci M, Rice T, Kosel ML, Smirnov IV, Sarkar G, Caron AA, Kollmeyer TM, Praska CE, Chada AR, Halder C, Hansen HM, McCoy LS, Bracci PM, Marshall R., Zheng S, Reis GF, Pico AR, O'Neill BP, Buckner JC, Giannini C, Huse JT, Perry A, Tihan T, Berger MS, Chang SM, Prados MD, Wiemels J, Wiencke JK, Wrensch MR, Jenkins RB.**

Glioma Groups Based on 1p/19q, IDH, and TERT Promoter. *N Engl J Med. Mutations in Tumors.* 2015, Vol. 372(26): 2499-2508.

16. **Crocetti E, Trama A, Stiller C, Caldarella A, Soffiotti R, Jaal J, Weber DC, Ricardi U, Slowinski J, Brandes A e group, RARECARE working.** Epidemiology of glial and non-glial brain tumours in Europe. *Eur J Cancer.* 2012, Vol. 48(10): 1532-42.

17. **Hardell L, Carlberg M, Söderqvist F, Hansson Mild K.** Meta-analysis of long-term mobile phone use and the association with brain tumours. *Int J Oncol.* 2008, Vols. 32(5): 1097-103.

18. **AIOM, Linee Guida Neoplasie Cerebrali, Edizione 2013.**

19. **P, Ohgaki H and Kleihues.** Epidemiology and etiology of gliomas. *Acta Neuropathol.* 2005, Vol. 109(1): 93-108.

20. **Stefanaki K, Alexiou GA, Stefanaki C, Prodromou N.** Tumors of central and peripheral nervous system associated with inherited genetic syndromes. *Pediatr Neurosurg.* 2012, Vols. 48(5):271-85.

21. **Michael B. Foote, Nickolas Papadopoulos, and Luis A. Diaz, Jr.** Genetic Classification of Gliomas: Refining Histopathology. *Cancer Cell.* 2015, Vol. 28, July 13, p. 28, July 13.

22. **Lindberg N, Kastemar M, Olofsson T, Smits A, Uhrbom L.** Oligodendrocyte progenitor cells can act as cell of origin for experimental glioma. *Oncogene.* 2009, Vol. 28: 2266-75.

23. **GJ, Ruiz J and Lesser.** Low-Grade Gliomas. *Current Treatment Options in Oncology.* 2009, Vols. 10: 231-242.

24. **Shaw EG, Scheithauer BW, O'Fallon JR.** Supratentorial gliomas: a comparative study by grade and histologic type. *J Neurooncol.* 1997, Vol. 31:273-278.

25. **MJ, Van den Bent.** Practice changing mature results of RTOG study 9802: another positive PCV trial makes adjuvant chemotherapy part of standard of care in low-grade glioma. *Neuro Oncol.* 2014, Vol. 16(12): 1570-1574.

26. **Schiff D, Brown PD, Giannini C.** Outcome in adult low-grade glioma. *Neurology.* 2007, Vol. 69: 1366-1373.

27. **Soffiotti R, Baumert BG, Bello L, von Deimling A, Duffau H, Frénay M, Grisold W, Grant R, Graus F, Hoang-Xuan K, Klein M, Melin B, Rees J, Siegal T, Smits A, Stupp R, Wick W.** Guidelines on management of low-grade gliomas: report of an EFNS-EANO Task Force. *Eur J Neurol.* 2010, Vols. 17(9): 1124-1133.

28. **D, Pouratian N and Schiff.** Management of Low-Grade Glioma. *Curr Neurol Neurosci Rep.* 2010, Vol. 10: 224-231.

29. **D, Bourne TD and Schiff.** Update on molecular findings, management and outcome in low-grade gliomas. *Nat Rev Neurol.* 2010, Vol. 6(12): 695-701.

30. **Sanai N, Chang S, Berger MS.** Low-grade gliomas in adults. *J Neurosurg.* 2011, Vol. 115(5): 948-965.

31. **Jakola AS, Myrnel KS, Kloster R, Torp SH, Lindal S, Unsgard G, Solheim O.** Comparison of a strategy favoring early surgical resection vs a strategy favoring watchful waiting in low-grade gliomas. *JAMA*. 2012, Vol. 308(18): 1881-1888.
32. **Hai Yan, M.D., Ph.D., D. Williams Parsons, M.D., Ph.D., Genglin Jin, Ph.D., Roger. McLendon, M.D., B. Ahmed Rasheed, Ph.D., et al.** IDH1 and IDH2 Mutations in Gliomas. *New England Journal of Medicine*. 2009, Vol. 19; 360(8): 765–773.
33. **Okamoto Y, Di Patre PL, Burkhard C, et al.** Population-based study on incidence, survival rates, and genetic alterations of low-grade diffuse astrocytomas and oligodendrogliomas. *Acta Neuropathol (Berl)*. 2004, Vol. 108: 49-56.
34. **Jiao Y, Killela PJ, Reitman ZJ, Rasheed AB, Heaphy CM, de Wilde RF, Rodriguez FJ, Rosemberg S, Oba-Shinjo SM, Nagahashi Marie SK, Bettegowda C, Agrawal N, Lipp E, Pirozzi C, Lopez G, He Y, Friedman H, Friedman AH, Riggins GJ, Holdhoff M, Burger. P, McLendon R, Bigner DD, Vogelstein B, Meeker AK, Kinzler KW, Papadopoulos N, Diaz LA, Yan H.** Frequent ATRX, CIC, FUBP1 and IDH1 mutations refine the classification of malignant gliomas. *Oncotarget*. 2012, Vol. 3(7): 709-722.
35. **Liu XY, Gerges N, Korshunov A, Sabha N, Khuong-Quang DA, Fontebasso AM, Fleming A, Hadjadj D, Schwartzenuber J, Majewski J, Dong Z, Siegel P, Albrecht S, Croul S, Jones DT, Kool M, Tonjes M, Reifenberger G, Faury D, Zadeh G, Pfister S.** Jabado N. Frequent ATRX mutations and loss of expression in adult diffuse astrocytic tumors carrying IDH1/IDH2 and TP53 mutations. *Acta Neuropathol*. 2012, Vol. 124(5): 615-625.
36. **Stupp R, Tonn JC, Brada M, Pentheroudakis G, & Group EGW.** High-grade malignant glioma: ESMO Clinical Practice Guidelines for diagnosis, treatment and follow-up. *Annals of oncology: official journal of the European Society for Medical Oncology*. 2010, Vol. ESMO 21 Suppl 5: v190-193.
37. **Parsons DW, Jones S, Zhang X, Lin JC, Leary RJ, Angenendt P, Mankoo P, Carter H, Siu IM, Gallia GL, et al.** An integrated genomic analysis of human glioblastoma multiforme. *Science*. 2008, Vol. 321: 1807-1812.
38. **Mellai, M., Monzeglio, O., Piazzini, A., et al.** MGMT promoter hypermethylation and its associations with genetic alterations in a series of 350 brain tumors. *J. Neurooncol*. 2012, Vol. 107 (3), 617–631.
39. **The Cancer Genome Atlas Research Network.** 2015.
40. **H, Kleihues P and Ohgaki.** Primary and secondary glioblastomas: from concept to clinical diagnosis. *Neuro Oncol*. 1999, Vol. 1: 44-51.
41. **Urbańska K, Sokołowska J, Szmidi M, Sysa P.** Glioblastoma multiforme - an overview. *Contemp Oncol (Pozn)*. 2014, Vol. 18(5): 307-12.
42. **Karcher S, Steiner HH, Ahmadi R, Zoubaa S, Vasvari G, Bauer H, Unterberg A, Herold-Mende C.** Different angiogenic phenotypes in primary and secondary glioblastomas. *Int J Cancer*. 2006, Vol. 118: 2182-9.
43. **Chen J, McKay RM, Parada LF.** Malignant Glioma: Lessons from Genomics, Mouse Models, and Stem Cells. *Cell*. 2012, Vol. 149(1): 36-47.

44. **Markus Bredel, M.D., Ph.D., Denise M. Scholtens, Ph.D., Ajay K. Yadav, Ph.D., Angel A. Alvarez, B.Sc., Jaclyn J. Renfrow, M.A., James P. Chandler, M.D., Irene L.Y. Yu, M.Sc., and Griffith R. Harsh IV, M.D.** NFKBIA Deletion in Glioblastomas. *New England Journal of Medicine*. 2011, Vol. 17; 364(7): 627–637.
45. **M., Karin.** Nuclear factor-kappaB in cancer development and progression. *Nature*. 2006, Vol. 441: 431–436.
46. **Verhaak RG, Hoadley KA, Purdom E, Wang V, Qi Y, Wilkerson MD, Miller CR, Ding L, Golub T, Mesirov JP, Alexe G, Lawrence M, O'Kelly M, Tamayo P, Weir BA, Gabriel S, Winckler W, Gupta S, Jakkula L, Feiler HS, Hodgson JG, James CD, Sarkaria JN.** Brennan C, Kahn A, Spellman PT, Wilson RK, Speed TP, Gray JW, Meyerson M, Getz G, Perou CM, Hayes DN. Integrated genomic analysis identifies clinically relevant subtypes of glioblastoma characterized by abnormalities in PDGFRA, IDH1, EGFR, and NF1. *Cancer Cell*. 2010, Vol. 17(1): 98-110.
47. **Singh, S.K., Hawkins, C., Clarke, I.D., Squire, J.A., Bayani, J., Hide, T., Henkel-Man, R.M., Cusimano, M.D., And Dirks, P.B.** Identification of human brain tumor initiating cells. *Nature*. 2004, Vol. 432: 396-401.
48. **Galli R, Binda E, Orfanelli U, Cipelletti B, Gritti A, De Vitis S, Fiocco R, Foroni C, Dimeco F, Vescovi A.** Isolation and characterization of tumorigenic, stem-like neural precursors from human glioblastoma. *Cancer Res*. 2004, Vol. 64(19): 7011-7021.
49. **Bao S, Wu Q, McLendon RE, Hao Y, Shi Q, Hjelmeland AB, Dewhirst MW, Bigner DD, Rich JN.** Glioma stem cells promote radioresistance by preferential activation of the DNA damage response. *Nature*. 2006, Vol. 444(7120): 756-60.
50. **Lee J, Kotliarova S, Kotliarov Y, Li A, Su Q, Donin NM, Pastorino S, Purow BW, Christopher N, Zhang W, Park JK, Fine HA.** Tumor stem cells derived from glioblastomas cultured in bFGF and EGF more closely mirror the phenotype and genotype of primary tumors than do serum-cultured cell lines. *Cancer Cell*. 2006, Vol. 9: 391-403.
51. **Pollard SM, Yoshikawa K, Clarke ID, Danovi D, Stricker S, Russell R, Bayani J, Head R, Lee M, Bernstein M, Squire JA, Smith A, Dirks P.** Glioma Stem Cell Lines Expanded in Adherent Culture Have Tumor-Specific Phenotypes and Are Suitable for Chemical and Genetic Screens. *Cell Stem Cell*. 2009, Vol. 4(6): 568-580.
52. **Laks DR, Masterman-Smith M, Visnyei K, Angenieux B, Orozco NM, Foran I, Yong WH, Vinters HV, Liau LM, Lazareff JA, Mischel PS, Cloughesy TF, Horvath S, Kornblum HI.** Neurosphere formation is an independent predictor of clinical outcome in malignant glioma. *Stem Cells*. 2009, Vol. 27: 980-987.
53. **Beier D, Hau P, Proescholdt M, Lohmeier A, Wischhusen J, Oefner PJ, Aigner L, Brawanski A, Bogdahn U, Beier CP.** CD133(+) and CD133(-) glioblastoma-derived cancer stem cells show differential growth characteristics and molecular profiles. *Cancer Res*. 2007, Vol. 67: 4010–4015.
54. **Sampetean O., Saya H.** Characteristics of glioma stem cells. *Brain Tumor Pathology*. 2013, Vol. 30(4): 209-14.

55. **Persson AI, Petritsch C, Swartling FJ, Itsara M, Sim FJ, Auvergne R, Goldenberg DD, Vandenberg SR, Nguyen KN, Yakovenko S, Ayers-Ringler J, Nishiyama A, Stallcup WB, Berger MS, Bergers G, McKnight TR, Goldman SA, Weiss WA.** Non-stem cell origin for oligodeoligodendroglioma . *Cancer Cell*. 2010, Vol. 18(6):669-682.
56. **Lindberg N, Kastemar M, Olofsson T, Smits A, Uhrbom L.** Oligodendrocyte progenitor cells can act as cell of origin for experimental glioma. *Oncogene*. 2009, Vol. 28(23):2266-2275.
57. **Jiang Y, Uhrbom L.** On the origin of glioma. *Ups J Med Sc*. 2012.
58. **Ghotra VP, Puigvert JC, Danen EH.** The cancer stem cell microenvironment and anti-cancer therapy. *Int J Radiat Biol*. 2009, Vol. 85: 955-62.
59. **Plaks V, Kong N, Werb Z.** The cancer stem cell niche: how essential is the niche in regulating stemness of tumor cells? *Cell Stem Cell*. Vol. 16(3): 225-238.
60. **Calabrese C, Poppleton H, Kocak M, Hogg TL, Fuller C, Hamner B, Oh EY, Gaber MW, Finklestein D, Allen M, Frank A, Bayazitov IT, et al.** A perivascular niche for brain tumor stem cells. *Cancer Cell*. 2007, Vol. 11: 69–82.
61. **H, Oh SY and Kim.** Molecular Culprits Generating Brain Tumor Stem Cells. *Brain Tumor Res Treat*. 2013, Vol. 1(1): 9-15.
62. **Gilbertson, R.J., Rich, J.N.** Making a tumour’s bed: glioblastoma stem cells and the vascular niche. *Nat. Rev. Cancer* . 2007, Vol. 7, 733–736.
63. **Cabarcas, S.M., Mathews, L.A., Farrar, W.L.** The cancer stem cell niche – there goes the neighborhood? *International Journal of Cancer*. 2011, Vol. 129: 2315-2327.
64. **Heddleston JM, Li Z, Lathia JD, Bao S, Hjelmeland AB, Rich JN.** Hypoxia inducible factors in cancer stem cells. *Br J Cancer*. 2010, Vol. 102: 789–95.
65. **Das B, Tsuchida R, Malkin D, Koren G, Baruchel S, Yeger H.** Hypoxia enhances tumor stemness by increasing the invasive and tumorigenic side population fraction. *Stem Cells*. 2008, Vol. 26: 1818–30.
66. **Silvan U, Diez-Torre A, Arluzea J, Andrade R, Sillio M, Arechaga J.** Hypoxia and pluripotency in embryonic and embryonal carcinoma stem cell biology. *Differentiation*. 2009, Vol. 78: 159–68.
67. **Cleaver O, Melton DA.** Endothelial signaling during development. *Nat Med*. 2003, Vol. 9: 661–668.
68. **Le DM, Besson A, Fogg DK, Choi KS, Waisman DM, Goodyer CG, Rewcastle B, Yong VW.** Exploitation of astrocytes by glioma cells to facilitate invasiveness: a mechanism involving matrix metalloproteinase-2 and the urokinase-type plasminogen activator-plasmin cascade. *J Neurosci*. 2003, Vol. 23: 4034-4043.
69. **Charles, N.A., Holland, E.C., Gilbertson, R., Glass, R., Kettenmann, H.** The Brain Tumor Microenvironment. *Glia*. 2011, Vol. 59: 1169-1180.
70. **RA, Hanahan D and Weinberg.** Hallmarks of cancer: the next generation. *Cell*. 2011, Vol. 144(5): 646-674.

71. **Radisky D., Hagios C., Bissel M.J.** Tumors are unique organs defined by abnormal signaling and context. *Cancer Biology*. 2001, Vol. 11: 87-95.
72. **Cirri, P., Chiarugi, P.** Cancer-associated-fibroblasts and tumour cells: a diabolic liaison driving cancer progression. *Cancer Metastasis Rev* . 2012, Vol. 31: 195-198.
73. **Cat, B., Stuhlmann, D., Steinbrenner, H., Alili, L., Holtkotter, O. Sies, H., et al.** Enhancement of tumor invasion depends on transdifferentiation of skin fibroblasts mediated by reactive oxygen species. *Journal of Cell Science*. 2006, Vol. 119(Pt 13), 27.
74. **Thiery JP, Acloque H, Huang RY, Nieto MA.** Epithelial-mesenchymal transitions in development and disease. *Cell*. 2009, Vol. 139: 871–90.
75. **Wang, W., Li, Q., Yamada, T., Matsumoto, K., Matsumoto, I., Oda, M., et al.** Crosstalk to stromal fibroblasts induces resistance of lung cancer to epidermal growth factor receptor tyrosine kinase inhibitors. *Clinical Cancer Research*. 2009, Vol. 15(21), 6.
76. **Hanahan D, Weinberg RA.** The hallmarks of cancer. *Cell*. 2000, Vol. 100(1):57-70.
77. **Graeber MB, Scheithauer BW, Kreutzberg GW.** Microglia in brain tumors. *Glia*. 2002, Vol. 40: 252–259.
78. **Watters JJ, Schartner JM, Badie B.** Microglia function in brain tumors. *J Neuroscience Res*. 2005, Vol. 81: 447–455.
79. **Bourkoula E, Mangoni D, Ius T, Pucer A, Isola M, Musiello D, Marzinotto S, Toffoletto B, Sorrentino M, Palma A, Caponnetto F, Gregoraci G, Vindigni M, Pizzolitto S, Falconieri G, De Maglio G, Pecile V, Ruaro ME, Gri G, Parisse P, Casalis L, Scoles G, Skrap M, Beltrami CA, Beltrami AP, Cesselli D.** Glioma-associated stem cells: a novel class of tumor-supporting cells able to predict prognosis of human low-grade gliomas. *Stem Cells*. 2014, Vol. 32(5): 1239-1253, p. 32(5): 1239-1253.
80. **Mueller MM, Werbowetski T, Del Maestro RF.** Soluble factors involved in glioma invasion. *Acta Neurochir (Wien)*. 2003, Vol. 145(11): 999-1008.
81. **Iwami K, Natsume A, Wakabayashi T.** Cytokine networks in glioma. *Neurosurgical Review*. 2011, Vol. 34(3):253–263.
82. **ThomasWurdinger, Katrin Deumelandt, Hans J. van der Vliet, PieterWesseling, Tanja D. de Gruijl.** Mechanisms of intimate and long-distance cross-talk between glioma and myeloid cells: How to break a vicious cycle. *Biochimica et Biophysica Acta*. 2014, Vol. 1846, 560–575 .
83. **Hao C, Parney IF, Roa WH, Turner J, Petruk KC, Ramsay DA.** Cytokine and cytokine receptor mRNA expression in human glioblastomas: evidence of Th1, Th2 and Th3 cytokine dysregulation. *Acta Neuropathol*. 2002, Vol. 103: 171–178.
84. **Sasaki A, Ishiuchi S, Kanda T, Hasegawa M, Nakazato Y.** Analysis of interleukin-6 gene expression in primary human gliomas, glioblastoma xenografts, and glioblastoma cell lines. *Brain Tumor Pathol*. 2001, Vol. 18: 13-21.

85. **Van Meir E, Sawamura Y, Diserens AC, Hamou MF, de Tribolet N.** Human glioblastoma cells release interleukin 6 in vivo and in vitro. *Cancer Res.* 1990, Vol. 50: 6683–6688.
86. **Inoue K, Slaton JW, Eve BY, Kim SJ, Perrotte P, Balbay MD, Yano S, Bar-Eli M, Radinsky R, Pettaway CA, Dinney CP.** Interleukin 8 expression regulates tumorigenicity and metastases in androgen-independent prostate cancer. *Clin Cancer Res.* 2000, Vol. 6: 2104–2119.
87. **Kubota Y, Oka S, Nakagawa S, Shirasuna K.** Interleukin-1alpha enhances type I collagen-induced activation of matrix metalloproteinase-2 in odontogenic keratocyst fibroblasts. *J Dent Res.* 2002, Vol. 81: 23–27.
88. **Kossakowska AE, Edwards DR, Prusinkiewicz C, Zhang MC, Guo D, Urbanski SJ, Grogan T, Marquez LA, Janowska-Wieczorek A.** Interleukin-6 regulation of matrix metalloproteinase (MMP-2 and MMP-9) and tissue inhibitor of metalloproteinase. (*TIMP-1*) expression in malignant non-Hodgkin's lymphomas. *Blood.* 1999, Vol. 94: 2080–2089.
89. **Braden C. McFarland, G. Kenneth Gray, Susan E. Nozell, Suk W. Hong, and Ety N. Benveniste.** Activation of the NF-κB pathway by the STAT3 inhibitor JSI-124 in human glioblastoma cells. *Mol Cancer Res.* 2013, Vol. 11(5): 494–505.
90. **YJ, Tang WZ and Xia.** Expression of nuclear factor-kappaBP65 in human brain glioma and human brain metastatic carcinoma and its significance. *Xue Xue Bao.* 2004, Vol. 24(1): 75–8.
91. *Oncotarget.* 2014 May; 5(9): 2551–2561).
92. **Cesselli D, Beltrami AP, Pucer A, Bourkoula E, Ius T, Vindigni M, Skrap M, Beltrami CA.** Human Low Grade Glioma Cultures. In: Diffuse High- and Diffuse Low-Grade Gliomas in Adults. *Springer.* 2013.
93. **Quail DF, Joyce JA.** Microenvironmental regulation of tumor progression and metastasis. *Nat Med.* 2013, Vol. 19: 1423–37.
94. **Felsberg J, Wolter M, Seul H, et al.** Rapid and sensitive assessment of the IDH1 and IDH2 mutation status in cerebral gliomas based on DNA pyrosequencing. *Acta Neuropathol.* 2010, Vol. 119:501–507.
95. **Beltrami AP, Cesselli D, Bergamin N, et al.** Multipotent cells can be generated in vitro from several adult human organs (heart, liver, and bone marrow). *Blood.* 2007, Vol. 110:3438–3446.
96. **Cesselli D, Beltrami AP, D'Aurizio F, et al.** Effects of age and heart failure on human cardiac stem cell function. *Am J Pathol.* 2011, Vol. 179:349–366.
97. **Cesselli D, Beltrami AP, Poz A, et al.** Role of tumor associated fibroblasts in human liver regeneration, cirrhosis, and cancer. *Int J Hepatol.* 2011, Vol. 120925.
98. **C. Trapnell, A. Roberts, L. Goff, G. Pertea, D. Kim, D. R Kelley, H. Pimentel, S. L Salzberg, J. L Rin & L. Pachter.** Differential gene and transcript expression analysis of RNA-seq experiments with TopHat and Cufflinks. *Nature Protocols.* 2012, Vol. 7, 562–578.
99. **Giltane, J.M. and D.L. Rimm.** Technology insight: Identification of biomarkers with tissue microarray technology. *Nat Clin Pract Oncol.* 2004, Vol. 1(2): p. 104–11.

100. **Yeung YT, McDonald KL, Grewal T, Munoz L.** Interleukins in glioblastoma pathophysiology: implications for therapy. *Br J Pharmacol.* 2013, Vol. 168(3): 591-606.
101. **S. C. Casey, Amedeo Amedei, Katia Aquilano, Asfar S. Azmi, Fabian Benencia, Dipita Bhakta, Alan E. Bilsland, Chandra S. Boosani, Sophie Chen, Maria Rosa Ciriolo.** Cancer prevention and therapy through the modulation of the tumor microenvironment. *Seminars in Cancer Biology.* 2015, Vol. Vol 35 (0): S199-S223.
102. **A P Beltrami, D Cesselli and C A Beltrami.** Stem Cell Senescence and Regenerative Paradigms. *Clinical Pharmacology & Therapeutics .* 2012, Vol. Volume 91, Issue 1, pages 21–29.
103. **Perez-Mancera PA, Young AR, Narita M,.** Inside and out: the activities of senescence in cancer. *Nat Rev Cancer.* 2014, Vol. 14(8): 547-558.
104. **Tarassishin L, Lim J, Weatherly DB, Angeletti RH, Lee SC.** Interleukin-1-induced changes in the glioblastoma secretome suggest its role in tumor progression. *J Proteomics.* 2014, Vol. 99: 152-168.
105. **Nijaguna MB, Schroder C, Patil V, Shwetha SD, Hegde AS, Chandramouli BA, Arivazhagan A, Santosh V, Hoheisel JD, Somasundaram K.** Definition of a serum marker panel for glioblastoma discrimination and identification of Interleukin 1beta in the microglial secretome as a novel mediator of endothelial cell survival induced by C-reactive protein. *J Proteomics .* 2015, Vol. 128: 251-261.
106. **Gianfranceschi G., Gri G., Cesselli D., & Beltrami A.P.** Stem Cell Senescence as the Memory of Past Injuries. *Current Pathobiology Reports.* 2015, Vol. 3(1): 17–26.
107. **Shukla S, Pia Patric IR, Thinagararjan S, Srinivasan S, Mondal B, Hegde AS, Chandramouli BA, Santosh V, Arivazhagan A, Somasundaram K.** A DNA methylation prognostic signature of glioblastoma: identification of NPTX2-PTEN-NF-kappaB nexus. *Cancer Res.* 2013, Vol. 73(22): 6563-6573.
108. **Bhat KP, Balasubramaniyan V, Vaillant B, Ezhilarasan R, Hummelink K, Hollingsworth F, Wani K, Heathcock L, James JD, Goodman LD, Conroy S, Long L, Lelic N, Wang S, Gumin J, Raj D, Kodama Y, Raghunathan A, Olar A, Joshi K, Pelloski CE, Heimberger A, Kim SH.** Mesenchymal differentiation mediated by NF-kappaB promotes radiation resistance in glioblastoma. *Cancer Cell.* 2013, Vol. 24(3): 331-346.
109. **al, Emily C. Brantley L. Burton Nabors et.** Loss of PIAS3 Expression in Glioblastoma Multiforme Tumors: Implications for STAT-3 Activation and Gene Expression. *Clin Cancer Res.* 2008, Vol. 14(15).
110. **M., Karin.** NF-kappaB as a critical link between inflammation and cancer. *Cold Spring Harb.* 1:a000141, 2009.
111. **Shan Y, He X, Song W, Han D, Niu J, Wang J.** Role of IL-6 in the invasiveness and prognosis of glioma. *Int J Clin Exp Med.* 2015, Vol. Jun 15;8(6):9114-20.
112. **Y. Du, L. Gao, K. Zhang, J. Wang.** Association of the IL6 polymorphism rs1800796 with cancer risk: a meta-analysis. *Genet. Mol. Res.* 2015, Vol. 14 (4) : 13236 - 13246.
113. **Krishanthan Vigneswaran1, Stewart Neill2, Costas G. Hadjipanayis.** Beyond the World Health Organization grading of infiltrating gliomas: advances in the molecular genetics of glioma classification. *Ann Transl Med.* 2015, Vol. 3(7):95.

114. **Shirin Ilkanizadeh, Jasmine Lau, Miller Huang, Daniel J. Foster, Robyn Wong, Aaron Frantz, Susan Wang, William A. Weiss, and Anders I. Persson.** Glial progenitors as targets for transformation in glioma. *Adv Cancer Res.* 2014, Vol. 121: 1–65, p. 121: 1–65.